

SANDIA REPORT

SAND98-1191
Unlimited Release
Printed July 1998

Exponential 6 Parameterization for the JCZ3-EOS

B. C. McGee, M. L. Hobbs, M. R. Baer

Inside of Cover Page

SAND98-1191
Unlimited Release
Printed July 1998

Exponential 6 Parameterization for the JCZ3-EOS

B. C. McGee, M. L. Hobbs,¹ M. R. Baer
Energetic and Multi-Phase Processes
Sandia National Laboratories
P. O. Box 5800
Albuquerque, New Mexico 87185-0834

Abstract

A database has been created for use with the Jacobs-Cowperthwaite-Zwisler-3 equation-of-state (JCZ3-EOS) to determine thermochemical equilibrium for detonation and expansion states of energetic materials. The JCZ3-EOS uses the exponential 6 intermolecular potential function to describe interactions between molecules. All product species are characterized by r^* , the radius of the minimum pair potential energy, and ϵ/k , the well depth energy normalized by Boltzmann's constant. These parameters constitute the JCZS (S for Sandia) EOS database describing 750 gases (including all the gases in the JANNAF tables), and have been obtained by using Lennard-Jones potential parameters, a corresponding states theory, pure liquid shock Hugoniot data, and fit values using an empirical EOS. This database can be used with the CHEETAH 1.40 or CHEETAH 2.0 interface to the TIGER computer program that predicts the equilibrium state of gas- and condensed-phase product species. The large JCZS-EOS database permits intermolecular potential based equilibrium calculations of energetic materials with complex elemental composition.

1. Correspondence concerning this report should be addressed to M. L. Hobbs

Acknowledgment

Many thanks to Arthur C. Ratzel for providing the opportunity and funding for this project. Helpful suggestions made by internal reviewers, R. G. Schmitt and S. A. Silling, are appreciated.

Table of Contents

Table of Contents	5
List of Figures	6
List of Tables	7
1. Executive Summary	9
2. JCZ3-EOS Background	9
3. Obtaining the Exponential 6 Potential Force Constants from Lennard-Jones Potential Parameters	10
4. Estimating the Exponential 6 Potential Force Constants from Critical Properties	12
5. Estimating the Exponential 6 Potential Force Constants through Correlation and Curve Fitting	14
5.1 Determining r^*	14
5.2 Determining ϵ/k	15
5.2.1 The BKW-EOS	15
5.2.2 The BKWR Parameterization	16
5.2.3 The BKWS Parameterization	16
5.2.4 The BKWC Parameterization	16
5.2.5 Using the BKWS-EOS to Determine ϵ/k	17
6. Pure Liquid Shock Hugoniot Data	18
7. DAKOTA Optimization	23
8. Validation of the JCZS-EOS	26
8.1 Explosive Performance	27
8.2 Expansion States	32
8.3 Detonation in Condensed Explosives with Low Initial Densities	32
8.4 High Pressure Gas Detonations	33
9. Summary and Conclusions	33
10. References	34
APPENDIX A	36
APPENDIX B	39
APPENDIX C	55

List of Figures

<p>Figure 1. Plot of the normalized exponential 6 potential function for Argon (solid line) with an r^* and ε/k of 3.85 Å and 122 K, respectively. The repulsive (dotted line) and attractive (dashed line) energy terms are also shown.</p> <p>Figure 2. Plot of the normalized Lennard-Jones potential function for Argon (solid) with an σ and ε/k of 3.43 Å and 122 K, respectively. The repulsive (dotted line) and attractive (dashed line) energy terms are also shown.</p> <p>Figure 3. Plot of the LJ potential function for AlCl_3 (solid line). The EXP 6 potential functions are plotted with the LJ characteristic diameter (dashed) and the corrected characteristic diameter (dash dotted)</p> <p>Figure 4. Plot of the r^*_{SCS} versus r^*_{4P} for 103 different molecules.</p> <p>Figure 5. Plot of r^*_{SCS} versus $\sigma \times 2^{1/6}$.</p> <p>Figure 6. Plot of $(\varepsilon/k)_{\text{SC}}$ versus $(\varepsilon/k)_{\text{LJ}}$</p> <p>Figure 7. Plot of the exponential 6 potential function for AlCl_3 using the SCS parameters ($r^* = 5.84$ Å, $\varepsilon/k = 509$ K) and the LJ corrected parameters AlCl_3 ($r^* = 2.76$ Å, $\varepsilon/k = 472$ K)</p> <p>Figure 8. Geometrical representation of CH_2O</p> <p>Figure 9. Correlation between molecular volume and A) r^*_{SCS} for 95 species and B) $\sigma \times 2^{1/6}$ for 195 species. The linear correlation in A is replotted in B and labeled as Eq. (5).</p> <p>Figure 10. Plot of poor correlation between LJ potential well depths and the electron density for 215 molecules. The monatomic species are shown as open circles.</p> <p>Figure 11. Formyl fluoride, CHFO, 298 K and 3000 K isentrope predictions using the ideal gas EOS, the BKWS-EOS, and the JCZS-EOS. Parameters for the JCZS-EOS were chosen to be $r^* = 4.50$ Å and $\varepsilon/k = 150$ K using Eq. (5) for r^* and fitting ε/k to match the high pressure 298 K isentrope.</p> <p>Figure 12. Carbon subnitride, C_4N_2, 298 K isentrope predictions using the ideal gas EOS, BKWS-EOS, and the JCZ3-EOS. The JCZ prediction labeled “Fit” uses r^* from Eq. (12) and the prediction labeled “Special Fit” used r^* to best fit the BKWS isentrope.</p> <p>Figure 13. Comparison of measured (symbols) liquid shock Hugoniot to predicted liquid shock Hugoniot (lines) using the BKWS-EOS, BKWC-EOS, and JCZS-EOS for H_2O and H_2.</p> <p>Figure 14. Comparison of measured (symbols) liquid shock Hugoniot to predicted liquid shock Hugoniot (lines) using the BKWS-EOS, BKWC-EOS, and JCZS-EOS for A) CH_3OH, B) CH_4, and C) CO_2.</p>	<p>10</p> <p>11</p> <p>11</p> <p>13</p> <p>13</p> <p>13</p> <p>13</p> <p>14</p> <p>14</p> <p>15</p> <p>17</p> <p>17</p> <p>19</p> <p>20</p>
---	---

Figure 15. Comparison of measured (symbols) liquid shock Hugoniot to predicted liquid shock Hugoniot (lines) using the BKWS-EOS, BKWC-EOS, and JCZS-EOS for A) NH ₃ , B) N ₂ , and C) O ₂	21
Figure 16. Comparison of measured (symbols) liquid shock Hugoniot to predicted liquid shock Hugoniot (lines) using the BKWS-EOS, BKWC-EOS, and JCZS-EOS for A) Ar, B) CBr ₂ H ₂ , and C) Cl ₂ H ₂	22
Figure 17. CHEETAH interface with DAKOTA.	24
Figure 18. Comparison of measured (symbols) detonation velocity and pressure for PETN to predictions using the BKWS-EOS (dashed lines) and the JCZS-EOS (solid lines).	32
Figure 19. Predicted (lines) and measured (symbols) detonation velocities for high pressure gases.....	33

List of Tables

Table 1. EXP 6 parameters used with JCZ3-EOS to best match liquid shock Hugoniot data	18
Table 2. DAKOTA optimized r^* values for major C, H, N, O, Cl, and F species	23
Table 3. Measured and predicted detonation velocities and pressures	25
Table 4. RMS percent errors - optimization	26
Table 5. RMS percent errors - optimization	26
Table 6. Overall percent RMS errors for D, P, and T	27
Table 7. Measured and predicted detonation temperatures using CHEETAH 1.4.....	27
Table 8. Measured and predicted detonation velocities and pressure with %RMS errors ..	28
Table 9. Percent RMS errors for E, E _{2.2} , E _{4.1} , E _{6.5}	32
Table A.1 Species with known critical volumes.....	36
Table A.2 Species with known critical temperatures	37
Table A. 3 Species with known Lennard-Jones parameters.....	38
Table B.1 The complete JCZS database of r^* and ϵ/k values	39

(Intentionally left blank)

Executive Summary

1. Executive Summary

Determination of product species and associated equations-of-state (EOS) for energetic materials with complex elemental compositions remains a major unsolved problem. A simple EOS model is needed to predict thermochemical behavior of product species for conditions ranging from high pressure detonation states to low pressure ideal conditions. Such an EOS model should be based on physical arguments, rather than excessive curve fittings to a limited set of specific conditions. The Jacobs-Cowperthwaite-Zwisler-3 EOS¹ (JCZ3-EOS) uses exponential 6 (EXP 6) intermolecular potentials to describe the P-V-T relationship of the gaseous product species resulting from detonation of energetic materials.

The primary disadvantage of using the JCZ3-EOS for equilibrium calculations of energetic materials is that only 20 species have known JCZ3 molecular potential force constants. Realistic thermochemical equilibrium calculations require an EOS with a large species database to encompass all possible product species in a detonation event. In this work, a new database for use with the JCZ3-EOS has been developed. This new database will be referred to as the JCZS (where the S refers to Sandia) EOS database. A methodology has been established to increase the size of the JCZS database to approximately 750 species. Among these species are all the gases in the JANNAF² database. For each species, force constants are obtained to parameterize an EXP 6 potential function. One technique of obtaining these constants relates Lennard-Jones (LJ) potential function parameters to the EXP 6 potential function parameters. Another technique uses a simple corresponding states (SCS) theory (SCS) that relates the unknown molecular potential force constants of a molecule to the constants of a corresponding states molecule, argon, through use of critical properties. This method was used by Ross and Ree³ for simple molecules. The remaining constants are obtained in the present work from a series of correlation and estimation techniques that are presented later. In addition to these techniques, a few important species constants were obtained by matching liquid shock Hugoniot data.

Hugoniot calculations with the JCZS-EOS are shown to adequately replicate Hugoniot data for various molecules. Various detonation and cylinder expansion calculations using the JCZS-EOS also compare favorably to experimental data. The JCZS-EOS is shown to adequately predict high pressure states from 500 kbar to expansion states near atmospheric pressure.

2. JCZ3-EOS Background

The JCZ3-EOS uses an equation based on P-V-T relationships similar to the Mie-Grüneisen EOS:⁴

$$P = \frac{G(V, T)nRT}{V} + P_0(V) \quad (1)$$

where P , n , R , T , and V represent the pressure, number of moles, universal gas constant, and volume, respectively. The form of the Grüneisen function, G , and the volume dependent internal pressure function, P_0 , is documented (e.g., Ref. 1). Both the internal pressure function, P_0 , and the Grüneisen function are composed of the EXP 6 potential function:

$$\phi(r) = \epsilon \left[\left(\frac{6}{\eta - 6} \right) \exp[\eta(1 - r/r^*)] - \left(\frac{\eta}{\eta - 6} \right) \left(\frac{r^*}{r} \right)^6 \right] \quad (2)$$

where ϵ is the well depth for the pair potential and r^* is the radius of the minimum pair potential energy. The molecular force parameters ϵ , η , and r^* are required for each product species. The force constant, ϵ , is often given as ϵ/k , where k is Boltzmann's constant. The explicit dependence of the Grüneisen function, G , and the internal pressure function, P_o , on the potential function, φ , is not obvious and the interested reader is referred to Ref. [1] for more information. Hobbs and Baer⁵ have shown that the investigators using $\eta = 13$ give the best agreement between measured and predicted pure liquid shock Hugoniots than other values of η . Therefore this study also assumes that η is 13 for all molecules, leaving r^* and ϵ/k to be determined for each molecule.

Figure 1 shows a plot of the repulsive and attractive energy terms in the EXP 6 potential function for Argon with $r^* = 3.85 \text{ \AA}$, $\epsilon/k = 122 \text{ K}$. Molecules attract each other when they are separated by distances greater than r^* . As the molecules come closer together than r^* , the molecules repel one another as modeled by the repulsive term.

3. Obtaining the Exponential 6 Potential Force Constants from Lennard-Jones Potential Parameters

Similar to the EXP 6 potential function, the Lennard-Jones (LJ) potential function describes the repulsion and attraction between spherical molecules as shown in Fig. 2 with characteristic diameter, σ , set equal to 3.43 \AA , and the well depth, ϵ/k , being set to 122 K . The value of the two potential func-

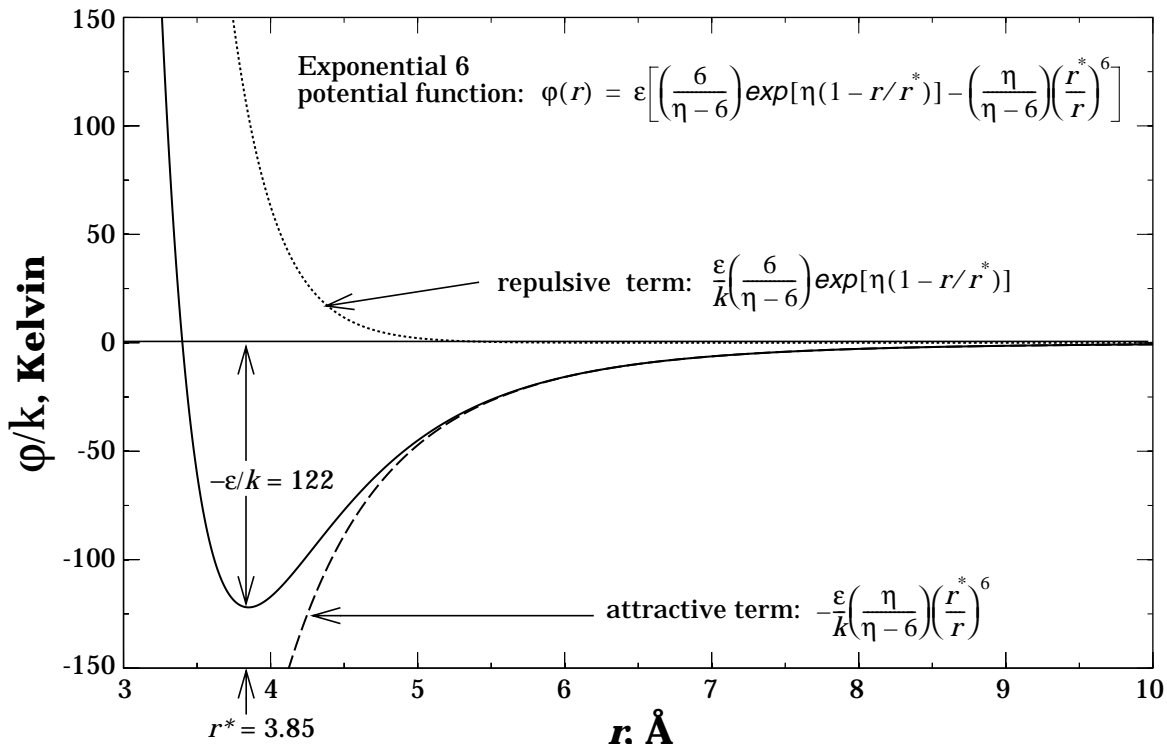


Fig. 1. Plot of the normalized EXP 6 potential function for Argon (solid line) with an r^* and ϵ/k of 3.85 \AA and 122 K , respectively. The repulsive (dotted line) and attractive (dashed line) terms are also shown.

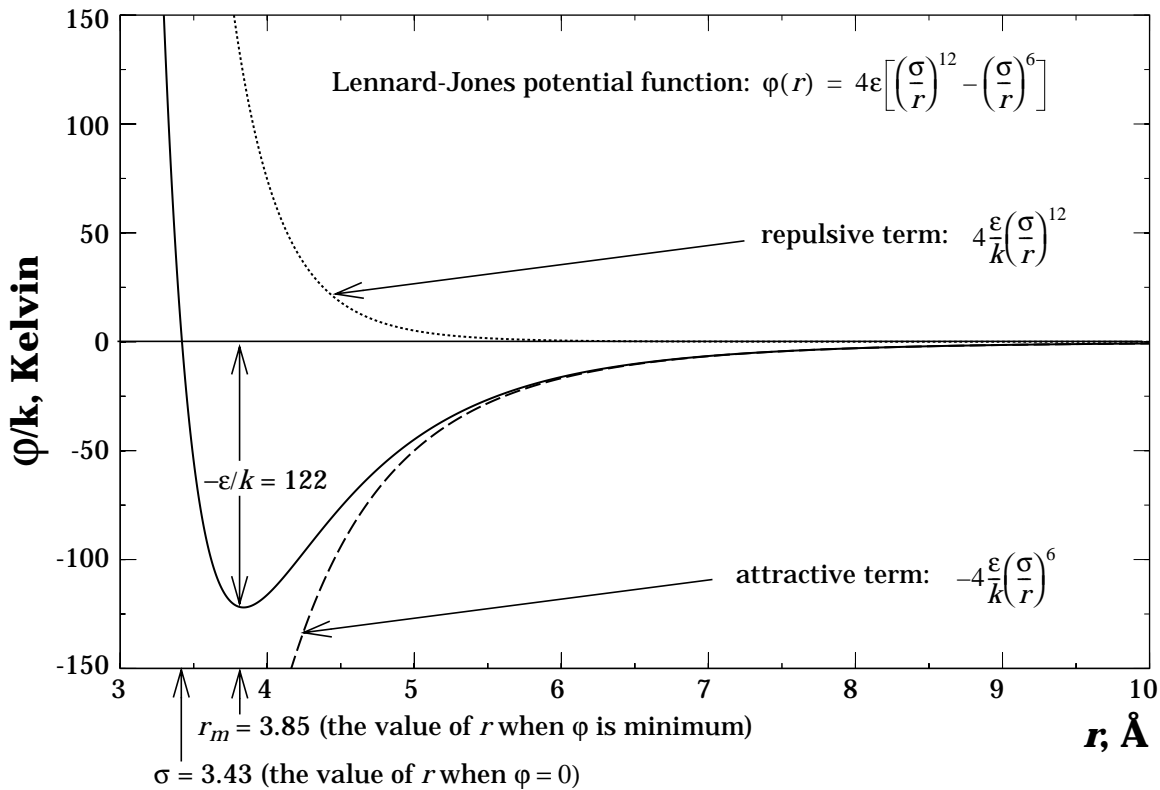


Fig. 2. Plot of the normalized LJ potential function for Argon (solid line) with an σ and ϵ/k of 3.43 Å and 122 K, respectively. The repulsive (dotted line) and attractive (dashed line) terms are also shown.

tions in Fig. 1 and 2 using the EXP 6 function and the LJ function are essentially identical. The primary difference between the two function is the location of the characteristic diameter depicted as r^* for the EXP 6 function and σ for the LJ function.

The LJ characteristic diameter, σ , is related to r^* of the EXP 6 potential function by:⁶ $\sigma/r^* = 0.8909$ or $r^* = \sigma \times 2^{1/6}$. The constant $2^{1/6}$ was determined by finding the minimum of the LJ potential function. As shown in Fig. 2, σ is the value of r when $\phi = 0$. But, r^* in the EXP 6 potential function is at the bottom of the potential well when ϕ is minimum. By taking the derivative of the LJ potential function, r_m , the value of r at the bottom of the potential well, can be determined. This value, r_m , is equivalent to the EXP 6 force constant r^* . Figure 3 demonstrates the method of obtaining EXP6 parameters from LJ parameters for AlCl₃. The

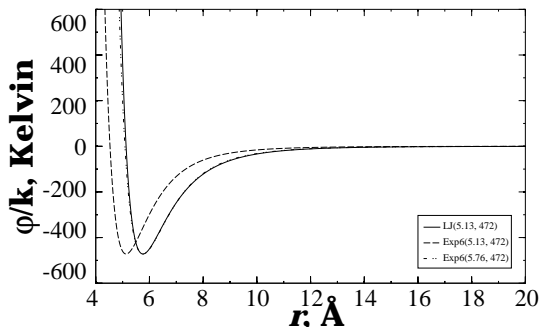


Fig. 3. Plot of the LJ potential function for AlCl₃ (solid line). The EXP 6 potential functions are plotted with the LJ characteristic diameter (dashed) and the corrected characteristic diameter (dash dotted).

Estimating the Exponential 6 Potential Force Constants from Critical Properties

solid curve represents the LJ potential function with the accepted experimental values of $\sigma = 5.13$, $\varepsilon/k = 472$. The dashed curve represents the EXP 6 potential function with the LJ force parameters used directly. The dashed curve is shifted to the left of the LJ potential function. The dash-dotted curve represents the EXP 6 potential using the adjusted LJ parameters ($r^* = 5.76 = \sigma \times 2^{1/6}$) while retaining the value of $\varepsilon/k = 472$. The dash-dotted curve is an acceptable fit to the original LJ potential function curve.

Of the 750 species listed in the JANNAF² tables, 200 have LJ parameters. References for LJ values used in this study are listed in Appendix A in Table A.3. EXP 6 parameters obtained from LJ data are assumed to be the most accurate since experimental data were used in obtaining most of these values.

4. Estimating the Exponential 6 Potential Force Constants from Critical Properties

At the beginning of this study, JCZS-EOS force constants were initially determined by the following four parameter corresponding states (4PCS) equation set:⁵

$$\frac{r^*}{V_c^{1/3}} = \underbrace{\frac{I_{ar}^*}{V_{c, ar}^{1/3}}}_{\text{Corresponding States}} + \underbrace{\frac{\alpha}{\alpha_{hx}} \left(\frac{I_{hx}^*}{V_{c, hx}^{1/3}} - \frac{I_{ar}^*}{V_{c, ar}^{1/3}} \right)}_{\text{Shape Corrections}} + \underbrace{\beta_{h2o} \left\{ \frac{I_{hx}^*}{V_{c, hx}^{1/3}} - \left[\frac{I_{ar}^*}{V_{c, ar}^{1/3}} + \frac{\alpha_{h2o}}{\alpha_{hx}} \left(\frac{I_{hx}^*}{V_{c, hx}^{1/3}} - \frac{I_{ar}^*}{V_{c, ar}^{1/3}} \right) \right] \right\}}_{\text{Polar Corrections}} \quad (3)$$

$$\frac{\varepsilon/k}{T_c} = \frac{\varepsilon_{ar}/k}{T_{c, ar}} + \frac{\alpha}{\alpha_{hx}} \left(\frac{\varepsilon_{hx}/k}{T_{c, hx}} - \frac{\varepsilon_{ar}/k}{T_{c, ar}} \right) + \frac{\beta}{\beta_{h2o}} \left\{ \frac{\varepsilon_{hx}/k}{T_{c, hx}} - \left[\frac{\varepsilon_{ar}/k}{T_{c, ar}} + \frac{\alpha_{h2o}}{\alpha_{hx}} \left(\frac{\varepsilon_{hx}/k}{T_{c, hx}} - \frac{\varepsilon_{ar}/k}{T_{c, ar}} \right) \right] \right\} \quad (4)$$

The first term of Eq. (3) and (4) represent the simple corresponding states (SCS) law used by Ross and Ree³ to determine force constants as proposed originally by Hirschfelder et al.⁷ The second and third terms of each equation represent shape and polar corrections obtained by the ELK method.⁸⁻⁹ The values r^* and ε/k were calculated using the critical temperature, critical volume, α and β values. α was calculated from the acentricity factor, β was calculated from polarity, and β_h was calculated from the heat of vaporization. Pure shock Hugoniot calculations with the JCZ3-EOS, using potential parameters determined with the SCS method yielded comparable results to JCZ3 Hugoniot estimates using parameters determined with the 4PCS method. The shape and polar corrections in Eq. (3) and (4) may not be necessary for Hugoniot calculations using the JCZ3-EOS.

The EXP 6 potential function implicitly assumes that molecules are both spherical and nonpolar. Including shape and polar effects are typically addressed by adding terms to the potential function, rather than changing r^* and ε/k , as in the 4PCS method. Figures 4 show that shape and polar corrections do not significantly influence r^* . Figure 4 shows a plot of r^*_{SCS} versus r^*_{4P} . The subscripts *SCS* and *4PCS* denote that r^* was calculating using the SCS technique and the 4PCS technique, respectively. Figure 4 shows that the difference between the two methods is minimal. In the present work, the SCS technique, without the shape or polar correction, is used to estimate r^* and ε/k .

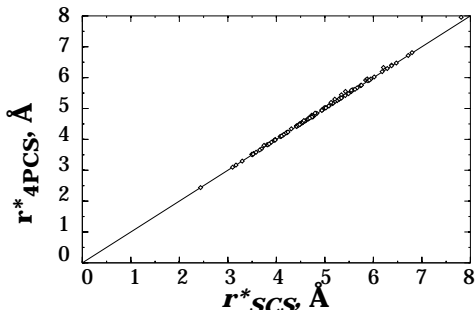


Fig. 4. Plot of the r^*_{SCS} versus r^*_{4PCS} , for 103 different molecules.

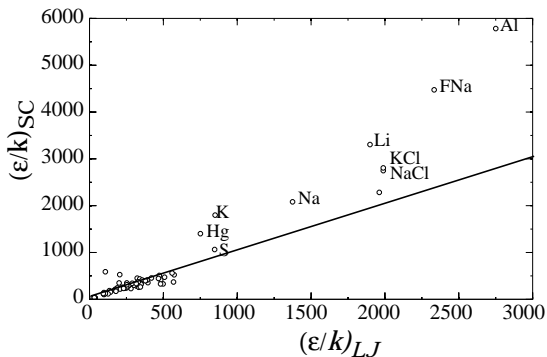


Fig. 6. Plot of $(\epsilon/k)_{SC}$ versus $(\epsilon/k)_{LJ}$.

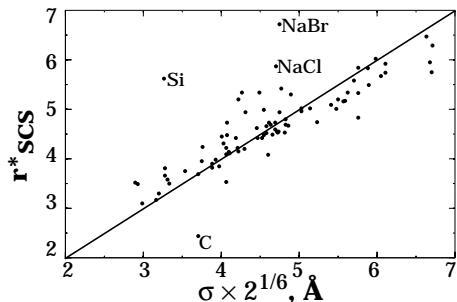


Fig. 5. Plot of r^*_{SCS} versus $\sigma \times 2^{1/6}$.

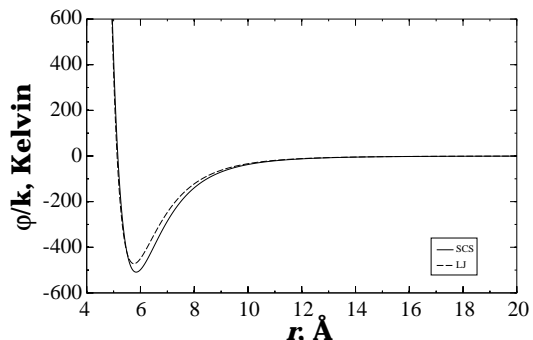


Fig. 7. Plot of the EXP 6 potential for AlCl_3 using the SCS method ($r^* = 5.84$, $\epsilon/k = 509$) and the LJ method ($r^* = \sigma \times 2^{1/6} = 5.13 \times 2^{1/6} = 2.76$, $\epsilon/k = 472$).

Figure 5 shows the agreement between the corrected LJ characteristic diameter as discussed in Section 3, $\sigma \times 2^{1/6}$, and r^*_{SCS} . The correlation is especially good for covalently bonded species. The species with poor correlation are either monatomic species or ionically bonded species. Table A.1 in Appendix A gives the literature reference to each critical volume found. Table A.2 in Appendix A gives the references for each critical temperature. Figure 6 shows a plots of $(\epsilon/k)_{LJ}$ versus $(\epsilon/k)_{SCS}$. Good correlation exists between the SCS technique and the experimentally determined values of ϵ/k . Large deviations exist for monatomic species and ionically bonded molecules as shown in Fig. 6.

Figure 7 shows the EXP 6 function for a typical molecule in the JANNAF database, AlCl_3 , determined using the SCS method and the LJ method. Both methods give similar predictions of the intermolecular potential. Unfortunately, not all chemical species have critical properties. Critical properties of unstable species are rare, and for free radical species, non-existent. For heavy metals and many ionic compounds, reported values are typically calculated with questionable accuracy. Out of the database of 750 species, 150 species have both the critical temperature and critical volume. Of these 150 species, 93 also have LJ parameters. Thus, the EXP 6 parameters for approximately 250 out of 750 JANNAF species can be obtained using either the SCS technique or can be estimated with known LJ constants.

5. Estimating the Exponential 6 Potential Force Constants through Correlation and Curve Fitting

This section describes the method used to obtain the remaining EXP 6 potential parameters for species without critical properties or LJ parameters. Some judgement was also required to determine whether these values could be used in the JCZS database. The methodology of achieving the values of the near 500 remaining species plus those uncertain cases is explained in Sections 5.1 and 5.2. The methods used to select the JCZS parameters, when more than one value exists, are discussed in Section 5.3.

5.1 Determining r^*

The BKWS study¹⁰ required the calculation of molecular volume of each species to estimate covolumes. Molecular volume is calculated from known and predicted van der Waals radii. Figure 8 shows a geometrical representation of CH₂O. When calculating the molecular volume of a species such as CH₂O, the volume of each atom is assumed to be represented by a sphere with the radius equal to van der Waals radius. When atoms overlap in a molecule, the volume is only represented once. Therefore the molecular volume is the same as the volume of a space-filling model with the appropriate units.

A strong correlation exists between the actual volume of a gas molecule calculated using van der Waals radii and the radius of the minimum pair potential energy, r^* . Figure 9.A shows the correlation between r^*_{SCS} and molecular volume to the third power for 93 species calculated with known critical volumes.

Most of the species that stray farthest from the linear correlation in Figure 9.A are monatomic. Because almost all of these have LJ potential parameters for use in the EXP 6 potential function anyway, the monatomic species were eliminated from the least squares fit to obtain an improved correlation. The least squared linear correlation of the polyatomic species in Fig. 9.A can be used to estimate r^* from molecular volumes:

$$r^* = 1.19(\text{Molecular Volume})^{(1/3)} + 0.68 \quad (5)$$



Fig. 8. Geometrical representation of CH₂O

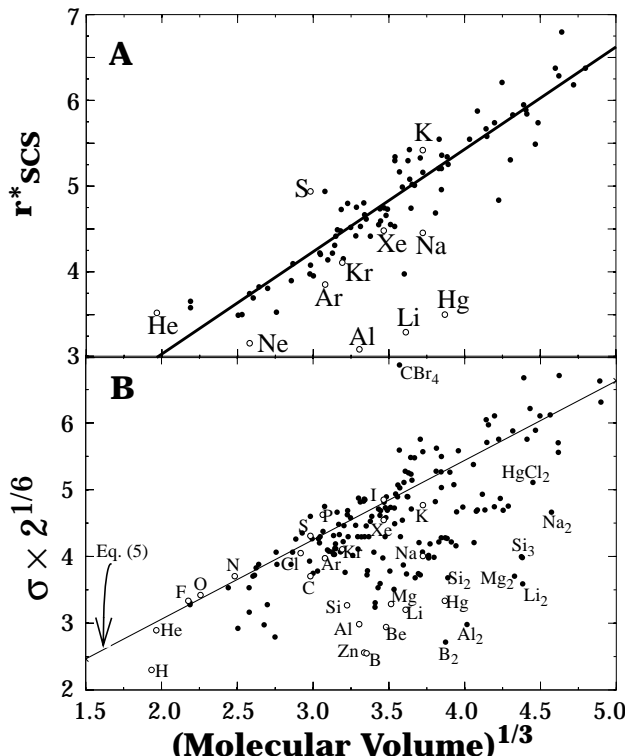


Fig. 9. Correlation between molecular volume and A) r^*_{SCS} for 95 species and B) $\sigma \times 2^{1/6}$ for 195 species. The linear correlation in A is replotted in B and labeled as Eq. (5).

As shown previously in Fig. 5, the corrected LJ characteristic diameter, $\sigma \times 2^{1/6}$, correlated adequately with r^* calculated using SCS theory. Thus, the $\sigma \times 2^{1/6}$ should also be correlated to (Molecular Volume) $^{1/3}$ as shown in Fig. 9.B. Again, most of the scatter in Fig. 9.B is attributed to monatomic species.

5.2 Determining ε/k

A similar correlation for ε/k with molecular volume was sought. Electron density can be calculated readily from the molecular volume and was initially thought to be correlated to the potential well depth. Unfortunately, Fig. 10 there is a poor relationship between the 215 LJ potential well depths, ε/k , and the electron density represented as the number of electrons, Z , divided by the molecular volume as shown in Fig. 10. References for the LJ potential well depths can be found in Appendix A Table A.3. The potential well depths determined with corresponding states methods are also poorly correlated with electron density. Unfortunately, an adequate correlation of ε/k was not found in this study. An alternative method for determining ε/k was developed. This method involves choosing r^* based on Eq. (5) and determining ε/k by matching high pressure, pure species, isentropes calculated with the BKWS-EOS which is described subsequently.

5.2.1 The BKW-EOS

The Becker-Kistiakowsky-Wilson equation-of-state (BKW-EOS) is used extensively to calculate detonation properties. Hobbs and Baer¹⁰ give the historical background and molecular covolumes for the BKW-EOS:

$$\frac{PV}{RT} = 1 + X e^{\beta X} \quad \text{with} \quad X = \frac{\kappa \sum n_i k_i}{V(T + \theta)^\alpha} \quad (6)$$

where P , V , R , T , and n_i represent pressure, molar gas volume, gas constant, absolute temperature, and mole fraction of the i^{th} gaseous component, respectively. The summation extends over all components of the gaseous mixture. The covolume factors, k_i , representing excluded volume, are discussed subsequently. The parameters α , β , κ , and θ are empirical constants. The quantity θ was added to the equation to prevent P from approaching infinity as T approaches zero.¹¹ Typically, the parameters α , β , κ , θ , and k_i are *adjusted to fit measured detonation properties*. Three different parameterizations of the BKW-EOS are in use: BKWC,¹² BKWR,¹³ and BKWS.¹⁰ The C, R, and S represent CHEETAH reparameterization, Finger et al.¹³ Reparameterization, and Sandia reparameterization, respectively. The BKWS parameterization with covolumes based on physical arguments should give better predictions of detonation properties than the empirical BKW parameterizations (BKWC and BKWR) with covolumes used as fitting parameters.

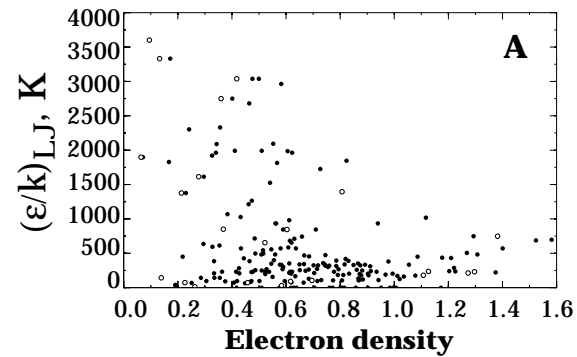


Fig. 10. Plot of poor correlation between LJ potential well depths, ε/k , and the electron density for 215 molecules. The monatomic species are shown as open circles.

5.2.2 The BKWR Parameterization

Parameters optimized in the BKWR-EOS included three BKW constants (β , κ , and θ) and 10 covolumes. The constants were calibrated using 10 measured detonation velocities (D), 10 measured detonation pressures (P), and 4 measured detonation temperatures (T). The BKWR-EOS produces adequate detonation velocities and pressures. However, the predicted detonation temperatures are about a thousand degrees too low and the energies of detonation are uniformly about 10% too high.¹⁴ To correct for these deficiencies, BKWR energies are corrected by normalizing with 1.62 g/cc PETN as a standard. The BKWR-EOS (13 gas and 1 condensed species) is only applicable to energetic materials consisting of C, H, N, O, and F. Thus the BKWR-EOS is inadequate to determine all the parameters for the JCZS-EOS with 750 species containing a variety of elements.

5.2.3 The BKWS-EOS Parameterization

Parameters optimized in the BKWS-EOS only include the three BKW constants (β , κ , and θ). Unlike the BKWR-EOS and BKWC-EOS, covolumes used in the BKWS-EOS were assumed to be invariant and based on the molecular structure of the product species. Covolumes were obtained using measured van der Waal radii, bond lengths, and bond angles. The three BKW constants were calibrated using a density weighted cost function comprised of 103 detonation velocities, 64 detonation pressures, and 14 detonation temperature measurements. The BKWS-EOS predicts higher detonation temperatures leading to lower detonation energies allowing calculated energies of detonation to be used without correction. Since covolumes are not used as adjustable constants, the BKWS-EOS can be applied to a large number of product species. Currently the BKWS library considers approximately 750 gaseous products and 400 condensed reaction products found in the JANNAF tables² and can be used to parameterize ε/k for the JCZS-EOS.

A thermal-elastic EOS¹⁵ was used for condensed reaction products. However, thermal expansion and compressibility data were not available for all 400 condensed species. In the BKWS database, most condensed phase species were assumed to be incompressible, although temperature and pressure dependent compressibility can be easily added when such information becomes available. Condensed Al, AlN, Al₂O₃, Al₄C₃, C and H₂O were included as compressible species.

5.2.4 The BKWC Parameterization

The success of the BKWS-EOS prompted Fried et al.¹² to optimize the BKW parameters again, including covolumes, freeze-out temperature, and condensed phase compressibility constants using a smaller product species database (23 gaseous products and 2 condensed products) determined from major species predicted using the BKWS-EOS. Parameters optimized in the BKWC-EOS include four BKW constants (a , β , κ , and θ), the freezing temperature used in cylinder expansion (T_f), three parameters in the condensed-phase carbon EOS (V_o , a , and b), and 23 covolumes. The 31 BKW constants were calibrated using an estimated error weighted cost function comprised of 32, 30, and 132 D, P, and expansion energies, respectively. With the large number of adjustable parameters, the BKWC-EOS was used to improve the prediction of detonation velocity and pressure over BKWS by about 1% for energetic materials composed of C, H, N, and O. However, improvement in detonation property prediction is not justified when experimental variability (5-10%) is considered. Also, the BKWC optimization was not constrained to consider measured properties such as H and O van der Waal radii. The optimized covolume of H₂ became larger than H₂O in the BKWC-EOS which is physically impossible. Significant errors are shown in Section 6 when the BKWC-EOS is used to predict shock Hugoniot data. Furthermore, with only a small set of product species, the BKWC-EOS cannot be used to parameterize the JCZS-EOS with 750 gaseous species.

5.2.5 Using the BKWS-EOS to Determine ε/k

Because the BKWS database provides acceptable results for high pressure detonation states and the ideal gas law provides accurate results for low pressure states, ε/k can be estimated by matching isentropes at high pressure and low pressure states using the calculated r^* from molecular volume data. In this study, the standard temperature and pressure (298 K and 1 atm) isentrope was chosen for fitting ε/k . Figure 11 shows the 298 K and 3,000 K isentrope for Formyl fluoride. Parameters for the JCZS-EOS were chosen to be $r^* = 4.50 \text{ \AA}$ and $\varepsilon/k = 150 \text{ K}$ using Eq. (5) for r^* and fitting ε/k to match the high pressure 298 K isentrope. The agreement between the JCZS-EOS and BKWS-EOS at high pressure for the 3,000 K isentrope in Fig. 11 indicates that fitting the 298 K isentrope is sufficient to match isentropes at significantly different conditions.

Not all values of r^* predicted with Eq. (5) were adequate to match the BKWS isentropes. For such species, r^* was adjusted to match the BKWS isentrope as shown in Fig. 12 for carbon subnitride, C_4N_2 . For such cases, Eq. (5) is used as an initial estimate of r^* and both r^* and ε/k are fit to the BKWS isentrope. The force parameters for these “specially fit” molecules are not unique and various combinations of parameters will give an adequate match to the BKWS isentrope.

As shown in Figures 11 and 12, the JCZS isentrope deviates from the BKWS isentrope at intermediate pressures. The JCZS isentropes matches the BKWS isentrope at high pressures. At intermediate pressures, the JCZS isentrope approaches the ideal gas isentrope whereas the BKWS isentrope remains at higher values. At low pressures, all three isentropes converge. As shown in the evaluation section, the JCZS-EOS model gives better predictions in this intermediate pressure regime giving better predictions of low density explosives and expansion states than the BKW-EOS. The intermediate pressure regimes in Fig. 11 and 12 show characteristics of the potential well described by the EXP 6 potential function.

Caution must be used when using the JCZS-EOS for molecules with ε/k estimated from BKWS predictions. The parameters for these molecules are only as good as the BKWS predictions. Because the BKWS-EOS was calibrated at high pressures with explosives composed primarily of C, H, N, O, F, and Cl, species with substantially different atomic compositions may be in error. One method to determine the accuracy of the BKWS and JCZS predictions would be to compare Hugoniot predictions to pure liquid shock Hugoniot data as discussed further in Section 6.

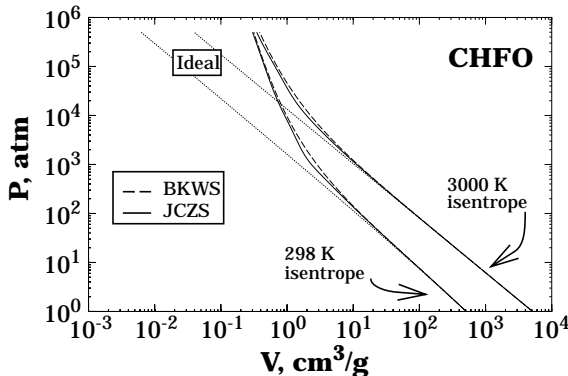


Fig. 11. Formyl fluoride, CHFO, 298 K and 3000 K isentrope predictions using the ideal gas EOS, BKWS-EOS, and the JCZS-EOS. Parameters for the JCZS-EOS were chosen to be $r^* = 4.50 \text{ \AA}$ and $\varepsilon/k = 150 \text{ K}$ using Eq. (5) for r^* and fitting ε/k to match the high pressure 298 K isentrope.

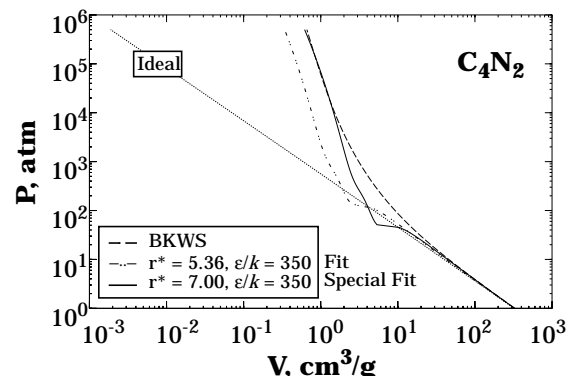


Fig. 12. Carbon subnitride, C_4N_2 , 298 K isentrope predictions using the ideal gas EOS, BKWS-EOS, and the JCZS-EOS. The JCZ prediction labeled “Fit” uses r^* from Eq. (5) and the prediction labeled “Special Fit” used r^* to best fit the BKWS isentrope.

6. Pure Liquid Shock Hugoniot Data

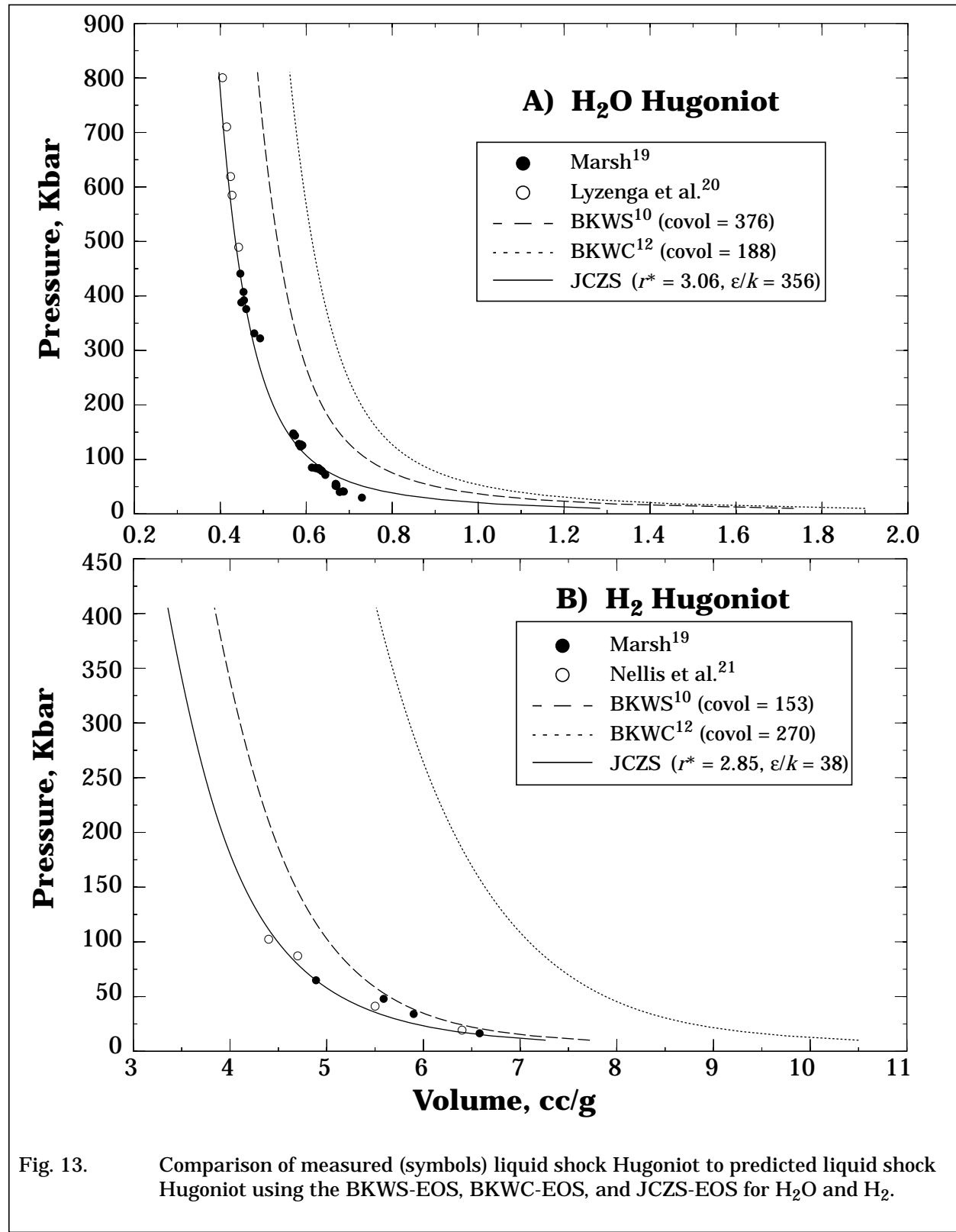
The accuracy of an EOS can be tested by comparing predictions to data of pure liquid shock Hugoniots. Some caution must be used when using pure liquid shock Hugoniot data since the species may break into smaller fragments at elevated temperatures and pressures. Sheffield¹⁷ suggests that if the Hugoniot deviates from the “universal” liquid Hugoniot¹⁸ the species is likely breaking into smaller fragments. Figures 13 through 16 show a comparison between liquid shock Hugoniot data and predicted liquid shock Hugoniot using the BKWS-EOS, BKWC-EOS, and the JCZ-EOS for water, hydrogen, methanol, methane, carbon dioxide, ammonia, nitrogen, oxygen, carbon tetrachloride, and trichloromethane, respectively. The source of the EXP 6 parameters is given in Table 1. Three of the JCZS parameters were obtained by the SCS method (CH_4 , N_2 , and O_2), three parameters were obtained by the LJ method (CO_2 , NH_3 , and CHCl_3), one parameter set was obtained by the 4PCS method, two parameter sets were obtained from literature values (H_2O and Ar), one parameter set was obtained by slightly adjusting the LJ value of r^* (H_2), and one parameter set was obtained by a combination of the SCS and LJ methods (CH_3OH).

Table 1. EXP 6 parameters used with JCZ3-EOS to best match liquid shock Hugoniot data

Species	r^*	ε/k	Source for JCZS Hugoniot fit
H_2O	3.06	356	Ref. 16
H_2	2.85	38	r^* constrained so that $r^*_{\text{H}_2} < r^*_{\text{H}_2\text{O}}$, ε/k selected from Ref. 34
CH_3OH	4.23	482	r^* taken as the average of SCS and LJ, ε/k taken from LJ
CH_4	4.23	154	SCS values
CO_2	4.22	244	LJ values
NH_3	3.33	481	LJ values
N_2	4.00	102	SCS values
O_2	3.86	125	SCS values
Ar	3.85	122	Ref. 3 (Argon is used as the corresponding molecule for all SC molecules)
CCl_4	5.98	631	4PCS (Ref. 5) used instead of SCS because of the better fit
CHCl_3	6.05	340	LJ values

The JCZS-EOS adequately predicts liquid shock Hugoniot data as shown in Figures 13-16. The better results of the BKWS predictions compared to the BKWC predictions are likely due to the values of the covolumes. Finger et al.,¹³ Mader,¹¹ and Cowan and Fickett²⁹ report covolume factors calibrated with shock Hugoniot data for CO_2 , H_2O , N_2 , and O_2 as 670, 360, 380, and 325, respectively. The geometrical covolumes calculated by Hobbs and Baer³⁰ are 70.3, 39.9, 39.9, and 33.5, respectively. The covolume factors divided by the geometric covolume for these species are 9.53, 9.02, 9.52, and 9.70, respectively, giving an average value of 9.43. The covolumes reported in Figures 13-16, are the geometrical covolumes multiplied by 9.43; the BKWS covolume factors for CO_2 , H_2O , N_2 , and O_2 are 663, 376, 376, and 316. Even though the geometrical covolumes are similar to the values used in the

Pure Liquid Shock Hugoniot Data



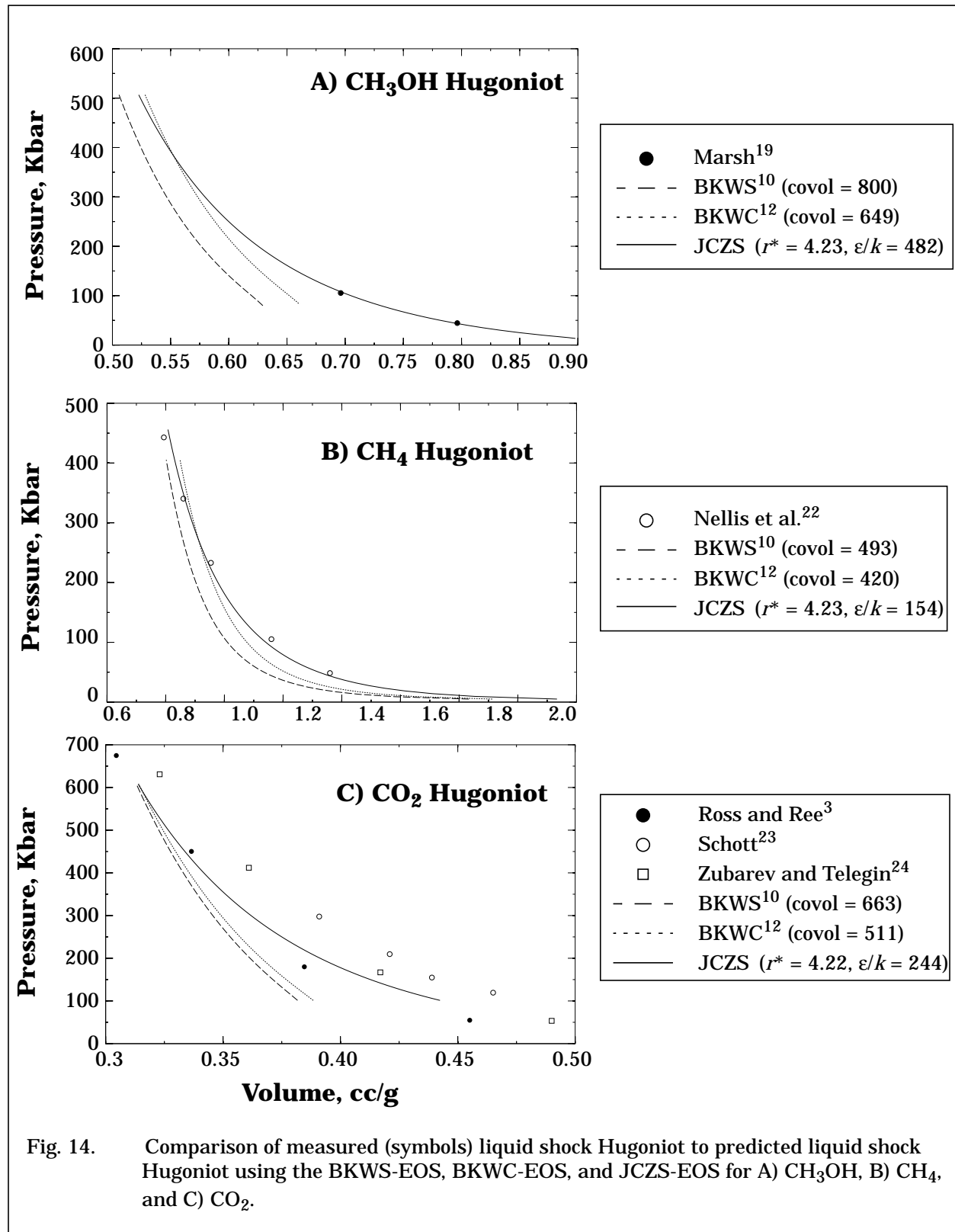
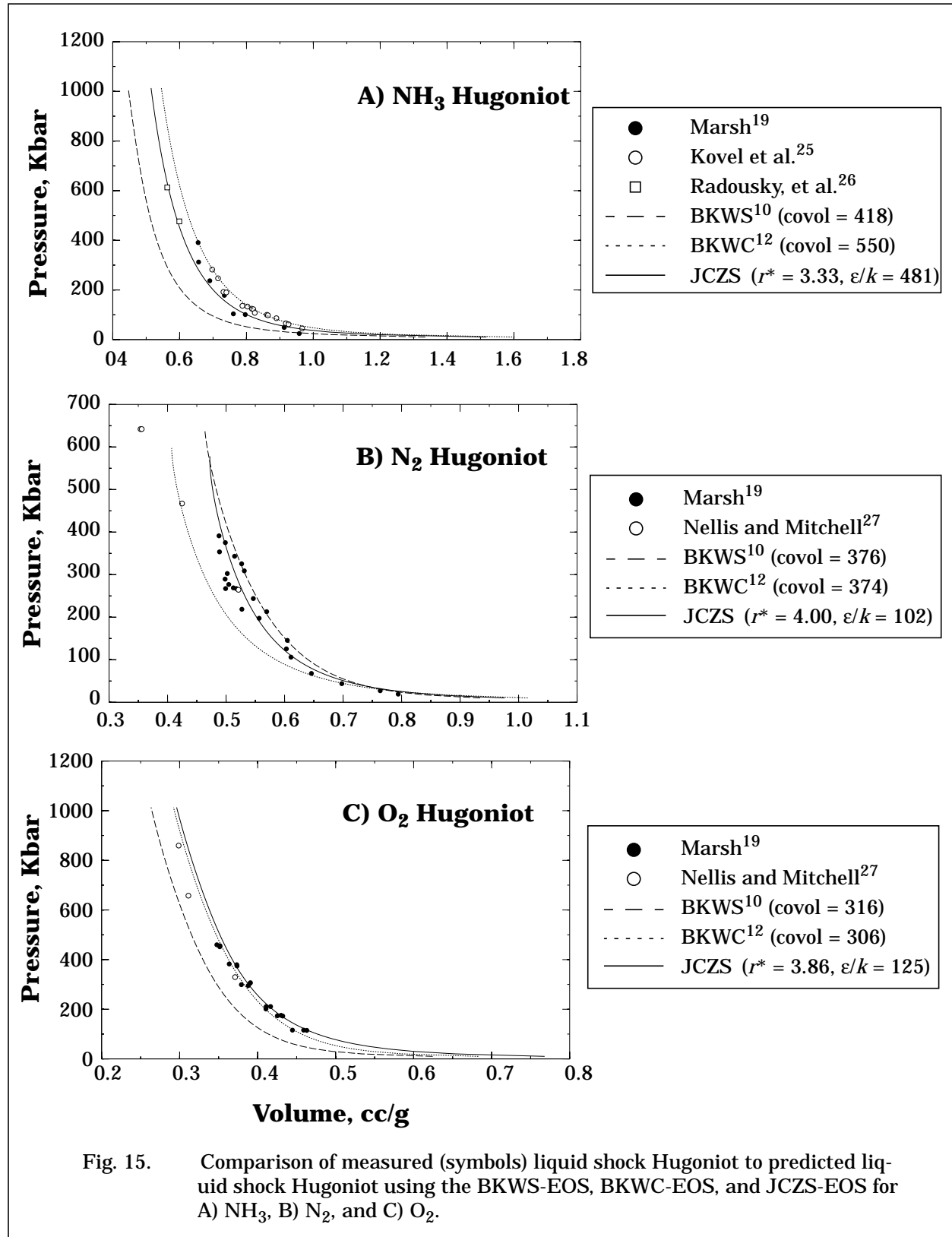


Fig. 14. Comparison of measured (symbols) liquid shock Hugoniot to predicted liquid shock Hugoniot using the BKWS-EOS, BKWC-EOS, and JCZS-EOS for A) CH_3OH , B) CH_4 , and C) CO_2 .

Pure Liquid Shock Hugoniot Data



Pure Liquid Shock Hugoniot Data

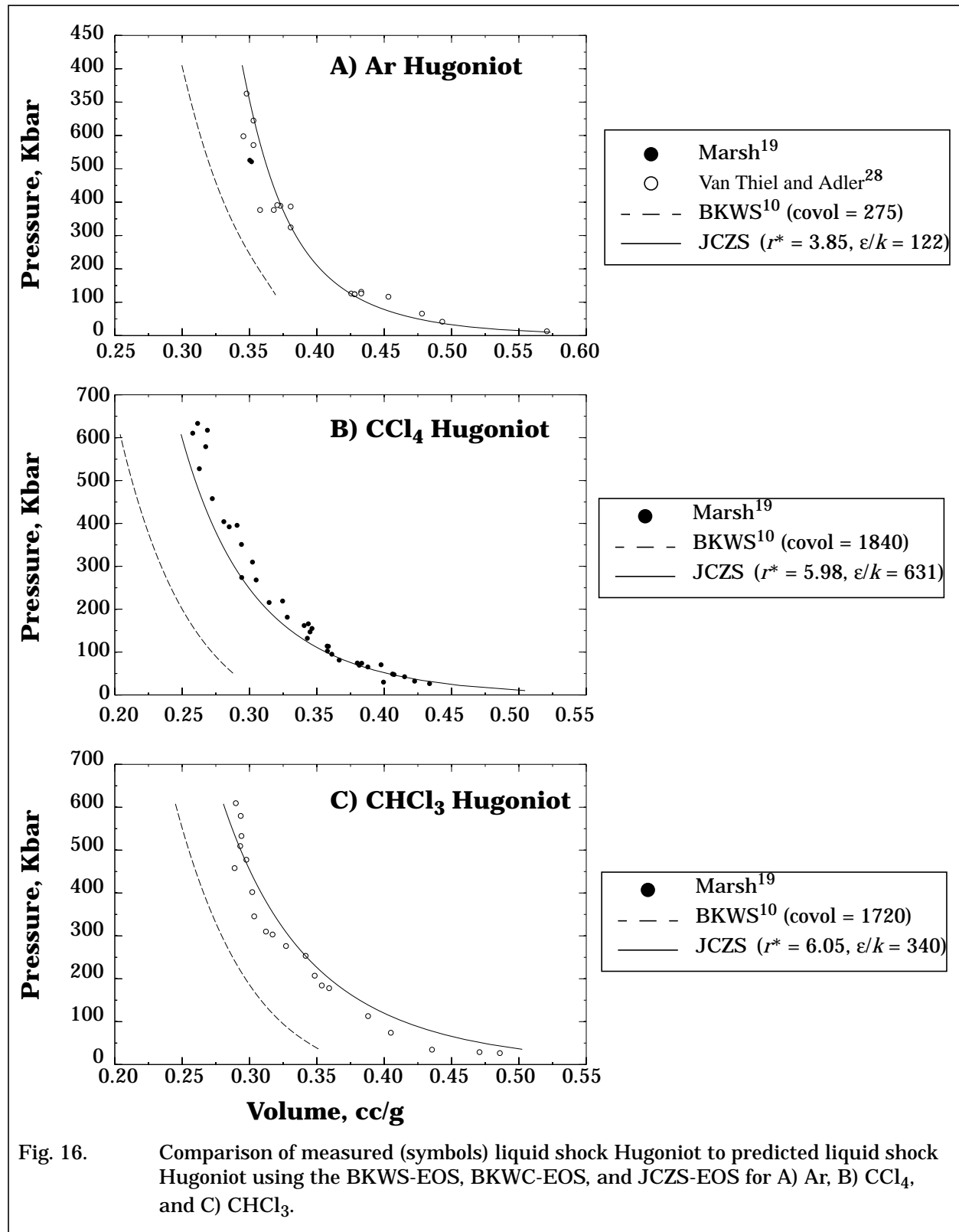


Fig. 16. Comparison of measured (symbols) liquid shock Hugoniot to predicted liquid shock Hugoniot using the BKWS-EOS, BKWC-EOS, and JCZS-EOS for A) Ar, B) CCl₄, and C) CHCl₃.

literature to predict Hugoniot data, the coefficients in the BKWS-EOS (β , κ , and θ) are different than the coefficients used in the literature and give slightly different results. Hugoniot calculations using the BKWC-EOS are not acceptable. The BKWC-EOS was developed by adjusting covolumes to match detonation states without regard to the physical significance of the covolume factors as discussed in Section 5.2.4. Although the BKWS covolumes were used as an initial estimate for the BKWC covolumes, the BKWC optimization was not constrained to consider measured properties such as H and O van der Waal radii. The optimized covolume of H_2 became larger than H_2O in the BKWC-EOS which is physically impossible. Such parameters lead to spurious results as shown in Fig. 13 for H_2O and H_2 . Caution must be used when using the BKWC-EOS.

7. DAKOTA Optimization

To avoid an unconstrained reparameterization of the JCZS-EOS, similar to the BKWC reparameterization of the BKWS-EOS, the JCZS parameters for major species were slightly adjusted using constrained optimization to obtain optimal agreement with detonation velocity measurements. The species chosen for this constrained optimization are listed in Table 2 with the initial values of r^* and the final optimized values of r^* . The initial r^* values are either from the LJ values (lj), isentrope fit values (fit), or the corresponding states values (cs). The source of the r^* values are labeled in the superscript of r^* initial. During the fitting process, r^* was found to be more sensitive than ε/k when fitting BKWS isentropes. The ε/k values were left as the original lj, fit, or cs values. The complete JCZS database is given in Appendix B.

Table 2. DAKOTA optimized r^* values for major C, H, N, O, Cl, and F species

Species	r^* initial	r^* opt.	Species	r^* initial	r^* opt.	Species	r^* initial	r^* opt.	Species	r^* initial	r^* opt.
CClF₃	5.16 ^{lj}	4.71	CH₂O	4.31 ^{cs}	4.40	CO	4.10 ^{lj}	3.88	H	2.30 ^{lj}	2.00
CClFO	5.07 ^{fit}	5.06	CH₂O₂	4.56 ^{fit}	4.46	CO₂	4.22 ^{lj}	4.22	H₂	3.28 ^{lj}	2.85
CF₂	4.08 ^{lj}	4.87	CH₃	4.27 ^{lj}	4.15	C₂F₃N	5.36 ^{cs}	5.83	H₂O	2.92 ^{lj}	3.06
CF₂O	4.75 ^{cs}	5.59	CH₃F	4.42 ^{cs}	4.93	C₂F₄	5.08 ^{cs}	6.03	H₃N	3.28 ^{lj}	3.33
CF₃	4.85 ^{lj}	5.65	CH₃OH	4.07 ^{lj}	4.23	C₂F₆	5.55 ^{cs}	7.36	HO	3.53 ^{lj}	3.29
CF₄	5.23 ^{lj}	6.40	CH₄	4.22 ^{cs}	4.23	C₂H₄	4.46 ^{lj}	4.50	N₂	4.10 ^{cs}	4.00
CF₄O	4.86 ^{fit}	6.40	CHF₃	4.67 ^{cs}	5.71	C₂H₆	4.8/3 ^{lj}	4.01	N₂O	4.30 ^{lj}	5.18
CFO	4.51 ^{fit}	4.72	CHFO	4.50 ^{fit}	4.50	C₃O₂	4.72 ^{cs}	5.22	NO	3.92 ^{lj}	4.15
CH₂ClF	5.03 ^{lj}	4.86	CHNO	4.30 ^{lj}	4.80	CLH	3.95 ^{cs}	3.35	NO₂	3.98 ^{sc}	4.77
CH₂F₂	4.58 ^{lj}	4.36	CNO	4.30 ^{lj}	4.89	FH	3.53 ^{lj}	3.70	O₂	3.82 ^{sc}	3.86

DAKOTA Optimization

CHEETAH,¹² a C version of the FORTRAN equilibrium code TIGER,¹⁵ was chosen as the analysis code to solve the CJ detonation problem for the 32 explosives listed in Table 3. Formation enthalpies can be found in Ref. 12. Starting with the initial r^* values listed in Table 2, an objective function was minimized using DAKOTA³¹ (Design Analysis Kit for OpTimizAtion). The objective function was the root mean square error (rms) between calculated ($D_{i,c}$) and measured ($D_{i,m}$) detonation velocities

$$rms = \sqrt{\frac{1}{N} \sum_{i=1}^N \left(\frac{D_{i,m} - D_{i,c}}{D_{i,m}} \right)^2} \quad (7)$$

where the subscripts i , m , and c represent the i^{th} explosive in Table 3, measured, and calculated, respectively. N represents the number of detonation velocity measurements, 32. Figure 17 shows the conceptualized CHEETAH interface with the DAKOTA³¹ toolkit which utilizes object-oriented design to interface analysis codes to various optimization techniques. The input deck generator is based on an algebraic preprocessor, APREPRO.³² The error calculator is a FORTRAN code used to read CHEETAH output and compute the error function given in Eq. (7). The input generator and error calculator are controlled by a C-shell script.

Table 4 shows the overall percent RMS error for predicted detonation velocity and detonation pressure for the explosives listed in Table 2 for the BKWS-EOS, BKWC-EOS, JCZS-40 EOS, and JCZS-132 EOS. The predictions were made using CHEETAH 1.40. During the course of this study, CHEETAH 2.0 was released. Predictions made using CHEETAH 2.0 are given in Table 5. The format of the libraries and formula cards were changed in CHEETAH 2.0. The discrepancy in Tables 4 and 5 are probably related to roundoff error in translating heats of formation for products and reactants to SI units. The JCZS-40 database only considered the 40 species listed in Table 2 for the detonation calculations. The JCZS-132 predictions considered all 132 species in the JANNAF tables composed of species containing C, H, N, O, Cl, or F. Since the RMS percent errors for both the JCZS-40 and JCZS-132 are similar, the JCZS-40 database is probably sufficient for energetic materials composed of C, H, N, O, Cl, or F. The CHEETAH input deck, DAKOTA input deck, C-shell script, and FORTRAN rms error program are given in Appendix C for reference.

Table 4 also shows the overall percent RMS error for predicted detonation velocities and detonation pressure for the explosives listed in Table 2 excluding the nonideal explosives HNB and TATB containing explosives (HNB, TATB, RX26, and LX17). These nonideal explosives may not reach complete equilibrium and probably should not be considered in the RMS percent error calculation. A more complete set of explosives will be used for validation of the JCZS-EOS in Section 8.

The 31 BKWC constants were optimized as discussed in Section 5.2.4 using the detonation velocities, detonation pressures, and expansion energies for the explosives shown in Table 3. Only detonation velocities were used in the DAKOTA optimization. Detonation velocities are thought to be the most accurate performance measurement provided a steady velocity has been reached. Detonation pressures, P_{cj} , are directly related to the detonation velocity D :

$$P_{cj} = \rho_0 D u \quad (8)$$

where ρ_0 and u represent the initial density and particle velocity, respectively. The detonation pressures are typically inferred from the detonation velocity and particle velocity. Since the JCZS-EOS predicts accurate detonation velocities, detonation pressure predictions are likely adequate.

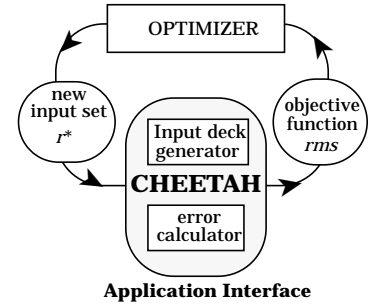


Fig. 17. CHEETAH interface with DAKOTA.

DAKOTA Optimization

Table 3. Measured¹² and predicted detonation velocities and pressures*

Explosive and density, g/cm ³	D _m , km/s	P _m , kbar	D _{BKWS} , km/s	D _{BKWC} , km/s	D _{JCZS-small} , km/s	D _{JCZS-large} , km/s	P _{BKWS} , kbar	P _{JCZS-small} , kbar	P _{JCZS-large} , kbar
btf, 1.85	8.49	340.	8.12 (4.32)	8.57 (0.94)	8.57 (0.92)	8.55 (0.73)	307. (9.77)	327. (3.94)	327. (3.93)
hm_x, 1.89	9.10	405.	9.35 (2.74)	9.24 (1.58)	9.11 (0.15)	9.11 (0.09)	374. (7.64)	399. (1.52)	399. (1.55)
hm_x, 1.18	6.67	155.	6.72 (0.68)	6.73 (0.90)	6.61 (0.91)	6.61 (0.92)	147. (5.28)	138. (11.04)	138. (11.03)
hnb, 1.97	9.34	430.	8.86 (5.14)	9.25 (0.87)	8.76 (6.14)	8.71 (6.74)	373. (13.28)	348. (18.99)	347. (19.33)
hns, 1.66	7.03	215.	7.08 (0.70)	7.00 (0.39)	7.07 (0.63)	7.07 (0.62)	203. (5.56)	204. (4.94)	204. (4.95)
hns, 1.40	6.34	160.	6.26 (1.30)	6.27 (1.12)	6.26 (1.27)	6.26 (1.27)	143. (10.42)	140. (12.40)	140. (12.41)
hns, 1.20	5.74	115.	5.73 (0.23)	5.71 (0.59)	5.69 (0.88)	5.69 (0.88)	109. (4.81)	103. (10.55)	103. (10.55)
hns, 1.00	5.10	73.	5.27 (3.39)	5.15 (1.00)	5.13 (0.66)	5.13 (0.65)	81. (11.38)	71. (2.16)	71. (2.17)
nm, 1.13	6.28	120.	6.59 (4.88)	6.03 (4.02)	6.17 (1.70)	6.17 (1.70)	130. (8.62)	115. (3.77)	115. (3.77)
petn, 1.76	8.27	310.	8.68 (4.86)	8.50 (2.74)	8.40 (1.52)	8.40 (1.46)	312. (0.71)	296. (4.52)	296. (4.52)
petn, 1.50	7.48	240.	7.66 (2.43)	7.64 (2.15)	7.36 (1.59)	7.36 (1.59)	223. (7.22)	202. (16.01)	202. (16.01)
petn, 1.26	6.59	160.	6.85 (3.98)	6.63 (0.61)	6.49 (1.57)	6.49 (1.56)	160. (0.17)	139. (12.84)	139. (12.82)
rx23, 1.42	8.64	258.	8.68 (0.48)	8.71 (0.82)	8.31 (3.82)	8.31 (3.82)	236. (8.69)	210. (18.44)	210. (18.44)
tatb, 1.83	7.58	260.	8.00 (5.48)	7.75 (2.18)	8.02 (5.75)	8.02 (5.75)	266. (2.19)	280. (7.88)	280. (7.87)
tnm, 1.65	6.45	155.	5.53 (14.32)	6.36 (1.42)	6.27 (2.72)	6.27 (2.72)	116. (25.19)	148. (4.42)	144. (7.37)
tnt, 1.63	7.07	205.	7.15 (1.12)	6.81 (3.63)	6.99 (1.10)	6.99 (1.10)	200. (2.30)	192. (6.10)	192. (6.11)
lx14, 1.83	8.80	370.	9.00 (2.22)	8.78 (0.22)	8.75 (0.55)	8.75 (0.57)	341. (7.96)	347. (6.15)	347. (6.16)
rx26, 1.84	8.24	340.	8.54 (3.67)	8.25 (0.07)	8.39 (1.87)	8.39 (1.86)	307. (9.59)	321. (5.71)	321. (5.71)
anfo, 0.80	4.70	---	5.14 (9.46)	4.56 (2.93)	4.71 (0.19)	4.71 (0.19)	56. (--)	47. (--)	47. (--)
qm100, 1.51	7.70	---	8.08 (4.98)	7.17 (6.84)	7.56 (1.81)	7.56 (1.81)	217. (--)	188. (--)	188. (--)
dp12, 1.26	5.97	125.	5.88 (1.53)	6.11 (2.35)	5.93 (0.60)	5.93 (0.60)	166. (32.58)	154. (23.47)	155. (23.72)
afx902, 1.74	8.34	290.	8.11 (2.77)	8.08 (3.22)	8.38 (0.40)	8.38 (0.40)	249. (14.12)	257. (11.34)	257. (11.31)
fefo, 1.61	7.45	245.	7.36 (1.25)	7.36 (1.22)	7.41 (0.62)	7.40 (0.65)	227. (7.30)	248. (1.38)	240. (1.98)
fm1, 1.51	6.57	190.	7.23 (10.09)	6.91 (5.24)	6.99 (6.39)	6.99 (6.39)	204. (7.60)	189. (0.70)	189. (0.61)
pf, 1.83	7.29	270.	7.28 (0.15)	7.33 (0.55)	7.40 (1.48)	7.40 (1.48)	237. (12.10)	237. (12.30)	237. (12.20)
rx36, 1.83	8.51	335.	8.37 (1.60)	8.52 (0.16)	8.32 (2.21)	8.32 (2.24)	312. (6.96)	313. (6.63)	313. (6.60)
rx41, 1.86	8.81	350.	8.64 (1.99)	8.90 (0.94)	8.67 (1.68)	8.66 (1.74)	324. (7.32)	333. (4.93)	332. (5.16)
lx17, 1.91	7.63	260.	7.94 (4.12)	7.72 (1.13)	7.90 (3.53)	7.90 (3.53)	280. (7.59)	281. (8.10)	281. (8.12)
rx27, 1.64	6.93	200.	6.69 (3.38)	6.69 (3.47)	6.67 (3.67)	6.67 (3.67)	182. (8.79)	182. (8.96)	182. (8.89)
rx45, 1.75	7.71	250.	7.66 (0.62)	7.79 (1.05)	7.72 (0.11)	7.72 (0.11)	236. (5.46)	249. (0.27)	249. (0.25)
rx47, 1.82	7.66	260.	7.68 (0.33)	7.67 (0.22)	7.58 (0.99)	7.58 (0.99)	258. (0.82)	256. (1.47)	256. (1.44)
rx48, 1.85	7.76	263.	7.74 (0.19)	7.77 (0.15)	7.66 (1.27)	7.66 (1.28)	269. (2.20)	267. (1.56)	267. (1.58)

* Percent RMS errors are given in parenthesis

Table 4. RMS % errors - optimization*

EOS - # gases	D, [†] %	D, [‡] %	P, [†] %	P, [‡] %
BKWS - 132	4.52	4.21	10.7	10.9
BKWC - 22	2.32	2.28	8.01	7.96
JCZS - 40	2.45	1.83	9.82	9.52
JCZS - 132	2.48	1.85	9.72	9.43

* Calculated using **CHEETAH 1.40**

† All explosives in Table 3

‡ All explosives in Table 3 excluding nonideal explosives containing TATB and HNB

Table 5. RMS % errors - optimization*

EOS - # gases	D, [†] %	D, [‡] %	P, [†] %	P, [‡] %
BKWS - 132	5.12	5.18	9.47	9.54
BKWC - 22	2.34	2.45	8.15	8.16
JCZS - 40	2.61	2.12	8.48	8.13
JCZS - 132	2.64	2.16	8.34	7.99

* Calculated using **CHEETAH 2.0**

† All explosives in Table 3

‡ All explosives in Table 3 excluding nonideal explosives containing TATB and HNB

Experimental Chapman-Jouguet (C-J) detonation velocity, pressure, and temperature depend on composition, density, and size of the initial explosive charge. Detonation velocities are measured at various charge diameters and extrapolated to an “infinite diameter” for comparison with equilibrium calculations. Detonation velocities can typically be measured to within a few percent.¹¹ The RMS percent error for the JCZS-EOS is within experimental error. Detonation pressures determined by various indirect methods span a range of 10-20% (e.g. see Davis and Venable³³). The JCZS-EOS is 9.8% as shown in Tables 4 and 5. The lower percent RMS error for the BKWC-EOS was probably obtained at the cost of a larger percent error for detonation velocities.

8. Validation of the JCZS-EOS

Accuracy of detonation velocity and detonation pressure measurements were discussed in Section 7. Detonation velocity measurements are probably good to within 2%. Detonation pressure measurements are probably good to within 20%. Similar to detonation pressure measurements, detonation temperature measurements are probably good to within 20%. Detonation temperatures are measured by the brightness of the detonation front interacting with a detector. Void free systems such as liquid explosives or single crystal systems are believed to be more accurate. Measurements in porous systems include the effects of shocked air or perhaps low-density explosive material jetting into the voids rather than the brightness of the pure detonation products. Comparisons of measured detonation temperatures to calculated detonation temperatures should be done with caution.

Fried and Souers¹² estimated the accuracy of the total energy of detonation measured by bomb calorimetry to be within 5%. Fried also estimated the error in predicted adiabat energies at relative volumes of 2.2, 4.1, and 6.5 to be 5%. The total energy of detonation and the various adiabat energies can be calculated with CHEETAH using the “standard run” command. Experimental measurements for explosives within the Lawrence Livermore National Laboratories (LLNL) explosives database were reported by Fried and Souers.¹² These are the same explosives listed in Table 3 (excluding ANFO and QM100R).

Validation of the JCZS-EOS includes comparisons of predictions to measured detonation velocities, detonation pressures, detonation temperatures, total energy of detonation, and expansion energies at relative volumes of 2.2, 4.1, and 6.5. Hobbs and Baer¹⁰ presented an extensive table of explosives performance data from a large number of investigators. Hobbs and Baer’s¹⁰ explosive performance database covers a broad range of materials that include 111 detonation velocities, 67 deto-

nation pressures, and 14 detonation temperature measurements. The 32 detonation velocity measurements and 31 detonation pressure measurements in the LLNL performance database were compared previously in Tables 3-5 discussed in Section 7. The LLNL performance database will be used in Section 8.2 to examine total energy of detonation and expansion energies.

8.1 Explosive Performance

Table 6 shows the overall percent RMS error for the BKWS, BKWC, and JCZS-132 predictions of detonation velocity, detonation pressure, and detonation temperature for 62 various explosives which contain C, H, N, O, Cl, and F at various densities. The predictions were made using CHEETAH 1.4 and CHEETAH 2.0. The detonation temperatures predicted with CHEETAH 1.4 are shown in Table 7. Specific information regarding the composition and heat of formation of each explosive can be found in Ref. 10 or in Appendix C. Table 8 lists the percent RMS error between the calculated and measured performance for 111 detonation velocities and 67 detonation pressures using CHEETAH 1.4. The JCZS-40 only considered the 40 species listed in Table 2 for the detonation calculations. The JCZS-132 predictions considered 132 species as possible detonation products. Since the RMS percent errors for both the JCZS-40 and JCZS-132 are similar, the JCZS-40 data set is probably sufficient for energetic materials composed of C, H, N, O, Cl, or F.

Table 6 shows that the overall percent RMS error in predicted detonation velocity is almost a percent better using the JCZS-EOS than the BKWC-EOS. The better agreement with data is consistent with the results from the LLNL performance database given in Table 5. The overall percent RMS error in the detonation pressures are consistent between the JCZS-EOS and the BKWC-EOS. The overall percent RMS error in the predicted detonation temperatures is higher for the JCZS-EOS than the BKWC-EOS. However, the predicted RMS error is within the expected accuracy of the opti-

Table 7. Measured and predicted detonation temperatures using CHEETAH 1.4.

EM, g/cm ³	Exp. ¹⁰	BKWS	BKWC	JCZS	EM, g/cm ³	Exp. ¹⁰	BKWS	BKWC	JCZS
HMX, 1.60	4300	4266	4281	3986	RDX, 1.00	4600	4489	4323	4339
NG, 1.60	4260	4568	4523	4575	Tetryl, 1.61	4200	4269	4208	3792
NM, 1.13	3430	3583	3617	3394	Tetryl, 1.40	4130	4348	4201	3806
PETN, 1.60	4400	4395	4391	4378	Tetryl, 1.20	4300	4379	4153	3765
RDX, 1.66	4320	4234	4270	3943	Tetryl, 1.00	4390	4340	4076	3678
RDX, 1.40	4610	4387	4343	4146	TNT, 1.00	3400	3747	3558	3235
RDX, 1.20	4610	4463	4351	4257	TNM, 1.64	2800	2870	2723	2538

Validation of the JCZS-EOS

Table 8. Measured¹⁰ and predicted detonation velocities and pressures with %RMS errors.

Explosive and density, g/cm ³	D _m , km/s	P _m , kbar	D _{BKWS} , km/s	D _{BKWC} , km/s	D _{JCZS-small} , km/s	D _{JCZS-large} , km/s	P _{BKWS} , kbar	P _{JCZS-small} , kbar	P _{JCZS-large} , kbar
abh, 1.64	7.20	---	7.14 (0.78)	7.36 (2.18)	7.28 (1.09)	7.28 (1.09)	211. (--)	216. (--)	216. (--)
compa3, 1.64	8.47	---	8.25 (2.55)	7.75 (8.51)	7.91 (6.63)	7.91 (6.63)	266. (--)	254. (--)	254. (--)
compb, 1.72	7.92	295.	8.20 (3.59)	7.97 (0.68)	7.98 (0.73)	7.98 (0.73)	276. (6.52)	273. (7.45)	273. (7.46)
compb3, 1.72	7.89	287.	8.16 (3.43)	7.97 (1.00)	7.95 (0.79)	7.95 (0.79)	273. (4.71)	271. (5.42)	271. (5.42)
compc3, 1.60	7.63	---	7.74 (1.38)	7.53 (1.31)	7.53 (1.29)	7.53 (1.29)	230. (--)	225. (--)	225. (--)
compc4, 1.66	8.37	---	8.32 (0.59)	7.89 (5.78)	7.99 (4.57)	7.99 (4.57)	273. (--)	263. (--)	263. (--)
7822, 1.76	8.31	317.	8.53 (2.62)	8.39 (0.95)	8.29 (0.24)	8.29 (0.23)	302. (4.65)	300. (5.23)	300. (5.24)
7723, 1.74	8.25	313.	8.44 (2.25)	8.30 (0.65)	8.20 (0.56)	8.20 (0.56)	294. (6.15)	291. (7.08)	291. (7.09)
7525, 1.76	8.30	316.	8.49 (2.31)	8.34 (0.48)	8.25 (0.58)	8.25 (0.58)	300. (5.07)	299. (5.29)	299. (5.30)
7525, 1.62	7.95	265.	7.95 (0.04)	7.86 (1.13)	7.75 (2.49)	7.75 (2.49)	249. (5.96)	244. (7.87)	244. (7.88)
7030, 1.73	8.06	---	8.32 (3.16)	8.16 (1.21)	8.09 (0.38)	8.09 (0.38)	285. (--)	283. (--)	283. (--)
6535, 1.72	8.04	292.	8.22 (2.22)	8.05 (0.07)	8.00 (0.46)	8.00 (0.46)	277. (5.07)	275. (5.73)	275. (5.74)
6040, 1.74	8.09	---	8.24 (1.84)	8.03 (0.69)	8.03 (0.79)	8.03 (0.79)	281. (--)	280. (--)	279. (--)
6040, 1.72	7.90	---	8.16 (3.30)	7.97 (0.87)	7.95 (0.67)	7.95 (0.67)	273. (--)	271. (--)	271. (--)
5050, 1.63	7.66	231.	7.71 (0.60)	7.53 (1.76)	7.53 (1.76)	7.53 (1.76)	235. (1.78)	231. (0.04)	231. (0.05)
datb, 1.80	7.60	251.	7.86 (3.46)	7.65 (0.65)	7.82 (2.89)	7.82 (2.89)	258. (2.61)	265. (5.42)	265. (5.41)
datb, 1.78	7.60	251.	7.79 (2.46)	7.58 (0.21)	7.74 (1.86)	7.74 (1.86)	250. (0.26)	256. (1.97)	256. (1.97)
degn, 1.38	6.76	---	7.19 (6.42)	6.66 (1.47)	6.75 (0.16)	6.75 (0.16)	183. (--)	160. (--)	160. (--)
dipm, 1.76	7.40	---	7.56 (2.16)	7.54 (1.93)	7.57 (2.25)	7.57 (2.25)	239. (--)	245. (--)	245. (--)
expd. 1.55	6.85	---	6.91 (0.87)	6.65 (2.98)	6.76 (1.29)	6.76 (1.29)	176. (--)	166. (--)	166. (--)
expd, 1.48	6.70	---	6.66 (0.67)	6.41 (4.28)	6.50 (3.05)	6.50 (3.05)	158. (--)	148. (--)	148. (--)
hmx, 1.89	9.11	390.	9.35 (2.62)	9.24 (1.47)	9.11 (0.04)	9.11 (0.05)	374. (4.09)	399. (2.27)	399. (2.24)
hmx, 1.60	7.91	280.	8.14 (2.94)	8.16 (3.19)	8.04 (1.60)	8.04 (1.61)	259. (7.44)	260. (7.02)	260. (7.03)
hmx, 1.40	7.30	210.	7.41 (1.57)	7.46 (2.17)	7.35 (0.64)	7.35 (0.65)	199. (5.27)	196. (6.90)	195. (6.91)
hmx, 1.20	6.85	160.	6.78 (1.04)	6.80 (0.77)	6.68 (2.48)	6.68 (2.47)	151. (5.52)	143. (10.9)	143. (10.9)
hmx, 1.00	5.80	110.	6.20 (6.89)	6.11 (5.42)	6.01 (3.64)	6.01 (3.65)	110. (0.19)	99. (9.65)	99. (9.65)
hmx, 0.75	4.88	60.	5.42 (11.1)	5.19 (6.31)	5.06 (3.60)	5.06 (3.62)	64. (7.08)	52. (12.8)	52. (12.7)
hnab, 1.60	7.31	205.	7.09 (3.02)	7.29 (0.27)	7.19 (1.62)	7.19 (1.62)	204. (0.63)	207. (1.12)	207. (1.11)
hns, 1.60	6.80	---	6.88 (1.15)	6.83 (0.49)	6.88 (1.15)	6.88 (1.15)	187. (--)	187. (--)	187. (--)
hns, 1.70	7.00	---	7.22 (3.09)	7.12 (1.64)	7.21 (2.96)	7.21 (2.96)	214. (--)	217. (--)	216. (--)
lx01, 1.24	6.84	---	7.05 (3.03)	6.79 (0.77)	6.79 (0.74)	6.79 (0.74)	165. (--)	152. (--)	152. (--)

Validation of the JCZS-EOS

Table 8. Measured¹⁰ and predicted detonation velocities and pressures with %RMS errors.

Explosive and density, g/cm ³	D _m , km/s	P _m , kbar	D _{BKWS} , km/s	D _{BKWC} , km/s	D _{JCZS-small} , km/s	D _{JCZS-large} , km/s	P _{BKWS} , kbar	P _{JCZS-small} , kbar	P _{JCZS-large} , kbar
lx14, 1.84	8.83	370.	9.04 (2.36)	8.82 (0.14)	8.79 (0.45)	8.79 (0.44)	345. (6.79)	353. (4.65)	353. (4.66)
men, 1.02	5.49	---	6.00 (9.34)	5.19 (5.42)	5.22 (4.90)	5.22 (4.91)	94. (--)	75. (--)	75. (--)
ng, 1.60	7.70	253.	8.02 (4.18)	7.70 (0.04)	7.64 (0.81)	7.64 (0.76)	251. (0.66)	221. (12.7)	221. (12.7)
nm, 1.13	6.35	125.	6.59 (3.73)	6.03 (5.08)	6.17 (2.79)	6.17 (2.79)	130. (4.28)	115. (7.62)	115. (7.62)
nona, 1.70	7.40	---	7.26 (1.94)	7.38 (0.27)	7.36 (0.60)	7.36 (0.59)	221. (--)	226. (--)	226. (--)
nq, 1.78	8.59	---	8.56 (0.40)	8.37 (2.52)	8.85 (3.02)	8.85 (3.02)	274. (--)	293. (--)	293. (--)
nq, 1.72	---	245.	8.29 (--)	8.12 (--)	8.51 (--)	8.51 (--)	252. (3.01)	264. (7.66)	264. (7.66)
nq, 1.62	7.93	---	7.85 (1.04)	7.70 (2.93)	7.97 (0.51)	7.97 (0.51)	219. (--)	221. (--)	221. (--)
nq, 1.55	7.65	---	7.55 (1.31)	7.40 (3.21)	7.61 (0.51)	7.61 (0.51)	199. (--)	195. (--)	195. (--)
7822, 1.82	---	342.	8.76 (--)	8.58 (--)	8.50 (--)	8.50 (--)	326. (4.76)	326. (4.77)	326. (4.78)
7623, 1.81	8.45	338.	8.70 (3.00)	8.53 (0.92)	8.45 (0.01)	8.45 (0.00)	321. (5.16)	322. (4.70)	322. (4.71)
7525, 1.81	8.48	---	8.69 (2.45)	8.51 (0.31)	8.44 (0.51)	8.44 (0.51)	320. (--)	321. (--)	321. (--)
6040, 1.80	8.16	320.	8.47 (3.80)	8.23 (0.83)	8.25 (1.07)	8.25 (1.07)	304. (5.08)	305. (4.70)	305. (4.70)
9007, 1.64	8.09	---	8.08 (0.16)	7.72 (4.59)	7.79 (3.67)	7.79 (3.67)	256. (--)	248. (--)	248. (--)
9011, 1.77	8.50	324.	8.65 (1.72)	8.30 (2.36)	8.37 (1.55)	8.37 (1.55)	307. (5.22)	308. (5.05)	308. (5.05)
9205, 1.67	8.17	---	8.25 (0.94)	7.94 (2.78)	7.96 (2.52)	7.96 (2.52)	271. (--)	265. (--)	265. (--)
9501, 1.84	8.83	---	9.07 (2.69)	8.89 (0.67)	8.83 (0.04)	8.83 (0.05)	348. (--)	358. (--)	358. (--)
pentolit, 1.71	7.75	---	7.91 (2.05)	7.66 (1.16)	7.70 (0.62)	7.70 (0.62)	258. (--)	251. (--)	251. (--)
pentolit, 1.70	7.53	---	7.87 (4.53)	7.63 (1.31)	7.67 (1.80)	7.67 (1.80)	255. (--)	247. (--)	247. (--)
pentolit, 1.68	7.65	251.	7.80 (1.92)	7.57 (1.08)	7.59 (0.73)	7.59 (0.73)	248. (1.18)	240. (4.25)	240. (4.25)
pentolit, 1.64	7.53	---	7.65 (1.60)	7.44 (1.14)	7.45 (1.03)	7.45 (1.03)	235. (--)	227. (--)	227. (--)
petn, 1.76	8.27	337.	8.68 (4.91)	8.50 (2.79)	8.40 (1.57)	8.40 (1.57)	312. (7.36)	296. (12.2)	296. (12.2)
petn, 1.70	8.07	307.	8.43 (4.46)	8.29 (2.76)	8.15 (1.04)	8.15 (1.04)	289. (5.91)	271. (11.6)	271. (11.6)
petn, 1.60	7.75	266.	8.03 (3.68)	7.96 (2.71)	7.75 (0.02)	7.75 (0.02)	254. (4.63)	234. (12.0)	234. (12.0)
petn, 1.45	7.18	208.	7.48 (4.23)	7.42 (3.30)	7.17 (0.12)	7.17 (0.12)	208. (0.23)	187. (10.1)	187. (10.1)
petn, 1.23	6.37	139.	6.76 (6.09)	6.51 (2.21)	6.38 (0.21)	6.38 (0.23)	153. (10.2)	133. (4.41)	133. (4.38)
petn, 0.99	5.48	87.	5.99 (9.35)	5.59 (2.00)	5.58 (1.74)	5.58 (1.77)	100. (14.6)	85. (2.03)	85. (2.00)
petn, 0.88	5.06	68.	5.61 (10.9)	5.19 (2.55)	5.18 (2.37)	5.18 (2.40)	78. (15.2)	65. (4.11)	65. (4.08)
petn, 0.48	3.60	24.	4.12 (14.3)	3.83 (6.36)	3.50 (2.89)	3.50 (2.81)	26. (7.48)	18. (23.6)	18. (23.5)
petn, 0.30	2.99	13.	3.44 (15.0)	3.25 (8.85)	2.96 (0.85)	2.97 (0.71)	12. (5.13)	10. (23.3)	10. (23.1)

Validation of the JCZS-EOS

Table 8. Measured¹⁰ and predicted detonation velocities and pressures with %RMS errors.

Explosive and density, g/cm ³	D _m , km/s	P _m , kbar	D _{BKWS} , km/s	D _{BKWC} , km/s	D _{JCZS-small} , km/s	D _{JCZS-large} , km/s	P _{BKWS} , kbar	P _{JCZS-small} , kbar	P _{JCZS-large} , kbar
petn, 0.25	2.83	8.	3.25 (14.8)	3.10 (9.44)	2.85 (0.85)	2.86 (1.00)	9. (18.4)	8. (0.12)	8. (0.36)
picratol, 1.63	6.97	---	7.19 (3.10)	6.87 (1.41)	7.04 (0.97)	7.04 (0.97)	200. (--)	191. (--)	191. (--)
picric, 1.76	7.57	---	7.52 (0.64)	7.48 (1.17)	7.51 (0.82)	7.51 (0.82)	237. (--)	239. (--)	239. (--)
picric, 1.71	7.26	---	7.35 (1.19)	7.33 (1.00)	7.33 (1.00)	7.33 (1.00)	222. (--)	223. (--)	223. (--)
picric, 1.60	7.10	---	6.97 (1.77)	7.01 (1.31)	6.96 (1.98)	6.96 (1.98)	192. (--)	190. (--)	190. (--)
rdx, 1.80	8.75	341.	8.96 (2.45)	8.91 (1.83)	8.78 (0.34)	8.78 (0.34)	334. (2.00)	347. (1.88)	347. (1.86)
rdx, 1.77	8.70	338.	8.84 (1.58)	8.80 (1.12)	8.67 (0.38)	8.67 (0.38)	322. (4.86)	332. (1.66)	332. (1.68)
rdx, 1.72	8.46	313.	8.63 (1.99)	8.61 (1.78)	8.48 (0.24)	8.48 (0.24)	302. (3.65)	309. (1.20)	309. (1.22)
rdx, 1.66	8.24	---	8.38 (1.75)	8.39 (1.81)	8.26 (0.24)	8.26 (0.24)	279. (--)	284. (--)	284. (--)
rdx, 1.60	8.13	263.	8.15 (0.24)	8.17 (0.50)	8.04 (1.07)	8.04 (1.06)	260. (1.24)	261. (0.76)	261. (0.77)
rdx, 1.46	7.60	211.	7.63 (0.41)	7.67 (0.97)	7.56 (0.57)	7.56 (0.57)	216. (2.37)	214. (1.44)	214. (1.43)
rdx, 1.40	7.46	213.	7.42 (0.51)	7.47 (0.09)	7.35 (1.42)	7.35 (1.41)	199. (6.36)	196. (7.95)	196. (7.96)
rdx, 1.29	7.00	166.	7.06 (0.88)	7.10 (1.39)	6.99 (0.18)	6.99 (0.17)	172. (3.65)	166. (0.27)	166. (0.27)
rdx, 1.20	6.77	152.	6.79 (0.24)	6.81 (0.53)	6.69 (1.22)	6.69 (1.21)	152. (0.26)	143. (5.93)	143. (5.93)
rdx, 1.10	6.18	122.	6.49 (5.09)	6.50 (5.13)	6.35 (2.82)	6.36 (2.83)	130. (6.81)	120. (1.28)	120. (1.27)
rdx, 1.00	6.10	89.	6.21 (1.76)	6.12 (0.36)	6.02 (1.34)	6.02 (1.33)	110. (23.7)	100. (12.0)	100. (12.0)
rdx, 0.95	5.80	96.	6.06 (4.52)	5.93 (2.30)	5.85 (0.78)	5.85 (0.80)	100. (4.58)	90. (6.59)	90. (6.58)
rdx, 0.70	4.65	48.	5.25 (12.9)	5.01 (7.74)	4.83 (3.97)	4.84 (3.99)	57. (17.9)	45. (7.05)	45. (7.02)
rdx, 0.56	4.05	32.	4.72 (16.5)	4.49 (10.9)	4.17 (2.95)	4.17 (2.99)	38. (18.1)	28. (13.4)	28. (13.3)
tacot, 1.85	7.25	---	7.62 (5.13)	7.56 (4.29)	7.71 (6.32)	7.71 (6.32)	253. (--)	267. (--)	267. (--)
tatb, 1.88	7.76	---	8.19 (5.53)	7.91 (1.96)	8.23 (6.00)	8.23 (6.00)	285. (--)	308. (--)	308. (--)
tatb, 1.85	7.66	259.	8.07 (5.39)	7.81 (1.99)	8.10 (5.74)	8.10 (5.74)	273. (5.51)	291. (12.4)	291. (12.4)
tetryl, 1.73	7.72	---	7.81 (1.14)	7.74 (0.22)	7.72 (0.02)	7.72 (0.02)	255. (--)	257. (--)	257. (--)
tetryl, 1.71	7.85	---	7.74 (1.45)	7.68 (2.21)	7.65 (2.55)	7.65 (2.55)	248. (--)	250. (--)	250. (--)
tetryl, 1.68	7.50	239.	7.63 (1.71)	7.59 (1.15)	7.55 (0.65)	7.55 (0.65)	239. (0.13)	239. (0.14)	239. (0.13)
tetryl, 1.61	7.58	226.	7.38 (2.59)	7.38 (2.69)	7.32 (3.47)	7.32 (3.47)	218. (3.73)	217. (3.96)	217. (3.97)
tetryl, 1.40	---	---	6.70 (--)	6.75 (--)	6.66 (--)	6.66 (--)	165. (--)	161. (--)	161. (--)
tetryl, 1.36	6.68	142.	6.59 (1.41)	6.63 (0.72)	6.54 (2.03)	6.54 (2.03)	157. (10.4)	152. (7.32)	152. (7.31)
tetryl, 1.20	6.34	---	6.15 (3.00)	6.16 (2.77)	6.09 (3.89)	6.09 (3.89)	127. (--)	120. (--)	120. (--)
tetryl, 1.00	---	---	5.68 (--)	5.59 (--)	5.55 (--)	5.55 (--)	95. (--)	85. (--)	85. (--)

Validation of the JCZS-EOS

Table 8. Measured¹⁰ and predicted detonation velocities and pressures with %RMS errors.

Explosive and density, g/cm ³	D _m , km/s	P _m , kbar	D _{BKWS} , km/s	D _{BKWC} , km/s	D _{JCZS-small} , km/s	D _{JCZS-large} , km/s	P _{BKWS} , kbar	P _{JCZS-small} , kbar	P _{JCZS-large} , kbar
tnt, 1.64	6.93	210.	7.19 (3.69)	6.84 (1.25)	7.03 (1.42)	7.03 (1.42)	203. (3.20)	195. (6.93)	195. (6.93)
tnt, 1.45	6.50	144.	6.51 (0.21)	6.27 (3.60)	6.37 (1.97)	6.37 (1.97)	153. (6.54)	147. (1.85)	147. (1.84)
tnt, 1.36	6.20	124.	6.22 (0.29)	6.00 (3.30)	6.09 (1.84)	6.09 (1.85)	134. (8.39)	128. (3.27)	128. (3.26)
tnt, 1.00	5.00	67.	5.21 (4.26)	4.98 (0.34)	5.06 (1.14)	5.06 (1.14)	77. (15.5)	70. (3.78)	70. (3.78)
tnt, 0.80	4.34	37.	4.74 (9.21)	4.48 (3.13)	4.45 (2.53)	4.45 (2.52)	53. (43.6)	43. (15.8)	43. (15.7)
btf, 1.86	8.49	360.	8.16 (3.95)	8.60 (1.24)	8.60 (1.32)	8.60 (1.34)	310. (13.8)	331. (8.16)	331. (8.15)
btf, 1.76	8.26	---	7.84 (5.04)	8.34 (0.96)	8.26 (0.01)	8.26 (0.04)	278. (--)	292. (--)	292. (--)
hnb, 1.97	9.30	---	8.86 (4.78)	9.25 (0.50)	8.76 (5.78)	8.77 (5.69)	373. (--)	348. (--)	347. (--)
tnm, 1.64	6.36	159.	5.50 (13.5)	6.32 (0.60)	6.24 (1.89)	6.28 (1.30)	114. (28.1)	145. (8.56)	141. (11.1)
tntab, 1.74	8.58	---	8.02 (6.52)	8.79 (2.41)	8.48 (1.13)	8.49 (1.09)	286. (--)	303. (--)	303. (--)
fefo, 1.59	7.50	250.	7.30 (2.66)	7.30 (2.69)	7.35 (1.97)	7.45 (0.66)	222. (11.1)	243. (2.65)	235. (5.95)
lx04, 1.86	8.46	350.	8.34 (1.38)	8.28 (2.11)	8.35 (1.26)	8.36 (1.20)	310. (11.4)	310. (11.5)	310. (11.5)
lx07, 1.87	8.64	---	8.68 (0.45)	8.60 (0.47)	8.61 (0.40)	8.61 (0.35)	332. (--)	338. (--)	338. (--)
lx09, 1.84	8.81	377.	9.05 (2.76)	8.93 (1.39)	8.84 (0.32)	8.84 (0.33)	348. (7.67)	360. (4.58)	360. (4.60)
lx10, 1.86	8.82	375.	8.94 (1.31)	8.85 (0.29)	8.78 (0.45)	8.78 (0.42)	345. (7.93)	356. (5.05)	356. (5.05)
lx11, 1.86	8.32	---	8.04 (3.32)	8.00 (3.85)	8.15 (2.09)	8.15 (2.01)	293. (--)	297. (--)	297. (--)
ap, 1.00	3.70	---	4.02 (8.57)	3.66 (1.18)	3.73 (0.88)	3.71 (0.15)	40. (--)	36. (--)	35. (--)
lx15, 1.58	6.84	---	6.70 (2.04)	6.61 (3.41)	6.64 2.870	6.64 (2.85)	179. (--)	177. (--)	177. (--)
lx17, 1.91	7.63	---	7.96 (4.34)	7.73 (1.35)	7.92 (3.80)	7.92 (3.81)	282. (--)	283. (--)	284. (--)
9010, 1.78	8.37	328.	8.33 (0.46)	8.34 (0.33)	8.06 (3.66)	8.06 (3.65)	300. (8.44)	289. (11.8)	289. (11.8)
9404, 1.84	8.80	375.	9.01 (2.37)	8.90 (1.12)	8.81 (0.13)	8.81 (0.13)	344. (8.15)	353. (5.74)	353. (5.76)
94071.60	7.91	287.	7.94 (0.43)	7.90 (0.16)	7.76 (1.87)	7.76 (1.86)	251. (12.4)	245. (14.8)	245. (14.8)
9502, 1.91	7.71	---	8.08 (4.82)	7.83 (1.52)	8.07 (4.62)	8.07 (4.63)	287. (--)	298. (--)	298. (--)
9503, 1.90	7.71	---	8.21 (6.49)	7.98 (3.50)	8.13 (5.51)	8.14 (5.51)	296. (--)	306. (--)	306. (--)

*The acronyms and heats of formations for these explosives can be found in Ref. 10.

cal temperature measurements which may be as high as 20%. Table 8 shows the specific measured and predicted detonation temperatures used to calculate the overall percent RMS error for the temperatures. The JCZS predicted detonation temperatures are similar to measured detonation temperatures for homogeneous explosive. For example, the RMS error for the NM case is 1.05% for the JCZS-EOS compared to 5.45% for the BKWC-EOS.

8.2 Expansion States

As an additional evaluation of the JCZS-EOS at expanded states, the total energy of detonation and expansion energies at relative volumes of 2.2, 4.1, and 6.5 were compared to the tabulated values¹² for the explosives in the LLNL performance database. Table 9 gives the percent RMS error for the total energy of detonation which is labeled as E, and the expansion energies as relative volumes of 2.2, 4.1, and 6.5 labeled as E_{2.2}, E_{4.1}, and E_{6.5}.

The JCZS prediction of the total energy of detonation was better than the BKW predictions. The expansion energies for the BKWC-EOS was better than the BKWS and JCZS predictions. However, the BKWC used the expansion states to calibrate 31 constants and is expected to match the experimental measurements closest. A better comparisons of the expansion energy would be to compare cylinder wall velocities as predicted with a shock physics code.

8.3 Detonation in Condensed Explosives with Low Initial Densities

Figure 18 shows the measured and predicted detonation velocity and pressure for PETN for a wide range of initial densities. The agreement is good over the entire density range for both detonation velocity and pressure. The predictions made using the BKWS-EOS do not agree with the data as well as the predictions made using the JCZS-EOS especially at low initial densities.

Table 9. Percent RMS errors for E, E_{2.2}, E_{4.1}, E_{6.5}*

EOS	E		E _{2.2}		E _{4.1}		E _{6.5}	
	1.4 [†]	2.0 [‡]						
BKWS	11.7	8.0	12.2	10.8	10.4	9.1	8.7	7.4
BKWC	9.3	6.5	5.8	5.8	5.4	5.2	5.3	4.9
JCZS	8.5	6.5	11.9	8.0	8.9	6.9	7.9	7.0

* JCZS-small and JCZS-large give essentially the same results

† CHEETAH 1.4 ‡ CHEETAH 2.0

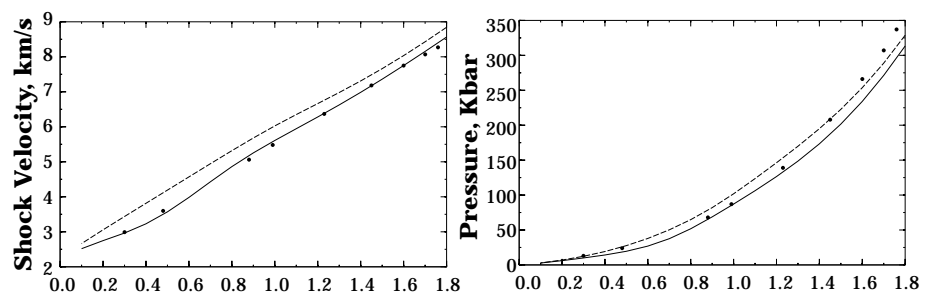


Fig. 18. Comparison of measured (symbols) detonation velocity and pressure for PETN to predictions using the BKWS-EOS (dashed lines) and the JCZS-EOS (solid lines).

Summary and Conclusions

8.4 High Pressure Gas Detonations

Another method of evaluating the JCZS-EOS database is to compare measured detonation velocity of gases at high initial pressures to predictions. The detonation velocity of various gases at high initial pressures were measured by Bauer³⁵ and evaluated by Schmitt.³⁶

Figure 6 shows predicted (lines) and measured (symbols) detonation velocities of various gases at different elevated initial pressures. The compositions of the gas mixtures are also shown in Figure 6. The BKWC database does not consider H and OH as reaction products and cannot adequately predict the detonation velocities for the hydrogen oxygen system as shown in Figure 6.A. The JCZS-EOS database adequately predicts the detonation velocity for all the gas mixtures in Figure 6.

9. Summary and Conclusions

The JCZ3 product species library has been expanded to include approximately 750 gas-phase products. The force constants for this library, r^* and ϵ/k , have been obtained by using pure liquid shock Hugoniot data, by correcting the LJ characteristic approach radii (σ) to conform to the mathematical form of the EXP 6 potential function and using literature values for the potential well depth, using corresponding states theory to calculate the EXP 6 force constants, using a semiempirical formula based on the species volume to determine the approach radii and obtaining the potential well depth by matching isentropes with the BKWS-EOS. Some of the EXP 6 parameters were slightly adjusted to predict optimal detonation velocities using the optimization toolkit, DAKOTA.

Detonation simulations have been performed with the JCZS-EOS database and have displayed adequate agreement with experimental results for detonation velocity, detonation pressure, and detonation temperature. Predicted detonation velocities with the JCZS-EOS are shown to be within 2% of measured values for many explosives. The predicted velocities with the BKWC-EOS for the same set of explosives was shown to be within 3%. The detonation pressure, temperature, and expansion states were all shown to be within 10% of reported values. The JCZS-EOS is shown to predict low density explosives and high pressure gaseous detonations with the same accuracy as high density explosives. The better agreement at these intermediate states is attributed to modeling molecular interactions which is not done in the semiempirical BKW-EOS.

The JCZ-EOS with the improved product species library has been shown to adequately predict detonation states as well as expansion states for various explosives. Better agreement between measured detonation performance and predicted detonation performance for low density explosives such as PETN is attributed to a better description of molecular interaction at intermediate pressure regimes. Such predictions supports the hypothesis that improved predictions of explosive performance can be realized by using a more fundamental EOS with an adequate number of product species, rather than merely increasing the number of fitting parameters used by empirical based equations-of-states.

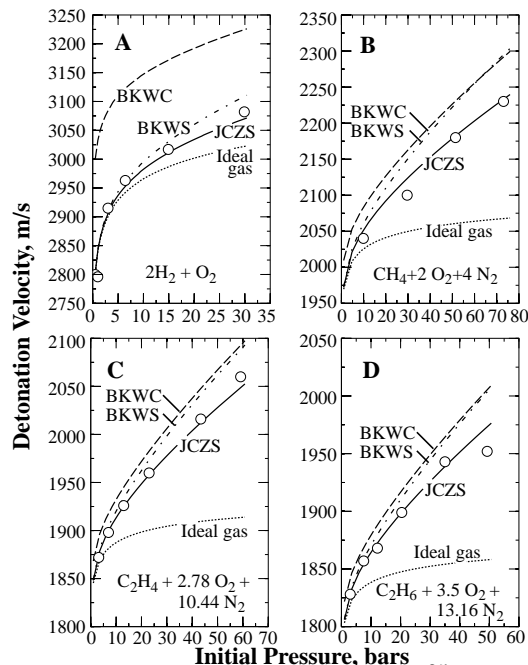


Fig. 19. Predicted (lines) and measured³⁵ (symbols) detonation velocities for high pressure gases.

References

10. References

1. Cowperthwaite, M. and Zwisler, W. K., "The JCZ Equations of State for Detonation Products and Their Incorporation into the TIGER Code," *Sixth Symposium (International) on Detonation*, ACR-221, Office of Naval Research, Naval Surface Weapons Center, 162 (1976).
2. Chase, M. W. Jr., Davies, C. A., Downey, J.R. Jr., Frurip, D. J., McDonald, R. A., Syverud, A. N., *JANAF Thermochemical Tables*, Third Edition, *Journal of Physical and Chemical Reference Data*, **14**, Supplement No. 1 (1985).
3. Ross, M. and Ree, F. H., "Repulsive forces of simple molecules and mixtures at high density and temperature," *J. Chem. Phys.* **73**(12), 6146 (1980).
4. Jacobs, S. J., "On the Equation of State of Compressed Liquids and Solids," NOLTR 68-214, United States Naval Ordnance Laboratory, White Oak, Maryland (1968).
5. Hobbs, M. L., and Baer, M. R., "Four Parameter Corresponding States Method Applied to the JCZ3 Force Constants," Internal Memorandum to A. C. Ratzel, Sandia National Laboratories, Albuquerque, New Mexico (December 12, 1994). See also Hobbs, M. L. and Baer, M. R., "Using Corresponding State Theory to Obtain Intermolecular Potentials to Calculate Pure Liquid Shock Hugoniots," *Twenty-Seventh International Symposium on Combustion*, Submitted, Boulder, CO (August 2-7, 1998).
6. Hirschfelder, J. O., Curtiss, C. F., and Bird, R. B., *Molecular Theory of Gases and Liquids*, Wiley, New York, 34 (1954).
7. Hirschfelder, J. O., Curtiss, C. F., and Bird, R. B., *Molecular Theory of Gases and Liquids*, Wiley, New York, 234 (1954).
8. Wilding, W. V., and Rowley, R. L., "Four-Parameter corresponding states Method for the Prediction of Thermodynamic Properties of Polar and Nonpolar Fluids," *International Journal of Thermophysics*, **7** (3), 525 (1986).
9. Rowley, R. L., "ELK, Extended Lee-Kesler--A Four-Parameter Corresponding States Method for Prediction of Thermophysical Properties of Pure Fluids and Mixtures," IBM PC compatible software and manual, Dept. of Chem. Eng., Brigham Young University, Provo, Utah (1993).
10. Hobbs, M. L., and Baer, M. R., "Calibrating the BKW-EOS with a Large Product Species database and Measured C-J Properties," Tenth Symposium (International) on Detonation, Boston, MA, (1993).
11. Mader, C. L., *Numerical Modeling of Detonations*, Univ. of California Press, Los Angeles, CA 1979.
12. Fried, L. E., "CHEETAH 1.22 User's Manual", UCRL-MA-117541 Rev.2, Lawrence Livermore National Laboratory (August, 3, 1995). See also Fried, L. E. and Souers, P. C., "BKW: An Empirical BKW parameterization based on cylinder test data," *Propellants, Explosives, and Pyrotechnics*, **21**, 215 (1996).
13. Finger, M., Lee, E., Helm, F. H., Hayes, B., Hornig, H., McGuire, R., Kahara, M., and Guidry, M., "The Effect of Elemental Composition on the Detonation Behavior of Explosives," *Sixth Symposium (International) on Detonation*, ACR-221, 1976, p. 710.
14. Souers, P. C. and Kury, J. W., "Comparison of Cylinder Data and Code Calculations for Homogeneous Explosives," UCRL-JC-110661, Lawrence Livermore National Laboratory, Livermore, California (May 1992).
15. Cowperthwaite, M. and Zwisler, W. H., *TIGER Computer Program Documentation*, Stanford Research Institute, Menlo Park, California, 1973.
16. Ree, F. H., "A statistical theory of chemically reacting multiphase mixture: application to the detonation properties of PETN," *J. Chem. Phys.*, **81**, 1251 (1984).
17. Sheffield, S. A., private communication at Sandia National Laboratories (1996).
18. Woolfolk, R. W., Cowperthwaite, M., and Shaw, R., "A 'Universal' Hugoniot for Liquids," *Thermochimica Acta*, **5**, 409 (1973).
19. Marsh, S. P., editor, *LASL Shock Hugoniot Data*, University of California Press, Berkeley, California (1980).
20. Lyzenga, G. A., Ahrens, T. J., Nellis, W. J., and Mitchell, A. C., "The temperature of shock-compressed water," *J. Chem. Phys.*, **76** (12), 6282 (1982).
21. Nellis, W. J., Mitchell, A. C., van Thiel, M., Devine, G. J., and Trainor, R. J., "Equation-of-state data for molecular hydrogen and deuterium at shock pressures in the range 2-76 GPa (20-760 kbar)," *J. Chem. Phys.*, **79** (3), 1480 (1983).
22. Nellis, W. J., Ree, F. H., van Thiel, M., Mitchell, A. C., "Shock Compression of Liquid Carbon Monoxide and

References

- Methane to 90 GPa (900 kbar)," *J. Chem. Phys.*, **75** (6), 3055 (1981).
- 23. Schott, G. L., "Shocked Liquid Carbon Dioxide," *Bull. Am. Phys. Soc.*, **31**, 824 (1986).
 - 24. Zubarev, V. N., Telegin, G. S., "The Impact Compressibility of Liquid Nitrogen and Solid Carbon Dioxide," *Soviet Physics - Doklady*, **7** (1), 34 (1962).
 - 25. Kovel, M. I., "The Shock Wave Hugoniot and Electrical Conductivity of Liquid Ammonia in the Pressure Range 45 kb to 282 kb," Ph.D. Theses, Lawrence Livermore Laboratory, UCRL-51367, University of California, Livermore, California (1973).
 - 26. Radousky, H. B., Mitchell, A. C., Nellis, W. J., and Ross, M., "Shock Temperature Measurements in Ammonia," in *Shock Waves in Condensed Matter*, edited by Gupta, Y. M., Plenum Press, New York (1986).
 - 27. Nellis, W. J. and Mitchell, A. C., "Shock Compression of Liquid Argon, Nitrogen, and Oxygen to 90 GPa (900 kbar)," *J. Chem. Phys.*, **73** (12), 6137 (1980).
 - 28. van Thiel, M. and Alder, B. J., "Shock Compression of Argon," *J. Chem. Phys.*, **44**(3), 1056 (1966).
 - 29. Cowan, R. D., and Fickett, W., "Calculation of the detonation properties of solid explosives with the Kistiakowsky-Wilson equation of state," *J. Chem. Phys.*, **24**, 932 (1956).
 - 30. Hobbs, M. L., and Baer, M. R., *Nonideal Thermoequilibrium Calculations Using a Large Product Species Data Base*, SAND92-0482, UC-741, Sandia National Laboratories, Albuquerque, NM, 13 (1992).
 - 31. Eldred, M. S., Hart, W. E., Bohnhoff, W. J., Romero, V. J., Hutchinson, S. A., and Salinger, A. G., "Utilizing Object-Oriented Design to Build Advanced Optimization Strategies with Generic Implementation," AIAA-4164 in *Proceedings of the 6th AIAA/USAF/NASA/ISSMO Symposium on Multidisciplinary Analysis and Optimization*, Bellevue, WA, 1568 (Sept. 4-6, 1996). See also Eldred, M. S., Outka, D. E., Bohnhoff, W. J., Witkowski, W. R., Romero, V. J., Ponslet, E. R., and Chen, K. S., "Optimization of Complex Mechanics Simulations with Object-Oriented Software Design," *Computer Modeling and Simulation in Engineering*, **1**, 3 (August 1996).
 - 32. Sjaardema, G. D., "APREPRO: An Algebraic Preprocessor for Parameterizing Finite Element Analyses," SAND92-2291, UC-705, Sandia National Laboratories, Albuquerque, NM (1994).
 - 33. Davis, W. C., and Venable, D., "Pressure Measurements for Composition B-3," *Fifth Symposium (International) on Detonation*, ACR-184, 13 (1970).
 - 34. Fickett, W., "Intermolecular Potential Functions for Some Simple Molecules from Available Experimental Data," Los Alamos National Laboratory Report No. LA-2665, TID-4500 (1962).
 - 35. Bauer, P. A., "Contribution of L'Etude De La Detonation De Melanges Explosifs Gazeux A Pression Initiale Elevvee," Ph. D. Thesis L'Universite De Pointiers (1985).
 - 36. Schmitt, R. G., "Analysis of Gas-phase Detonation Wave Structure at Elevated Initial Pressures," Ph. D Thesis, The University of Iowa (1994). See also, Schmitt, R. G., and Butler, P. B., "Detonation Properties of Gases at Elevated Initial Pressures," *Combust. Sci. and Tech.*, **106** 167 (1995).
 - 37. Daubert, T. E., Danner, R. P., Sibul, H. M., and Stebbins, C. C., *Physical and Thermodynamic Properties of Pure Compounds: Data Compilation*, extant 1994 (core with 4 supplements), Taylor & Francis, Bristol, PA (1994).
 - 38. Stephenson, R. M., Malanowski, S., Ambrose, D., "Vapor-Liquid Critical Constants of Fluids," in the *Handbook of Thermodynamics of Organic Compounds*, Elsevier, New York (1987).
 - 39. McCormick, S., *TAPP (version 2.20) - A Database of Thermochemical and Physical Properties*, E. S. Microware, Hamilton, OH (1996).
 - 40. Reid, R. C., Prausnitz, J. M., and Poling, B. E., *The Properties of Gases and Liquids*, 4th ed., McGraw-Hill, New York (1987).
 - 41. TRCTHERMO data search, Sandia Laboratories Technical Library, Albuquerque, NM (1997).
 - 42. Svehla, R. A., "Estimated Viscosities and Thermal Conductivities of Gases at High Temperatures," NASA Technical Report R-132 (1962).
 - 43. Warnatz, J., "Calculation of the Structure of Laminar Flat Flames I: Flame Velocity of Freely Propagating Ozone Decomposition Flames," *Ber. Beunsenges. Phys. Chem.*, **82**, 193 (1978). See also Warnatz, J., "Influence of Transport Models and Boundary Conditions on Flame Structure," in *Numerical Methods in Flame Propagation*, Editors N. Peters and J. Warnatz, Friedr. Vieweg and Sohn, Wiesbaden (1982).

Appendix A

Appendix A

Appendix A documents the resources of all the critical properties and Lennard-Jones parameters used to establish the JCZS database.

This table indicates the source of each critical volume obtained in the literature search.

Table A.1 Species with known critical volumes

Al ^a	Br ₃ HSi ^b	CF ₂ O ^a	CH ₃ OH ^a	C ₂ N ₂ ^a	Cl ₃ HSi ^a	D ₂ S ^b	F ₄ Si ^a	H ₄ N ₂ ^a	N ₂ O ^a
AlBr ₃ ^a	Br ₂ Hg ^b	CF ₄ ^a	CH ₄ ^a	C ₃ H ₆ ^a	Cl ₃ P ^a	D ₃ N ^e	F ₆ Mo ^b	H ₄ Si ^a	N ₂ O ₃ ^a
AlCl ₃ ^a	Br ₃ P ^b	CHBr ₃ ^c	CO ^a	C ₃ H ₈ ^a	Cl ₄ OW ^b	FH ^a	F ₆ S ^a	He ^c	N ₂ O ₄ ^a
AlI ₃ ^c	Br ₄ Si ^b	CHClF ₂ ^a	COS ^a	C ₃ H ₉ Cl ₃ Si ^a	Cl ₄ Si ^a	FNa ^a	F ₆ W ^b	Hg ^a	Na ^a
Ar ^d	Br ₄ Ti ^b	CHCl ₂ F ^a	CO ₂ ^a	C ₃ O ₂ ^e	Cl ₄ Ti ^a	FNO ₂ ^e	Fe ^a	HgI ₂ ^e	Ne ^c
BBr ₃ ^b	Br ₄ Zr ^b	CHCl ₃ ^a	CS ₂ ^a	ClD ^e	Cl ₄ Zr ^b	F ₂ ^a	Hf ^a	I ₄ Si ^b	O ₂ ^a
BCl ₃ ^a	Br ₅ Nb ^b	CHF ₃ ^a	C ₂ Cl ₄ ^a	ClF ₅ ^b	Cl ₅ Mo ^b	c-F ₂ N ₂ ^e	HNO ₃ ^a	I ₄ Ti ^d	O ₂ S ^a
BF ₃ ^a	C ^c	CHN ^a	C ₂ Cl ₆ ^a	ClF ₅ S ^e	Cl ₅ Nb ^c	t-F ₂ N ₂ ^e	HNaO ^a	I ₄ Zr ^b	O ₃ ^a
BI ₃ ^b	CBrF ₃ ^a	CH ₂ ClF ^a	C ₂ F ₃ N ^d	ClH ^a	Cl ₅ P ^e	F ₂ O ^e	H ₂ ^a	K ^a	O ₃ S ^a
B ₂ H ₆ ^a	CClF ₃ ^a	CH ₂ Cl ₂ ^a	C ₂ F ₄ ^a	CINO ^a	Cl ₅ Ta ^b	F ₃ N ^a	H ₂ O ^a	Kr ^c	P ^e
BrH ^c	CClN ^a	CH ₂ F ₂ ^a	C ₂ F ₆ ^a	ClNa ^a	Cl ₆ W ^b	F ₃ NO ^b	H ₂ O ₂ ^a	Li ^a	S ^c
BrI ^e	CCl ₂ F ₂ ^a	CH ₂ O ^a	C ₂ H ₂ ^a	Cl ₂ ^a	Cs ^e	F ₃ P ^e	H ₂ S ^a	MgO ^a	Si ^a
BrK ^a	CCl ₂ O ^a	CH ₂ O ₂ ^a	C ₂ H ₄ ^a	Cl ₂ H ₂ Si ^a	DH ^e	F ₃ PS ^e	H ₂ SO ₄ ^a	NO ^a	UF ₆ ^b
BrNa ^a	CCl ₃ F ^a	CH ₃ Cl ^a	C ₂ H ₄ O ^a	Cl ₂ Hg ^e	D ₂ ^c	F ₄ N ₂ ^a	H ₃ N ^a	NO ₂ ^a	Xe ^c
Br ₂ ^a	CCl ₄ ^a	CH ₃ F ^a	C ₂ H ₆ ^a	Cl ₂ O ₂ S ^c	D ₂ O ^c	F ₄ S ^e	H ₃ P ^a	N ₂ ^a	Zn ^c

a. Ref. [35], Daubert, T. E., Danner, R. P., Sibul, H. M. and Stebbins, C. C., *Physical and Thermodynamic Properties of Pure Compounds: Data Compilation*, Taylor & Francis, Bristol, PA (1994).

b. Ref. [36], Stephenson, R. M., Malanowski, S., Ambrose, D., "Vapor-Liquid Critical Constants of Fluids" in *Handbook of Thermodynamics of Organic Compound*, Elsevier, New York (1987).

c. Ref. [37], McCormick, S., *TAPP (version 2.20) - A Database of Thermochemical And Physical Properties*, E. S. Microware, Hamilton, OH (1996).

d. Ref. [38], Reid, R. C., Prausnitz, J. M., and Poling, B. E., *The Properties of Gases and Liquids*, 4th ed., McGraw-Hill, New York (1987).

e. Ref. [39], TRCTHERMO data search (1997).

Appendix A

This table indicates the source of each critical temperature obtained in the literature search.

Table A.2 Species with known critical temperatures

Al ^a	Br ₃ HSi ^b	CHF ₃ ^a	C ₂ F ₄ ^a	ClH ^a	Cl ₅ Ta ^b	t-F ₂ N ₂ ^b	H ₂ O ₂ ^a	Mg ^c	P ^a
AlBr ₃ ^b	Br ₃ P ^b	CHN ^a	C ₂ F ₆ ^a	ClNO ^a	Cl ₆ W ^b	F ₂ O ^d	H ₂ S ^a	MgO ^a	P ₂ ^c
AlCl ₃ ^a	Br ₄ Si ^b	CH ₂ ClF ^a	C ₂ H ₂ ^a	ClNa ^a	Cs ^c	F ₃ N ^a	H ₂ SO ₄ ^a	Mn ^c	P ₄ ^c
AlI ₃ ^b	Br ₄ Ti ^b	CH ₂ Cl ₂ ^a	C ₂ H ₄ ^a	ClO ₂ ^a	Cs ₂ ^c	F ₃ NO ^b	H ₃ N ^a	Mo ^c	Pb ^c
Ar ^c	Br ₄ Zr ^b	CH ₂ F ₂ ^a	C ₂ H ₄ O ^a	Cl ₂ ^a	Cu ^c	F ₃ P ^d	H ₃ P ^a	NO ^a	Pb ₂ ^c
BBr ₃ ^b	Br ₅ Nb ^b	CH ₂ O ^a	C ₂ H ₆ ^a	Cl ₂ H ₂ Si ^a	Cu ₂ ^c	F ₃ PS ^b	H ₄ N ₂ ^a	NO ₂ ^a	S ^c
BCl ₃ ^a	C ^c	CH ₂ O ₂ ^a	C ₂ N ₂ ^a	Cl ₂ Hg ^b	D ^c	F ₄ N ₂ ^a	H ₄ Si ^a	N ₂ ^a	S ₂ ^c
BF ₃ ^a	CBrF ₃ ^a	CH ₃ Cl ^a	C ₃ H ₆ ^a	Cl ₂ O ₂ S ^c	DH ^e	F ₄ S ^b	He ^c	N ₂ O ^a	S ₈ ^c
BI ₃ ^b	CClF ₃ ^a	C ₃ H ₉ Cl ₃ Si ^a	C ₃ H ₈ ^a	Cl ₃ FSi ^b	D ₂ ^c	F ₄ Si ^a	Hg ^a	N ₂ O ₃ ^a	Si ^a
B ₂ H ₆ ^a	CClN ^a	CH ₃ F ^a	C ₃ O ₂ ^d	Cl ₃ HSi ^a	D ₂ O ^c	F ₆ Mo ^b	HgI ₂ ^b	N ₂ O ₄ ^a	Sn ^c
Ba ^c	CCl ₂ F ₂ ^a	CH ₃ OH ^a	Ca ^c	Cl ₃ OPa	D ₂ S ^b	F ₆ S ^a	I ^c	Na ^a	Sr ^c
Be ^c	CCl ₂ O ^a	CH ₄ ^a	CaCl ₂ ^a	Cl ₃ P ^a	D ₃ N ^b	F ₆ W ^b	I ₂ Mg ^c	Na ₂ ^c	Ta ^c
Bi ^c	CCl ₃ F ^a	CNNa ^a	Ca ₂ ^c	Cl ₄ OW ^b	F ^c	Fe ^a	I ₄ Si ^b	Nb ^c	U ^c
Bi ₂ ^c	CCl ₄ ^a	CO ^a	Cl ^c	Cl ₄ Si ^a	FH ^a	H ^c	I ₄ Ti ^d	Ne ^c	UF ₆ ^b
BrH ^c	CF ₂ O ^a	COS ^a	ClCu ^a	Cl ₄ Ti ^a	FNO ^b	HI ^a	I ₄ Zr ^b	Ni ^c	V ^c
BrI ^e	CF ₄ ^a	CO ₂ ^a	ClD ^b	Cl ₄ Zr ^b	FNO ₂ ^b	HNO ₃ ^a	K ^a	O ₂ ^a	W ^c
BrK ^a	CHBr ₃ ^c	CS ₂ ^a	ClF ₃ ^c	Cl ₅ Mo ^b	FNa ^a	HNaO ^a	Kr ^c	O ₂ S ^a	Xe ^c
BrNa ^a	CHClF ₂ ^a	C ₂ Cl ₄ ^a	ClF ₃ Si ^b	Cl ₅ Nb ^c	F ₂ ^a	H ₂ ^a	Li ^a	O ₃ ^a	Zn ^c
Br ₂ ^a	CHCl ₂ F ^a	C ₂ Cl ₆ ^a	ClF ₅ ^b	Cl ₅ P ^c	c-F ₂ N ₂ ^d	H ₂ O ^a	Li ₂ ^c	O ₃ S ^a	Zr ^c
Br ₂ Hg ^b	CHCl ₃ ^a	C ₂ F ₃ N ^d	ClF ₅ S ^b						

- a. Ref. [36], Stephenson, R. M., Malanowski, S., Ambrose, D., "Vapor-Liquid Critical Constants of Fluids" in the *Handbook of Thermodynamics of Organic Compound*, Elsevier, New York (1987).
- b. Ref. [35], Daubert, T. E., Danner, R. P., Sibul, H. M. and Stebbins, C. C., *Physical and Thermodynamic Properties of Pure Compounds: Data Compilation*, Taylor & Francis, Bristol, PA (1994).
- c. Ref. [37], McCormick, S., *TAPP (version 2.20) - A Database of Thermochemical And Physical Properties*, E. S. Microware, Hamilton, OH (1996).
- d. Ref. [38], Reid, R. C., Prausnitz, J. M., and Poling, B. E., *The Properties of Gases and Liquids*, 4th ed., McGraw-Hill, New York (1987).
- e. Ref. [39], TRCTHERMO data search (1997).

Appendix A

This table indicates the source of each Lennard-Jones parameters obtained in the literature search.

Table A.3 Species with known Lennard-Jones parameters

Al ^a	B ₂ ^a	CCl ^a	CHO ^b	CS ^a	ClLi ^a	F Mg ^a	HNaO ^a	KO ^b	OP ^a
AlCl ^a	B ₂ H ₆ ^a	CClF ₃ ^a	CH ₂ ^b	CS ₂ ^a	ClMg ^a	F Na ^a	HO ^a	Kr ^a	OS ^b
AlCl ₃ ^a	B ₂ O ₃ ^a	CClN ^a	CH ₂ ClF ^a	C ₂ ^b	ClNO ^a	FO ^a	HO ₂ ^b	K ^b	OSi ^a
AlF ^a	Be ^a	CCl ₂ ^a	CH ₂ Cl ₂ ^a	C ₂ Cl ₄ ^a	ClNa ^a	FP ^a	HS ^a	Li ^a	O ₂ ^b
AlF ₃ ^a	BeBr ₂ ^a	CCl ₂ F ₂ ^a	CH ₂ F ₂ ^a	C ₂ H ^b	ClO ^a	FSi ^a	HSi ^a	LiO ^a	O ₂ S ^b
AlN ^a	BeCl ^a	CCl ₃ ^a	CH ₂ O ^b	C ₂ H ₂ ^a	ClP ^a	F ₂ ^b	H ₂ ^b	Li ₂ ^a	O ₂ Si ^a
AlO ^a	BeCl ₂ ^a	CCl ₃ F ^a	CH ₃ ^b	C ₂ H ₄ ^b	ClSi ^a	F ₂ Mg ^a	H ₂ N ^b	Li ₂ O ^a	O ₃ ^b
AlS ^a	BeF ^a	CCl ₄ ^a	CH ₃ Cl ^a	C ₂ H ₆ ^b	Cl ₂ ^a	F ₂ O ^a	H ₂ N ₂ ^a	Mg ^a	O ₃ S ^b
Al ₂ ^a	BeF ₂ ^a	CF ^a	CH ₃ F ^a	C ₂ N ^b	Cl ₂ H ₂ Si ^b	F ₂ S ₂ ^a	H ₂ O ^b	Mg ₂ ^a	P ^a
Ar ^a	BeI ₂ ^a	CFN ^a	CH ₄ ^b	C ₂ N ₂ ^a	Cl ₂ Hg ^a	F ₃ HSi ^b	H ₂ O ₂ ^b	N ^b	PS ^a
B ^a	Br ^a	CF ₂ ^a	CH ₃ OH ^a	C ₂ O ^b	Cl ₂ Mg ^a	F ₃ N ^a	H ₂ S ^a	NO ^b	P ₂ ^a
BBr ₃ ^a	BrF ^a	CF ₃ ^a	CN ^a	C ₃ H ₆ ^b	Cl ₂ Si ^b	F ₃ P ^a	H ₃ N ^b	NO ₂ ^b	P ₄ ^a
BCl ^a	BrF ₃ ^a	CF ₄ ^a	CNNa ^a	C ₃ H ₈ ^b	Cl ₃ FSi ^a	F ₃ Si ^b	H ₃ P ^a	NP ^a	S ^b
BCl ₂ ^a	BrH ^a	CH ^a	CO ^b	Cl ^a	Cl ₃ P ^a	F ₄ Si ^a	H ₄ N ₂ ^b	N ₂ ^b	S ₂ ^a
BCl ₃ ^a	BrLi ^a	CHBr ₃ ^a	COS ^a	ClF ^a	Cl ₄ Si ^a	F ₆ S ^a	H ₄ Si ^a	N ₂ O ^b	Si ^a
BF ^a	BrNa ^a	CHClF ₂ ^a	CO ₂ ^b	ClF ₃ ^a	D ₂ ^b	H ^b	He ^b	Na ^a	Si ₂ ^a
BF ₂ ^a	Br ₂ ^a	CHCl ₃ ^a	CNN ^b	ClF ₃ Si ^a	F ^a	HI ^a	Hg ^a	NaO ^a	Si ₃ ^b
BF ₃ ^a	Br ₂ Hg ^a	CHF ₃ ^a	CN ₂ ^b	ClH ^a	FH ^b	HK ^b	HgI ₂ ^a	Na ₂ ^a	UF ₆ ^a
BI ₃ ^a	C ^b	CHN ^b	CNO ^b	ClI ^a	FHO ^a	HKO ^b	I ^a	Ne ^a	Xe ^a
BO ^a	CBrF ₃ ^a	CHNO ^b	CP ^a	CIK ^b	FLi ^a	HN ^a	ILi ^a	O ^a	Zn ^a

- a. Ref. [40], Svehla, R. A., *Estimated Viscosities and Thermal Conductivities of Gases at High Temperatures*, NASA Technical Report R-132, (1962).
- b. Ref. [41], Warnatz, J., "Calculation of the Structure of Laminar Flat Flames I: Flame Velocity of Freely Propagating Ozone Decomposition Flames," *Ber. Beunsenges. Phys. Chem.*, **82**, 193 (1978). See also Warnatz, J., "Influence of Transport Models and Boundary Conditions on Flame Structure," in *Numerical Methods in Flame Propagation*, Eds. N. Peters and J. Warnatz, Friedr. Vieweg and Sohn, Wiesbaden (1982).

Appendix B

All the constants in the JCZS database are given here. Information regarding this database should be directed to:

Michael L. Hobbs
Energetic and Multi-phase Processes, Dept. 9112
Engineering Sciences Center
Sandia National Laboratories
Albuquerque, NM 87185-0834

Voice: (505)844-5988
Fax: (505) 844-8251
Email: mlhobbs@sandia.gov

The method used to obtain the force constants are discussed in detail in the text.

Table B.1 The complete JCZS database of r^* and ε/k values

Species	r^*	ε/k	Method	Species	r^*	ε/k	Method
AL	2.98	2750	LJ	BCLF	5.14	150	FIT
AL*	2.98	2750	LJ	BCLF2	5.16	150	FIT
CAL	5.10	300	FIT	BCLO	5.15	350	FIT
ALCL	5.16	500	FIT	BCL2	4.74	682	LJ
ALCLF	5.27	300	FIT	BCL2F	5.44	250	FIT
ALCLF2	5.39	300	FIT	BCL3	5.75	338	LJ
ALCLO	5.29	500	FIT	BF	4.74	300	FIT
ALCL2	5.58	400	FIT	BFO	4.74	300	FIT
ALCL2F	5.70	300	FIT	BF2	3.98	399	LJ
ALCL3	5.76	472	LJ	BF3	4.71	186	LJ
ALF	4.76	200	FIT	BH	4.30	100	FIT
ALFO	4.91	300	FIT	BHO	4.76	450	FIT
ALF2	4.90	150	FIT	BHO2	4.83	400	FIT
ALF3	5.02	150	FIT	BH2	4.30	100	FIT

Appendix B

Table B.1 The complete JCZS database of r^* and ε/k values

Species	r^*	ε/k	Method	Species	r^*	ε/k	Method
ALH	4.71	300	FIT	BH2O2	4.76	200	FIT
ALHO	4.83	150	FIT	BH3	4.30	100	FIT
ALHO2	5.01	500	FIT	BH3O3	4.76	400	FIT
ALN	4.85	100	FIT	BN	4.81	200	FIT
ALO	4.78	100	FIT	BO	4.74	250	FIT
ALS	5.17	700	FIT	BS	5.09	500	FIT
A2CL6	6.98	500	FIT	B2CL4	6.12	325	FIT
AL2O	5.59	500	FIT	B2H6	5.09	100	FIT
AL2O2	5.48	150	FIT	B2O2	5.38	350	FIT
B	2.27	3300	LJ	B2O3	4.67	2092	LJ
B2	5.29	100	FIT	B3CL3O3	7.50	200	FIT
BCL	5.09	700	FIT	B3F3O3	5.93	300	FIT
B3H3O6	6.42	300	FIT	CCL2O	5.25	368	SCS
B3H6N3	5.77	300	FIT	CCL3F	5.74	381	SCS
B5H9	5.57	200	FIT	CCL4	5.98	631	HUG
B10H14	6.51	300	FIT	CF	4.37	300	FIT
BE	2.94	3603	LJ	CFN	4.56	300	FIT
C2BE	5.32	700	FIT	CF2	4.87	94.2	OPT, LJ
BECL	5.20	900	FIT	CF2O	5.59	240	OPT, SCS
BECLF	5.27	325	FIT	CF3	5.65	121	OPT, LJ
BECL2	5.53	400	FIT	CF4	6.40	134	OPT, LJ
BEF	4.89	400	FIT	CH	4.29	100	FIT
BEF2	3.87	1266	LJ	CHCF2	5.14	261	LJ
BEH	4.40	100	FIT	CHC2F	5.80	400	FIT
BEHO	4.90	350	FIT	CHCL3	6.05	340	HUG

Appendix B

Table B.1 The complete JCZS database of r^* and ε/k values

Species	r^*	ε/k	Method	Species	r^*	ε/k	Method
BEH2	4.40	100	FIT	CHFO	4.50	150	OPT, FIT
BEH2O2	4.97	100	FIT	CHF3	5.71	242	OPT, SCS
BEO	4.89	300	FIT	CHN	4.74	400	FIT
BE2CL4	7.40	300	FIT	CHNO	4.80	232	OPT, LJ
BE2O2	5.47	200	FIT	CHO	4.41	400	FIT
BE3O3	6.11	175	FIT	CH2	4.29	50.0	FIT
BE4O4	6.62	150	FIT	CH2CLF	4.86	318	OPT, LJ
BE5O5	7.05	200	FIT	CH2CL	5.26	200	FIT
BE6O6	7.13	200	FIT	CH2F2	4.36	318	OPT, FIT
C	3.70	71.4	LJ	CH2O	4.40	330	OPT, SCS
CCL	4.81	500	FIT	CH3	4.15	144	OPT, LJ
CCLFO	5.06	300	OPT, FIT	CH3CL	4.73	337	SCS
CCLF3	4.71	244	OPT, SCS	CH3CL3SI	6.15	275	FIT
CCLN	4.99	363	SCS	CH3F	4.95	256	OPT, SCS
CH3F3SI	5.34	550	FIT	CLF	4.12	203	LJ
CH4	4.23	154	SCS	CLFLI2	9.50	300	FIT
CH3OH	4.23	482	OPT, LJ	CLFMG	5.43	550	FIT
CN	4.33	75.0	LJ	CLF3	4.81	336	LJ
CNNA	5.58	500	FIT	CLF3SI	5.58	231	LJ
CO	3.88	98.0	OPT, LJ	CLH	3.35	345	OPT, SCS
COS	5.02	200	FIT	CLHO	4.50	350	FIT
CO2	4.22	244	LJ	CLH3SI	5.25	250	LJ
CP	4.94	227	LJ	CLLI	6.00	600	FIT
CS	4.73	199	LJ	CLLIO	7.00	500	FIT
CS2	5.03	467	LJ	CLMG	5.33	700	FIT

Appendix B

Table B.1 The complete JCZS database of r^* and ε/k values

Species	r^*	ε/k	Method	Species	r^*	ε/k	Method
C2	4.06	98.0	LJ	CLNO	4.74	356	LJ
C2F2	4.87	400	FIT	CLNA	5.54	800	FIT
C2F4	6.03	248	OPT, SCS	CLO	4.31	184	LJ
C2H2	4.42	249	LJ	CLO2	4.64	400	FIT
C2H4	4.50	281	OPT, LJ	CLSI	5.08	300	FIT
C2H4O	4.75	380	SCS	CLTI	5.43	200	FIT
C2H6	4.01	252	OPT, LJ	CL2H2SI	5.71	324	LJ
C3H6	5.59	267	LJ	CL2LI2	6.27	300	FIT
C3H8	5.59	267	LJ	CL2MG	6.00	500	FIT
C2N2	5.30	324	SCS	CL2O	5.07	300	FIT
C3	5.05	300	FIT	CL2SI	5.51	300	FIT
C3O2	5.22	361	OPT, LJ	CL2TI	6.30	500	FIT
C4	5.32	700	FIT	CL2ZR	6.25	500	FIT
C4N2	7.00	350	FIT	CL3FSI	6.22	329	LJ
C5	7.00	300	FIT	CL3HSI	5.89	388	SCS
CL	4.06	131	LJ	CL3LI3	7.10	250	FIT
CL3OP	5.79	350	FIT	F2O	4.35	161	LJ
CL3P	5.88	419	LJ	F2OS	4.78	150	FIT
CL3PS	6.12	200	FIT	F2O2S	4.89	100	FIT
CL3TI	6.15	300	FIT	F2P	4.69	100	FIT
F2FE	5.09	300	FIT	F2SI	4.81	100	FIT
CL3ZR	6.25	300	FIT	F3FE	5.26	250	FIT
CL4SI	6.71	390	LJ	F4S	4.81	294	SCS
CL4TI	6.38	516	SCS	F2TI	5.25	300	FIT
CL4ZR	6.24	629	SCS	F2ZR	5.46	150	FIT

Appendix B

Table B.1 The complete JCZS database of r^* and ε/k values

Species	r^*	ε/k	Method	Species	r^*	ε/k	Method
CL5P	5.94	523	SCS	F3HSI	5.25	181	LJ
F	3.33	113	LJ	F3LI3	6.31	200	FIT
FH	3.70	330	OPT, LJ	F3N	4.49	189	SCS
FHO	3.95	400	FIT	F3P	4.89	203	LJ
FH3SI	4.88	200	FIT	F3TI	5.35	100	FIT
FLI	5.05	1000	FIT	OS2	5.06	300	FIT
FLIO	6.00	500	FIT	F3ZR	5.54	100	FIT
FMG	4.98	200	FIT	F4SI	5.05	172	LJ
FN	4.01	300	FIT	F4TI	5.48	100	FIT
FNO	4.25	200	FIT	F4ZR	5.63	100	FIT
FNA	5.24	300	FIT	F6S	5.09	100	FIT
FO	3.83	110	LJ	H	2.00	145	OPT, LJ
FP	4.63	271	LJ	HLI	5.02	75.0	FIT
FPS	5.12	500	FIT	HLIO	5.11	500	FIT
FSI	4.67	150	FIT	HMG	4.94	200	FIT
F2H2SI	4.94	200	FIT	HMGO	5.07	300	FIT
F2LI2	5.57	150	FIT	HN	3.72	65.0	LJ
F2MG	5.11	200	FIT	HNA	5.13	50.0	FIT
HNAO	4.27	1962	LJ	NP	4.61	125	FIT
HO	3.29	80.0	OPT, LJ	NS	4.54	150	FIT
HP	4.42	200	FIT	NSI	4.76	100	FIT
HS	4.38	847	LJ	N2O	4.30	232	OPT, LJ
HSI	4.60	200	FIT	N2O3	5.30	344	SCS
H2LI2O2	5.60	200	FIT	N2O4	7.00	100	FIT
H2N	3.87	150	FIT	N2O5	7.00	100	FIT

Appendix B

Table B.1 The complete JCZS database of r^* and ε/k values

Species	r^*	ε/k	Method	Species	r^*	ε/k	Method
H2O	3.06	356	REE	NA	4.00	1375	LJ
H2O2	3.90	591	SCS	NAO	5.26	300	FIT
H2P	4.51	150	FIT	NA2	6.12	400	FIT
H2S	4.07	301	LJ	O	3.42	107	LJ
H3N	3.33	481	LJ	OP	4.69	264	LJ
H3P	4.58	100	FIT	OS	4.48	301	LJ
H4N2	4.75	205	LJ	OSI	3.79	569	LJ
H4SI	4.66	218	LJ	OTI	5.08	75.0	FIT
LI	3.30	3305	LJ	OZR	5.34	100	FIT
LIN	5.15	500	FIT	O2P	4.70	200	FIT
LIO	5.08	500	FIT	O2S	4.53	348	SCS
LIO2	5.17	150	FIT	O2SI	4.84	200	FIT
LI2	5.90	250	FIT	O2TI	5.17	100	FIT
LI2O	5.89	500	FIT	O2ZR	5.42	100	FIT
MG	3.28	1614	LJ	O3	4.60	180	LJ
MGO	5.00	150	FIT	O3S	4.59	397	LJ
MGS	5.35	400	FIT	O6P4	6.08	100	FIT
N	3.70	71.0	LJ	O10P4	7.50	100	FIT
NO	4.15	117	OPT, LJ	P	4.62	50.0	FIT
NO2	4.77	349	OPT, SCS	PS	4.97	200	FIT
P2	5.02	200	FIT	HI	4.53	343	LJ
P4	6.11	300	FIT	I	4.85	211	LJ
P4S3	6.92	500	FIT	ILI	7.00	500	FIT
S	4.31	50.0	FIT	I2LI2	6.64	300	FIT
SSI	5.09	300	FIT	ALBR	5.32	1000	FIT

Appendix B

Table B.1 The complete JCZS database of r^* and ε/k values

Species	r^*	ε/k	Method	Species	r^*	ε/k	Method
S2	4.92	200	FIT	ALBR3	6.18	617	SCS
S8	7.07	100	FIT	ALI	6.5	500	FIT
SI	5.62	4174	LJ	ALI3	6.77	795	SCS
SIOH	5.01	250	FIT	AL2BR6	7.33	200	FIT
OHSI	5.58	400	FIT	AL2I6	9.00	200	FIT
SI2	5.31	200	FIT	BBR	5.26	1000	FIT
SI3	6.50	500	FIT	BBR3	5.91	470	SCS
TI	4.00	100	FIT	BI3	6.63	570	LJ
ZR	4.50	100	FIT	BEBR	5.33	1000	FIT
CCL2F2	5.49	311	SCS	BEBR2	5.78	700	FIT
FTI	5.12	100	FIT	BEI	6.00	1000	FIT
LINA0	5.88	700	FIT	BEI2	6.18	1000	FIT
CLZR	5.64	300	FIT	BRHG	5.75	300	FIT
FZR	5.36	100	FIT	BRK	6.21	2850	SCS
BF2H	4.79	150	FIT	BRTI	5.59	1000	FIT
BR	4.12	237	LJ	BR2K2	6.95	300	FIT
BRH	4.24	294	SCS	BR4TI	6.86	644	SCS
BRLI	6.50	500	FIT	CLHG	5.64	500	FIT
BR2	4.69	473	LJ	CLK	7.81	2810	LJ
BR2LI2	6.36	200	FIT	CL2K2	6.77	200	FIT
BF2O	4.74	150	FIT	FHG	5.37	150	FIT
CCL0	4.92	250	FIT	FK	5.26	200	FIT
F2HG	5.48	200	FIT	FI	4.97	300	FIT
F2K2	6.17	200	FIT	FNO2	4.46	283	SCS
HG	3.50	1400	SCS	FPB	5.38	300	FIT

Appendix B

Table B.1 The complete JCZS database of r^* and ε/k values

Species	r^*	ε/k	Method	Species	r^*	ε/k	Method
HGI	5.95	300	FIT	F2PB	5.51	300	FIT
IK	7.00	500	FIT	F5I	5.41	100	FIT
I2K2	7.24	350	FIT	F7I	5.61	100	FIT
CFO	4.71	200	OPT, FIT	HKO	5.07	1213	LJ
I2TI	7.50	400	FIT	HPB	5.31	150	FIT
I4TI	7.27	841	SCS	HGI2	5.85	867	LJ
K	4.77	850	LJ	INO	6.00	500	FIT
K2	7.00	500	FIT	IPB	5.99	500	FIT
W	5.40	1000	FIT	I2PB	6.57	500	FIT
BBR2	5.69	300	FIT	I4ZR	7.39	777	SCS
BI2	6.08	400	FIT	OPB	5.37	300	FIT
C2F6	7.36	237	OPT, SCS	PB	5.26	50.0	FIT
FFE	4.96	100	FIT	PB2	6.29	300	FIT
BRNO	5.50	500	FIT	BLIO2	6.50	300	FIT
BRPB	5.79	500	FIT	BRF	4.29	239	LJ
BR2HG	5.70	686	LJ	BRF3	4.90	482	LJ
BR2PB	6.24	500	FIT	BR4PB	6.94	300	FIT
BR2ZR	6.90	400	FIT	CKN	5.67	500	FIT
BR4ZR	6.86	651	SCS	C2K2N2	7.20	300	FIT
CLI	5.26	437	LJ	F4OW	5.71	50.0	FIT
CLPB	5.61	500	FIT	F4PB	5.70	100	FIT
CL2HG	6.20	500	FIT	H2K2O2	6.39	200	FIT
CL2PB	6.02	500	FIT	I2ZR	6.50	400	FIT
CL4PB	6.59	300	FIT	CU	4.69	50.0	FIT
I4PB	7.46	300	FIT	B2BEO4	6.70	300	FIT

Appendix B

Table B.1 The complete JCZS database of r^* and ε/k values

Species	r^*	ε/k	Method	Species	r^*	ε/k	Method
OW	5.47	100	FIT	BEF3LI	5.11	400	FIT
O2W	5.73	100	FIT	BRN	4.75	500	FIT
O3W	5.62	100	FIT	BR5W	7.08	200	FIT
O9W3	7.18	200	FIT	BR6W	7.52	100	FIT
ALF4LI	6.00	300	FIT	CLS	4.91	300	FIT
BBRCL2	5.81	400	FIT	CLNO2	4.90	300	FIT
BBRF2	5.31	300	FIT	CL5W	6.70	100	FIT
BBR2CL	5.93	450	FIT	CL6W	6.87	100	FIT
BBR2F	5.70	300	FIT	F2N	4.24	150	FIT
BF4K	6.70	300	FIT	H2O4W	5.68	200	FIT
CBRN	6.00	500	FIT	KO	5.29	150	FIT
BRCL	5.04	500	FIT	B3FH2O3	5.75	300	FIT
BRF5	5.26	100	FIT	B3F2HO3	6.00	300	FIT
BRI	4.73	582	SCS	B3HO	5.13	350	FIT
CIN	6.50	500	FIT	BR3OP	6.14	300	FIT
CL2O2W	6.14	300	FIT	BR3PS	6.43	300	FIT
CL2W	6.02	500	FIT	CLF2OP	5.33	300	FIT
CL4OW	6.36	633	FIT	CL2FOP	5.53	300	FIT
CL4W	6.52	200	FIT	FNO3	4.73	200	FIT
FW	5.47	100	FIT	F3OP	4.94	150	FIT
F6W	5.77	50.0	FIT	F3PS	5.52	280	SCS
BBRCL	6.00	500	FIT	HK	5.16	100	FIT
BBRF	5.29	500	FIT	HNO	4.06	500	FIT
BBRO	5.70	500	FIT	O12W4	8.20	200	FIT
CB	5.00	100	FIT	BI	6.30	500	FIT

Appendix B

Table B.1 The complete JCZS database of r^* and ε/k values

Species	r^*	ε/k	Method	Species	r^*	ε/k	Method
BF2HO	4.83	300	FIT	BO2	4.82	100	FIT
BEN	4.96	300	FIT	F2NA2	6.02	200	FIT
BRP	5.15	800	FIT	F4MG2	6.70	300	FIT
CLP	5.11	454	SCS	ITI	6.50	500	FIT
F5P	5.04	100	FIT	I3TI	6.95	300	FIT
HHG	5.32	100	FIT	I3ZR	6.95	300	FIT
HNO2	4.89	200	FIT	BRNA	6.72	400	FIT
NO2H	4.91	300	FIT	BRZR	5.77	300	FIT
HNO3	4.80	421	SCS	BR2NA2	6.74	300	FIT
HZR	5.31	150	FIT	IZR	6.02	700	FIT
NZR	5.41	200	FIT	B2F4	5.30	100	FIT
BE2O	5.61	300	FIT	CL2NA2	6.55	150	FIT
CLOTI	5.49	300	FIT	NO3	4.60	150	FIT
CL2OTI	5.85	350	FIT	NO3*	4.37	150	FIT
FOTI	5.18	200	FIT	BNAO2	6.20	300	FIT
F2OSI	4.95	200	FIT	FE	2.77	7556	SCS
F2OTI	5.27	100	FIT	FE*	2.77	7556	SCS
F3SI	4.89	310	LJ	CF4O	6.40	200	OPT, FIT
BR3P	6.11	575	SCS	CCL2	5.27	213	LJ
CBR4	6.34	200	FIT	CCL3	5.97	268	LJ
ALOH	4.91	600	FIT	CLFE	5.28	200	FIT
F4N2	5.46	250	SCS	CL2FE	5.90	500	FIT
HO2	3.97	300	FIT	CL3FE	6.04	300	FIT
LI2O2	5.68	100	FIT	CL6FE2	9.00	100	FIT
MGN	5.09	150	FIT	FEO	4.98	150	FIT

Appendix B

Table B.1 The complete JCZS database of r^* and ε/k values

Species	r^*	ε/k	Method	Species	r^*	ε/k	Method
BR2TI	6.50	400	FIT	F2N2	4.62	220	SCS
BR3TI	6.43	300	FIT	F2N2T	4.61	210	SCS
BR3ZR	6.50	300	FIT	H2N2	4.26	71.0	LJ
BBR2H	5.68	300	FIT	LINO	5.7	500	FIT
BCL2H	5.42	200	FIT	O6W2	6.5	200	FIT
B2H4O4	5.80	300	FIT	O8W3	9.5	200	FIT
C2N2NA	6.80	300	FIT	C2H	4.60	209	LJ
CLCU	5.19	250	FIT	CL10W2	7.85	200	FIT
CL3CU3	6.75	250	FIT	ACIDG	4.99	200	FIT
H2NA2O2	6.14	200	FIT	MO	5.21	100	FIT
ALBO2	5.52	500	FIT	CSI	5.03	250	FIT
BBEO2	6.00	500	FIT	CSI2	6.0	500	FIT
B2O	5.34	300	FIT	C2N	4.30	232	LJ
BE2F2O	6.00	300	FIT	C2SI	5.7	500	FIT
BRMG	6.50	300	FIT	NSI2	5.50	600	FIT
BR2MG	6.50	500	FIT	BRW	5.85	300	FIT
CNN	4.30	232	LJ	CBR	5.00	1000	FIT
CN2	4.30	232	LJ	CLW	5.73	500	FIT
C2O	4.30	232	LJ	H2MGO2	6.0	300	FIT
CLF5	5.16	100	FIT	HGO	5.38	200	FIT
CUF	4.84	100	FIT	MOO	5.30	100	FIT
CUF2	4.97	300	FIT	C2CL4	5.74	502	SCS
FEH2O2	5.42	300	FIT	C2CL6	6.20	300	FIT
BR2FE	6.50	400	FIT	COBALT	4.79	50.0	FIT
BR4FE2	9.00	200	FIT	C2HF	5.50	500	FIT

Appendix B

Table B.1 The complete JCZS database of r^* and ε/k values

Species	r^*	ε/k	Method	Species	r^*	ε/k	Method
CUO	4.86	150	FIT	ALO2	4.95	300	FIT
CU2	5.49	200	FIT	CLCS	6.08	700	FIT
FO2	4.20	300	FIT	CL2CS2	7.38	300	FIT
FEI2	7.00	500	FIT	CESIUM	5.71	50.0	FIT
FE2I4	6.58	100	FIT	CSF	5.81	200	FIT
CESIU2	6.99	1000	FIT	CAHO	5.29	500	FIT
CS2F2	6.82	300	FIT	CL2MOO2	5.94	200	FIT
MGOH	5.07	300	FIT	COF2	5.04	200	FIT
MOO2	5.38	100	FIT	F3NO	4.82	245	SCS
MOO3	5.46	100	FIT	F4MOO	5.58	100	FIT
C2CL2	6.50	300	FIT	F6MO	5.68	50.0	FIT
C2HCL	6.20	500	FIT	H2MOO4	5.61	200	FIT
CA	5.07	50.0	FIT	B2F4O	5.62	300	FIT
CAF	5.21	150	FIT	BA	5.69	50.0	FIT
CAF2	5.36	300	FIT	CNO	4.89	232	OPT, LJ
CL4MO	6.48	200	FIT	CL4FE2	9.00	200	FIT
CL5MO	6.68	100	FIT	N3	4.41	300	FIT
CL6MO	6.86	100	FIT	SR	5.32	50.0	FIT
CSO	5.83	300	FIT	BKO2	5.85	300	FIT
CS2O	6.90	500	FIT	CLFO2S	5.27	300	FIT
CBRF3	5.62	235	LJ	CL2O2S	5.55	441	SCS
CF3I	5.46	300	FIT	CSHO	6.50	500	FIT
CHCL	4.82	400	FIT	CS2H2O2	7.02	300	FIT
CHF	4.41	300	FIT	FHO3S	4.87	500	FIT
CHP	4.89	700	FIT	BACL	6.02	500	FIT

Appendix B

Table B.1 The complete JCZS database of r^* and ε/k values

Species	r^*	ε/k	Method	Species	r^*	ε/k	Method
C2F3N	5.86	252	OPT, SCS	BACL2	6.37	500	FIT
CL3SI	5.87	300	FIT	BAF	5.77	100	FIT
CL4MG2	9.00	100	FIT	BAF2	5.88	150	FIT
ALF4NA	6.50	300	FIT	CLSR	5.73	350	FIT
AL2F6	5.77	300	FIT	CL2SR	6.09	500	FIT
CACL	5.53	300	FIT	FSR	5.43	100	FIT
CACL2	6.50	500	FIT	F2SR	5.57	200	FIT
NB	5.23	50.0	FIT	CAI	7.00	500	FIT
TA	5.40	50.0	FIT	CAI2	8.00	300	FIT
CR	4.90	50.0	FIT	ISR	6.08	1000	FIT
PBS	5.70	1000	FIT	I2SR	8.20	300	FIT
V	4.94	50.0	FIT	BABR	6.15	300	FIT
OSR	5.45	200	FIT	BABR2	7.70	300	FIT
CLCO	5.26	200	FIT	BRCA	5.66	1000	FIT
CL2CO	6.00	500	FIT	BRSR	5.86	400	FIT
CL3CO	5.96	200	FIT	BR5NB	7.11	100	FIT
CL4CO2	9.00	100	FIT	CAO	5.22	100	FIT
CRN	5.07	100	FIT	CA2	6.19	1000	FIT
CRO	5.01	100	FIT	CL5NB	6.71	650	SCS
CRO2	5.12	100	FIT	CL5TA	6.74	621	SCS
CRO3	5.22	100	FIT	IMG	6.20	1000	FIT
NV	5.10	100	FIT	I2MG	7.00	500	FIT
NBO	5.30	100	FIT	MG2	5.83	500	FIT
NBO2	5.47	100	FIT	BAHO	6.30	500	FIT
OTA	5.46	100	FIT	HOSR	6.00	500	FIT

Appendix B

Table B.1 The complete JCZS database of r^* and ε/k values

Species	r^*	ε/k	Method	Species	r^*	ε/k	Method
OV	5.04	50.0	FIT	BHS	5.10	700	FIT
O2TA	5.52	100	FIT	BAH2O2	6.00	300	FIT
O2V	5.13	100	FIT	CAH2O2	6.50	300	FIT
BAI	6.35	500	FIT	H2O2SR	6.70	300	FIT
BAI2	8.50	300	FIT	ALF2O	5.05	200	FIT
BAO	5.80	200	FIT	FS	4.45	100	FIT
BR2CA	7.20	300	FIT	F2S	4.64	100	FIT
BR2SR	7.60	300	FIT	FSSF	5.19	300	FIT
BR4MG2	9.50	200	FIT	F2S2	5.28	206	LJ
F3S	4.81	207	FIT	D2S	4.40	100	DEUT
F5S	5.03	100	FIT	D3N	3.80	328	SCS
I4SI	7.52	764	SCS	BAS	6.05	500	FIT
BRH3SI	5.60	500	FIT	BES	5.50	550	FIT
BRSI	6.20	500	FIT	CAS	5.56	300	FIT
BR2H2SI	5.70	200	FIT	CLNI	5.23	250	FIT
BR2SI	5.78	500	FIT	CL2NI	5.63	550	FIT
BR3HSI	6.78	644	SCS	FES	5.31	250	FIT
BR4SI	6.15	494	SCS	SSR	5.77	400	FIT
HI3SI	6.73	300	FIT	BRF5S	5.61	200	FIT
H2I2SI	6.18	500	FIT	BR3SI	6.22	300	FIT
H3ISI	6.50	500	FIT	CF8S	5.55	150	FIT
ISI	6.20	500	FIT	CLF5S	5.37	316	SCS
I2SI	6.21	500	FIT	F10S2	5.88	250	FIT
NI	4.73	50.0	FIT	I3SI	6.76	350	FIT
NIS	5.25	300	FIT	C4NIO4	6.40	300	FIT

Appendix B

Table B.1 The complete JCZS database of r^* and ε/k values

Species	r^*	ε/k	Method	Species	r^*	ε/k	Method
D	2.30	145	DEUT	C5FEO5	6.29	300	FIT
CLD	3.75	345	DEUT	CL2S2	6.50	200	FIT
DF	3.53	330	DEUT	CLS2	5.40	400	FIT
DH	3.66	38.0	DEUT	CL2S	5.40	350	FIT
DHO	3.50	524	AVE	K2O4S	5.70	350	FIT
DN	3.72	65.0	DEUT	NA2O4S	6.26	300	FIT
DO	3.53	80.0	DEUT	MOBR	5.72	250	FIT
DS	4.38	847	DEUT	MOBR2	6.70	400	FIT
D2N	3.86	100	FIT	MOBR3	6.52	350	FIT
D2N2	4.11	200	FIT	MOBR4	6.82	200	FIT
D2O	3.50	521	SCS	IMO	5.94	500	FIT
I2MO	7.40	400	FIT	XE	4.54	231	LJ
I3MO	6.98	400	FIT	SN	4.94	50.0	FIT
I4MO	7.40	250	FIT	SNF	5.12	300	FIT
FMO	5.29	100	FIT	SNF2	5.28	300	FIT
F2MO	5.38	200	FIT	SNO	5.08	200	FIT
F3MO	5.46	100	FIT	CH2O2	4.44	200	OPT, FIT
F4MO	5.54	100	FIT	MN	4.86	50.0	FIT
F5MO	5.58	50.0	FIT	MNS	5.39	300	FIT
Li2O4S	7.00	300	FIT	BIZ	4.94	50.0	FIT
ZN	2.93	2565	SCS	BIZ2	5.93	500	FIT
CLDO	4.50	350	FIT	BIF	5.15	800	FIT
F10MO2	6.55	200	FIT	BIF3	5.52	400	FIT
F15MO3	9.00	200	FIT	UGAS	3.61	50.0	FIT
HF	3.64	2000	FIT	UF	5.20	500	FIT

Appendix B

Table B.1 The complete JCZS database of r^* and ε/k values

Species	r^*	ε/k	Method	Species	r^*	ε/k	Method
AL2	5.46	250	FIT	UF2	5.30	500	FIT
CS2O4S	7.75	300	FIT	UF3	5.50	300	FIT
CL2	4.73	316	LJ	UF4	5.50	300	FIT
F2	3.71	126	LJ	UF5	5.39	300	FIT
H2	2.85	38.0	HUG	UF6	5.53	100	FIT
N2	4.00	102	SCS	CHBR3	5.98	559	LJ
O2	3.86	125	SCS	F2H2	2.60	2000	FIT
AR	3.98	93.3	LJ	F3H3	2.20	2000	FIT
D2	3.31	39.3	LJ	F4H4	2.20	2000	FIT
HE	2.89	10.2	LJ	F5H5	2.20	2000	FIT
KR	4.10	179	LJ	F6H6	2.20	2000	FIT
NE	3.17	33.0	LJ	F7H7	2.20	2000	FIT

Appendix C

Appendix C

Appendix C contains the CHEETAH input deck for the explosives listed in Table 2, the Formula deck with all the explosives in the CHEETAH input deck, the DAKOTA input deck, C-shell script used in the DAKOTA optimization, the FORTRAN code used to construct the APREPRO include file for the DAKOTA optimization, a FORTRAN code used to calculate the root mean square error, rms.f., and the CHEETAH input deck for the explosives listed in Table 5.

CHEETAH INPUT DECK FOR THE EXPLOSIVES LISTED IN TABLE 2

```
# Template for standard CHEETAH run
library file, jc2.chl
gas eos, jc2
set, jc2, m,    6
set, jc2, l,    13
##dp12
composition, dp12, 100.
hug0, p, 1, rho, 1.26
c-j
##afx902
composition, nq, 95, viton, 5
hug0, p, 1, rho, 1.742
c-j
##fefo
composition, fefo, 100.
hug0, p, 1, rho, 1.61
c-j
##fm1
composition, fefo, 23, mf-1, 52, bdnpf, 25
hug0, p, 1, rho, 1.509
c-j
##pf
composition, picfluoride, 100.
hug0, p, 1, rho, 1.833
c-j
##rx36ah
composition, hmx, 51.32, btf, 43.68, viton, 5
hug0, p, 1, rho, 1.830
c-j
##rx41ab
composition, k-6, 95, viton, 5
hug0, p, 1, rho, 1.857
c-j
##lx17
composition, tatab, 92.5, kel-f, 7.5
hug0, p, 1, rho, 1.905
c-j
##rx27ad
composition, tacot, 92.5, kel-f, 7.5
hug0, p, 1, rho, 1.638
c-j
##rx45aa
composition, anta, 95, kel-f, 5
hug0, p, 1, rho, 1.752
c-j
##rx47aa
composition, cl-14, 92.51, kel-f, 7.49
```

Appendix C

```
hug0, p, 1, rho, 1.823
c-j
##rx48aa
composition, adnbf, 92.37, kel-f, 7.63
hug0, p, 1, rho, 1.848
c-j
composition, fefo, 100.
hug0, p, 1, rho, 1.59
c-j
# The following entry is for LX04
composition, hmx, 85., viton, 15.
hug0, p, 1, rho, 1.86
c-j
# The following entry is for LX07
composition, hmx, 90., viton, 10.
hug0, p, 1, rho, 1.87
c-j
composition, LX9, 100.
hug0, p, 1, rho, 1.84
c-j
# The following entry is for LX10
composition, hmx, 95., viton, 5.
hug0, p, 1, rho, 1.86
c-j
# The following entry is for LX11
composition, hmx, 80., viton, 20.
hug0, p, 1, rho, 1.86
c-j
# The following entry is for LX15
composition, hns, 95., kel-f, 5.
hug0, p, 1, rho, 1.58
c-j
# The following entry is for LX17
composition, tatb, 92.5, kel-f, 7.5
hug0, p, 1, rho, 1.91
c-j
composition, PBX9010, 100.
hug0, p, 1, rho, 1.78
c-j
composition, BKWC9404, 100.
hug0, p, 1, rho, 1.84
c-j
composition, PBX9407, 100.
hug0, p, 1, rho, 1.60
c-j
# The following entry is for PBX-9502
composition, tatb, 95.0, kel-f, 5.0
hug0, p, 1, rho, 1.91
c-j
# The following entry is for PBX-9503
composition, tatb, 80.0, hmx, 15, kel-f, 5.0
hug0, p, 1, rho, 1.90
c-j
STOP
```

Formula deck with all the explosives in the CHEETAH input deck is also included.

```
#Lawrence Livermore National Laboratory CHEETAH Reactant Library V1.0
# Explosives
for, be, 0.0, 5.0, 0.0, be, 1
```

Appendix C

for, lithium din, -63300.0, 45.919, 0, li, 1, n, 3, o, 4
for, al, 0., 9.985, 0., al, 1
for, k2so4, -343640.0, 65.488, 0.0, k, 2, s, 1, o, 4
for, sio2, -215940., 26.12, 0., si, 1, o, 2
for, adn, -35700., 68.92, 0., h, 4, n, 4, o, 4
for, adnbf, 36790., 126.8, 0., c, 6, h, 3, n, 5, o, 6
for, ammazole, 20400., 44.65, 0., h, 4, n, 4
for, ammpicrate, 000., 143.27, 0., c, 6, h, 6, n, 4, o, 7
for, anpz, -5400., 111.0, 0., c, 4, h, 4, n, 6, o, 4
for, anta, 14400., 70.96, 0., c, 2, h, 3, n, 5, o, 2
for, bicyclohmx, 25000., 157.46, 0., c, 4, h, 6, n, 8, o, 8
for, btf, 144500., 132.62, 0., c, 6, n, 6, o, 6
for, cl-12, 81000., 214.80, 0., c, 6, h, 6, n, 12, o, 12
for, cl-14, 20630., 131.89, 0., c, 6, h, 4, n, 6, o, 6
for, cl-20, 90000., 214.38, 0., c, 6, h, 6, n, 12, o, 12
for, datb, -29230., 132.35, 0., c, 6, h, 5, n, 5, o, 6
for, dftnb, -49690., 132.90, 0., c, 6, h, 1, n, 3, o, 6, f, 2
for, dina, -75400., 161.4, 0., c, 4, h, 8, n, 4, o, 8
for, dipam, -20100., 249.03, 0., c, 12, h, 6, n, 8, o, 12
for, dipehn, -233790., 321.59, 0., c, 10, h, 16, n, 6, o, 19
for, dnb, -6200., 106.73, 0., c, 6, h, 4, n, 2, o, 4
for, dnbt, 94000., 125.6, 0., c, 4, h, 2, n, 8, o, 4
for, dnbtzl, 0., 113.7, 0., c, 6, h, 3, n, 5, o, 4
for, dni24, 4900., 108.96, 0., c, 3, h, 2, n, 4, o, 4
for, dnpa, -110000., 138.84, 0., c, 6, h, 8, n, 2, o, 6
for, dnt, -16300., 119.72, 0., c, 7, h, 6, n, 2, o, 4
for, dp12, -48000., 116.00, 0., c, 3, h, 6, n, 2, f, 4
for, edd, -155766., 118.01, 0., c, 2, h, 10, n, 4, o, 6
for, edna, -24706., 87.78, 0., c, 2, h, 6, n, 4, o, 4
for, ednp, -140000., 172.02, 0., c, 7, h, 12, n, 2, o, 6
for, ethcarb, -138900., 66.66, 0., c, 3, h, 4, o, 3
for, ethpicrate, -48020., 165.93, 0., c, 8, h, 7, n, 3, o, 7
for, fefo, -177530., 199.20, 0., c, 5, h, 6, n, 4, o, 10, f, 2
for, hk6, 25000., 115.1, 0., c, 3, h, 5, n, 5, o, 5
for, hmx, 17930., 155.46, 0., c, 4, h, 8, n, 8, o, 8
for, hnb, 15700., 172.33, 0., c, 6, n, 6, o, 12
for, hnab, 67900., 251.37, 0., c, 12, h, 4, n, 8, o, 12
for, hndp, 9570., 267.81, 0., c, 12, h, 5, n, 7, o, 12
for, hne, 28600., 162.22, 0., c, 2, n, 6, o, 12
for, hns, 18700., 258.80, 0., c, 14, h, 6, n, 6, o, 12
for, hnx, 104000., 206.1, 0., c, 8, h, 5, o, 6, n, 13
for, hydrazine, 12050., 19.02, 0., h, 4, n, 2
for, hydnitrate, -59000., 56.41, 0., h, 5, n, 3, o, 3
for, k-6, -10000., 122.2, 0., c, 3, h, 4, n, 6, o, 7
for, licom, -78400., 114.9, 0., c, 2, h, 3, n, 5, o, 6, li, 1, cl, 1
for, medina, -13840., 78.42, 0., c, 1, h, 4, n, 4, o, 4
for, mf-1, -160115., 206.10, 0., c, 6, h, 9, n, 4, o, 10, f, 1
for, ng, -88600., 142.29, 0., c, 3, h, 5, n, 3, o, 9
for, nglycol, -58250., 102.5, 0., c, 2, h, 4, n, 2, o, 6
for, nibtn, -54600., 170.3, 0., c, 4, h, 6, n, 4, o, 11
for, nm, -27030., 54.02, 0., c, 1, h, 3, n, 1, o, 2
for, nq, -22100., 58.63, 0., c, 1, h, 4, n, 4, o, 2
for, nto, -28000., 67.39, 0., c, 2, h, 2, n, 4, o, 3
for, petn, -128700., 177.61, 0., c, 5, h, 8, n, 4, o, 12
for, petrin, -134000., 176.0, 0., c, 5, h, 9, n, 3, o, 10
for, picchloride, 6410., 137.78, 0., c, 6, h, 2, n, 3, o, 6, cl, 1
for, picfluoride, -62000., 126.1, 0., c, 6, h, 2, n, 3, o, 6, f, 1
for, picric acid, -51300., 129.44, 0., c, 6, h, 3, n, 3, o, 7
for, pran, 50000., 158.4, 0., c, 7, h, 4, n, 8, o, 6
for, pzo, -3100., 113.0, 0., c, 4, h, 4, n, 6, o, 5

Appendix C

for, rdx, 14710., 122.99, 0., c, 3, h, 6, n, 6, o, 6
for, styp acid,-103900., 133.9, 0., c, 6, h, 3, n, 3, o, 8
for, tacot, 110500., 209.85, 0., c, 12, h, 4, n, 8, o, 8
for, tatab, -36850., 133.21, 0., c, 6, h, 6, o, 6, n, 6
for, tena, -11690., 146.28, 0., c, 6, h, 3, n, 5, o, 8
for, tetrazene, 45200., 110.71, 0., c, 2, h, 8, n, 10, o, 1
for, tetryl, 4670., 165.98, 0., c, 7, h, 5, n, 5, o, 8
for, tna, -17790., 129.46, 0., c, 6,h, 4, n, 4, o, 6
for, tnan, -36610., 150.99, 0., c, 7, h, 5, n, 3, o, 7
for, tnaz, 2800., 104.40, 0., c, 3, h, 4, n, 4, o, 6
for, tnb, -8480., 121.00, 0., c, 6, h, 3, n, 3, o, 6
for, tnc, -60290., 144.70, 0., c, 7, h, 5, n, 3, o, 7
for, tneb, -21650., 148.87, 0., c, 8, h, 7, n, 3, o, 6
for, tneoc, -282130., 397.9, 0., c, 9, h, 8, n, 12, o, 28
for, tngu, 12000., 157.9, 0., c, 4, h, 2, n, 8, o, 10
for, tnm, 13000., 118.81, 0., c, 1, n, 4, o, 8
for, tnp, 79000., 120.96, 0., c, 5, h, 2, n, 4, o, 6
for, tnt, -15000., 137.3, 0., c, 7, h, 5, n, 3, o, 6
for, urea, -79610., 45.39, 0., c, 1, h, 4, n, 2, o, 1
for, ureanit, -130610., 73.21, 0., c, 1, h, 5, n, 3, o, 4

binders

for, cabosil, -215940., 27.31, 0., si, 1, o, 2
for, cellulose, -230800., 179.96, 0., c, 6, h, 10, o, 5
for, estane, -184820., 165.02, 0., c, 10, h, 14.59, n, 0.37, o, 3.42
for, ethglycol, -108700., 55.97, 0., c, 2, h, 6, o, 2
for, eva, 250000., 3942.4, 0., c, 240, h, 440, o, 40
for, for, -60700., 39.72, 0., c, 1, h, 3, n, 1, o, 1
for, gap, 28200., 75.79, 0., c, 3.13, h, 5.25, n, 2.87, o, 1.06
for, hdi, 9400., 132.82, 0., c, 8, h, 8, n, 2, o, 2
for, htpb, -620., 147.05, 0., c, 10, h, 15.71, n, 0.13, o, 0.12
for, ipdi, -58000., 210.11, 0., c, 12, h, 18, n, 2, o, 2
for, kel-f, -578000., 204.68, 0., c, 8, h, 2, f, 11, cl, 3
for, kraton, -161230., 769.52, 0., c, 51, h, 87
for, lecithin, -252860., 720.24, 0., c, 36, h, 76, n, 4, o, 7
for, melamine, -20810., 80.18, 0., c, 3, h, 6, n, 6
for, n-100, 9082., 419.82, 0., c, 23, h, 38, n, 6, o, 5
for, ncellulose-11, -180000., 164.80, 0., c, 6, h, 8, n, 2, o, 9
for, ncellulose-12, -174000., 159.61, 0., c, 6, h, 7.74, n, 2.26, o, 9.52
for, ncellulose-13, -163000., 171.45, 0., c, 6, h, 7.29, n, 2.71, o, 10.41
for, ncellulose-14, -156000., 179.10, 0., c, 6, h, 7, n, 3, o, 11
for, paraffin, -183000., 396.28, 0., c, 25, h, 52
for, pcl, -371008., 928.11, 0., c, 46, h, 72, o, 23
for, pe, -12700., 30.16, 0., c, 2, h, 4
for, pgn, 68000., 82.12, 0., c, 3, h, 5, n, 1, o, 4
for, phenoxy, -110000., 240.98, 0., c, 18, h, 20, o, 3
for, pnimmo, 73900., 114.94, 0., c, 5, h, 9, n, 1, o, 4
for, pvc, -19750., 44.64, 0., c, 2, h, 3, cl, 1
for, pvf, -479740., 676.42, 0., c, 38, h, 69, o, 19
for, saran, -1200., 25.50, 0., c, 1.0, h, 1.29, n, 0.15, cl, 0.37
for, sylgard, -24900., 70.62, 0., c, 2, h, 6, o, 1, si, 1
for, viton, -332700., 102.50, 0., c, 5, h, 3.5, f, 6.5
for, water, -68315., 18.02, 0., h, 2, o, 1

for, an, -87280., 46.40, 0., h, 4, n, 2, o, 3
for, ap, -70580., 60.25, 0., h, 4, n, 1, o, 4, cl, 1
for, calcium nit, -224200., 65.53, 0., n, 2, o, 6, ca, 1
for, lithium nit, -115500., 28.97, 0., n, 1, o, 3, li, 1
for, lithium per, -91060., 43.78, 0., o, 4, cl, 1, li, 1

Appendix C

for, magnesium per, -140600., 101.0, 0., o, 8, cl, 2, mg, 1
for, nitric acid, -41610., 41.92, 0., h, 1, n, 1, o, 3
for, potassium nit, -118200., 47.94, 0., o, 3, n, 1, k, 1
for, potassium per, -103400., 55.00, 0., o, 4, cl, 1, k, 1
for, sodium nit, -111800., 37.59, 0., n, 1, o, 3, na, 1
for, sodium per, -91610., 48.98, 0., o, 4, cl, 1, na, 1

for, bdnpa, -151300., 234.69, 0., c, 8, h, 14, n, 4, o, 10
for, bdnlpf, -142700., 224.60, 0., c, 7, h, 12, n, 4, o, 10
for, cef, -300000., 200.35, 0., c, 6, h, 12, o, 4, cl, 3, p, 1
for, dop, -268200., 396.15, 0., c, 24, h, 38, o, 4
for, tegdn, -145400., 180.58, 0., c, 6, h, 12, n, 2, o, 8
for, tmetn, -105800., 173.56, 0., c, 5, h, 9, n, 3, o, 9

reducers

for, al, 0., 9.985, 0., al, 1
for, al inert, 0., 9.985, 0., al inert, 1
for, b, 0., 4.62, 0., b, 1
for, fuel oil, 70000., 115.9, 0., c, 7, h, 12
for, graphite, 0., 5.34, 0., c, 1

for, ABH, 116000., 533.0, 75.0, C, 24, H, 6, N, 14, O, 24
for, COMPA3, 2840., 59.8, 70.0, C, 1.87, H, 3.74, N, 2.46, O, 2.46
for, COMPA3, 2840., 59.8, 70.0, C, 1.87, H, 3.74, N, 2.46, O, 2.46
for, COMPB, 1000., 139.3, 75.0, C, 2.03, H, 2.64, N, 2.18, O, 2.67
for, COMPC3, -6450., 59.9, 75.0, C, 1.90, H, 2.83, N, 2.34, O, 2.60
for, COMPC4, 3330., 59.9, 75.0, C, 1.82, H, 3.54, N, 2.46, O, 2.51
for, DATB-SNL, -23600., 132.3, 70.0, C, 6, H, 5., N, 5., O, 6.
for, DEGN, -99400., 141.0, 70.0, C, 4, H, 8, N, 2, O, 7
for, DIPM, -6800., 253.7, 70.0, C, 12, H, 6, N, 8, O, 12
for, EXPD, -94000., 150.9, 70.0, C, 6, H, 6, N, 4, O, 7
for, LX9, 2004., 53.6, 70.0, C, 1.43, H, 2.74, N, 2.59, O, 2.72, F, 0.02
for, MEN, -74300., 98.3, 70.0, C, 2.06, H, 7.06, N, 1.33, O, 3.10
for, NONA, 27400., 374.0, 75.0, C, 18, H, 5, N, 9, O, 18
for, PBX9007, 7130., 58.9, 70.0, C, 1.97, H, 3.22, N, 2.43, O, 2.44
for, PBX9010,-7870.,55.,70.0,C,1.39,H,2.43,N,2.43,O,2.43,CL,.09,F,.26
for, PBX9011, -4050., 55.7, 70.0, C, 1.73, H, 3.18, N, 2.45, O, 2.61
for, PBX9205, 5810., 58.1, 70.0, C, 1.83, H, 3.14, N, 2.49, O, 2.51
for, PBX9404,80.,53.6,70.,C,1.40,H,2.75,N,2.57,O,2.69,CL,.03,P,.01
for, BKWC9404,80.,53.6,70.,C,1.40,H,2.75,N,2.57,O,2.69,CL,.03
for, PBX9407,810.,55.2,70.,C,1.41,H,2.66,N,2.54,O,2.54,CL,.07,F,.09
for, PBX9501, 2300., 54.0, 70.0, C, 1.47, H, 2.86, N, 2.60, O, 2.69
for, PBX9502,-20800.,51.5,70.,C,2.30,H,2.23,N,2.21,O,2.21,CL,.038,F, 0.13
for, PBX9503, -17700.,51.7,70.0,C,2.16,H,2.28,N,2.26,O,2.26,CL,.038
for, NPRO, -30000.,24464.0, 85.0, C, 3, H, 7, N, 1, O, 2
for, tntab, 270000., 193.1, 75.0, C, 6, N, 12, O, 6

DAKOTA INPUT DECK

```
# DAKOTA INPUT FILE - dakota_sample.in
# NOTES: Sections are delimited by newline characters. Therefore, to continue a
# section onto multiple lines, the back-slash character is needed to
# escape the newline. Input is order-independent and white-space
# insensitive. Keywords may be abbreviated so long as the abbreviation
# is unique. Comments are preceded by #. Helpful NOTES precede each
# section specification; however, the definitive resource for input
# grammar is Dakota/src/dakota.input.spec.
```

Appendix C

```
# Interface section specification
# NOTES: input_filter and output_filter may be either an executable name or
# NO_FILTER. analysis_driver is the name of the analysis executable or
# driver script. parameters_file is the parameters file which Dakota
# creates, and results_file is the results file which Dakota will read.
# analysis_code_usage, file_tag, and file_save are optional and are not
# currently implemented. The names of the parameters and results files
# are passed on the command line either to the input_filter and
# output_filter respectively (if filters are specified) or to the
# analysis_driver (if NO_FILTER is used).

interface,
  application,
    analysis_driver=      'jcz.csh'          \
    parameters_file=      'params.in'        \
    results_file=         'results.out'

# Variables specification
# NOTES: Each of the n design parameters can have an initial point, a lower
# bound, an upper bound, and a descriptive tag. The uncertain variables
# specification is a placeholder for the time being.

variables,
  design = 17
  dv_descriptor 'c2f6' 'cf2' 'ch3f' 'cf4' 'clcf3' 'ccf0' 'ch2clf' \
    'fn' 'chf0' 'cf2o' 'chf3' 'ch2f2' 'c2f3n' 'cf3' \
    'c2f4' 'cf4o' 'cfo'
  initial_point  6.14 4.07 4.74 5.41 5.16 5.07 4.94 3.41 4.19 \
    5.64 4.76 4.91 5.36 4.85 5.08 4.86 4.51
  upper_bounds   9. 9. 9. 9. 9. 9. 9. 9. 9. 9. 9. 9. 9. 9. 9. 9. \
  lower_bounds   2. 2. 2. 2. 2. 2. 2. 2. 2. 2. 2. 2. 2. 2. 2. 2. \
  uncertain = 0

# Responses specification
# NOTES: This specification implements a generalized Dakota data set by
# specifying a set of functions and the types of gradients and hessians
# for these functions. This responses specification combines the
# previous "functions" and "derivatives" keywords and will simplify the
# specification of multiple data sets. Optimization data sets require
# specification of num_objective_functions, num_linear_constraints, and
# num_nonlinear_constraints. Multiobjective opt. is not yet supported,
# so num_objective_functions must be = 1. Uncertainty quantification
# data sets are specified by num_response_functions. Nonlinear least
# squares data sets are specified with num_least_squares_terms.
# Gradient type specification may be no_gradients, analytic_gradients,
# numerical_gradients or mixed_gradients:
# > no_gradients is invalid with gradient-based opt. methods
# > no_gradients or analytic_gradients are complete specifications
# > mixed_gradients uses id_numerical & id_analytic lists to specify
#   the gradient types for different function numbers. This capability
#   is not yet completely implemented within the Iterators.
# > if numerical_gradients, then:
#   >> method_source = vendor OR dakota
#   >> interval_type = forward OR central
#   >> fd_step_size = <float>
#   are additional optional parameters in the specification.
# Hessian type specification may currently be no_hessians or
# analytic_hessians. The only optimizer to currently support
# analytic_hessians is optpp_newton (full newton).
```

Appendix C

```
responses,          \
    num_objective_functions = 1      \
    num_linear_constraints = 0      \
    num_nonlinear_constraints = 0   \
numerical_gradients          \
method_source dakota          \
interval_type central          \
fd_step_size = 0.01            \
no_hessians

# Strategy specification
# NOTES: Contains placeholders for hybrid, SAO, and OUU. single_method should
#       be used for now.

strategy,           \
    single_method

# Method specification
# NOTES: method can currently be dot_frcg, dot_mmmfd, dot_bfgs, dot_slp,
#       dot_sqp, optpp_cg, optpp_q_newton, optpp_g_newton, optpp_newton,
#       optpp_fd_newton, optpp_ba_newton, optpp_baq_newton, optpp_bc_newton,
#       optpp_bcq_newton, optpp_bc_ellipsoid, optpp_pds, optpp_test_new,
#       npsol_sqp, lhs, or parameter_study. All optimization method control
#       parameters are now optional, although parameter_study and lhs still
#       have required control parameters. Default values for optional
#       parameters are defined in the static member initializations at the top
#       of ProblemDescDB.C. For a complete list of the optional parameters
#       supported by a particular optimizer, consult dakota.input.spec.

method,           \
    dot_sqp,          \
        max_iterations = 50,          \
        convergence_tolerance = 1e-9 \
        output verbose
```

C-shell script used to run the DAKOTA optimizer, jczi.csh

```
#!/bin/csh -f -x
#
# Optimize JCZ3 parameters
#
#
# Create jczi library to run with cheetah
#
./conapr
# Create jczi library
aprepro -q -W jczi.apr jczi.chi
cp jczi.chi /home/mlhobbs/cheetah.1.40/products
cd /home/mlhobbs/cheetah.1.40
make library
cd /home/mlhobbs/opt/run5
/home/mlhobbs/cheetah.1.40/cheetah input output
rm D.jcz P.jcz
grep shock output > D.jcz
grep '1.)' output > P.jcz
#
# Output filter function evaluation
#
./rms
#
```

Appendix C

```
echo "output filter created results.out"
#
```

FORTRAN code used to construct the APREPRO include file for the DAKOTA optimization

```
program conapr
implicit double precision (a-h,o-z)
c*****
c purpose: parse Dakota Optimizer output into aprepro input
c      include file
c*****
parameter(linp=10,lout=11)
c
c read the input from dakota.out and convert into an include file
c for making the Trex1d input file
c
character dumc*10
c-----c
c open files
c-----c
open(unit=linp,file='params.in',status='old',form='formatted')
open(unit=lout,file='params.inc',status='unknown')
c-----c
c Read number of variables (inum)
c-----c
read (linp,*,end=100,err=200) inum, dumc
c-----c
c Read number and variable name
c-----c
do 10 i = 1,inum
    read (linp,*,end=300,err=400) value, dumc
    write (lout,25) dumc,value
cMLH if (i.gt.12) write (lout,25) dumc,value
10  continue
c-----c
c output any other parameters that change
c-----c
stop
c-----c
c Error processing
c-----c
100 write(6,500)
    stop
200 write(6,510)
    stop
300 write(6,520) i
    stop
400 write(6,530) i
    stop
c-----c
c      Formats
c-----c
25  format(t5,'{,A10,'=,G20.10,}')
500 format(t2,'***** Error EOF reading input params.in *****')
510 format(t2,'***** Error reading input params.out *****')
520 format(t2,'***** Error EOF reading input params.out I=',I3,
    1 '*****')
530 format(t2,'***** Error reading input params.out I=',I3,
    1 '*****')
end
```

Appendix C

FORTRAN code used to calculate the root mean square error, rms.f.

```
program rms
C23456789x123456789x123456789x123456789x123456789x123456789x12
C-----C
C This program calculates the root mean square (rms) percent difference
C in calculated and measured Detonation properties.
C-----C
character*27 junk
character*7 junk2
character*6 spec(25)
parameter (nin1=10,nin2=12,nin3=13,nin4=14,nptmax=150)
parameter (nout1=20,nout2=30,nout3=40,nout4=45,nout5=55)
dimension dexp(nptmax),djcz(nptmax),pexp(nptmax),pjcz(nptmax)
data spec/ 'dp12','afx902','fefo','fm1','pf','rx36ah','rx41ab',
&      'lx17','rx27ad','rx45aa','rx47aa','rx48aa','fefo',
&      'lx04','lx07','lx09','lx10','lx11','lx15','lx17',
&      '9010','9404','9407','9502','9503'/
C-----C
C open input files
C-----C
open(nin1,file='D.exp',status='unknown',form='formatted')
open(nin2,file='D.jcz',status='unknown',form='formatted')
open(nin3,file='P.exp',status='unknown',form='formatted')
open(nin4,file='P.jcz',status='unknown',form='formatted')
open(nout1,file='D.all',status='unknown',form='formatted')
open(nout2,file='P.all',status='unknown',form='formatted')
open(nout3,file='results.out',status='unknown',form='formatted')
open(nout4,file='D.rms',status='unknown',form='formatted')
open(nout5,file='P.rms',status='unknown',form='formatted')
wt = 1.0
C-----C
C read in Detonation velocities
C-----C
i = 0
10   i = i + 1
      READ(nin1,* , end=15) dexp(i)
      goto 10
15   npt = i - 1
      i = 0
20   i = i + 1
      READ(nin2,2500, end=25) junk,djcz(i)
2500  format (a27,e11.5)
      djcz(i) = djcz(i)/1000.
      goto 20
25   if(i-1.ne.npt) then
      write(6,*) 'The # of points in D.exp and D.jcz are different'
      npt = i-1.
      wt = 2.0
      endif
C-----C
C Write out the detonation velocities
C-----C
do 100 i=1,npt
      if(dexp(i).ne.0.0) then
          write(nout1,*) dexp(i),djcz(i)
      endif
100  continue
C-----C
```

Appendix C

```
C Calculate the RMS error
C-----C
errd = 0.0
do 200 i=1,npt
  if(dexp(i).ne.0.0) then
    errd = errd+((dexp(i)-djcz(i))/dexp(i))**2.
    err = 100.*sqrt(((dexp(i)-djcz(i))/dexp(i))**2.)
    write(nout4,*) dexp(i),djcz(i),err,' ',spec(i)
  endif
200 continue
  errd = 100.*sqrt(errd/float(npt))
  errd = wt*errd
C-----C
C read in Detonation pressures
C-----C
wt = 1.0
count = 0.0
i = 0
50 i = i + 1
  READ(nin3,* , end=55) pexp(i)
  if (pexp(i).ne.0.) count = count+1.
  pexp(i) = 10.*pexp(i)
  goto 50
55 if(i-1.ne.npt) then
  write(6,*) 'The # of points in D.exp and P.exp are different'
  endif
  i = 0
60 i = i + 1
  READ(nin4,2600, end=65) junk2,pjcz(i)
2600 format (a7,f8.1)
  pjcz(i) = 1.01325*pjcz(i)/1000.
  goto 60
65 if(i-1.ne.npt) then
  write(6,*) 'The # of points in P.exp and P.jcz are different'
  npt = i-1.
  wt = 2.0
  endif
C-----C
C Write out the detonation pressures
C-----C
do 300 i=1,npt
  if(pexp(i).ne.0.0) then
    write(nout2,*) pexp(i),pjcz(i)
  endif
300 continue
C-----C
C Calculate the RMS error for the pressures
C-----C
errp = 0.0
do 400 i=1,npt
  if(pexp(i).ne.0.0) then
    errp = errp+((pexp(i)-pjcz(i))/pexp(i))**2.
    err = 100.*sqrt(((pexp(i)-pjcz(i))/pexp(i))**2.)
    write(nout5,*) pexp(i),pjcz(i),err,' ',spec(i)
  endif
400 continue
  errp = 100.*sqrt(errp/count)
  errp = wt*errp
C-----C
C Write out the rms error
```

Appendix C

```
C-----C
      write(nout4,*) errd
      write(nout5,*) errp
C-----C
C Calculate the RMS weighted error to be minimized
C by only considering the detonation velocities since
C these are measured accurately
C-----C
      write(nout3,1000) errd
1000  format(t5,e15.8,'   f)
      stop
      end
```

CHEETAH input deck for the explosives listed in Table 5

```
library file, bkwc.chl
#library file, bkws.chl
gas eos, bkw
#set, bkw, alpha,    0.5
#set, bkw, beta,    0.298
#set, bkw, theta,   6620.
#set, bkw, kappa,   10.5
#gas eos, jcz3
#set, jcz3, m, 6
#set, jcz3, l, 13
composition, abh, 1.
hug0, p, 1, rho, 1.64
c-j
composition, compa3, 1.
hug0, p, 1, rho, 1.64
c-j
composition, compb, 1.
hug0, p, 1, rho, 1.72
c-j
# The following entry is for comp B-3
composition, rdx, 60., tnt, 40.
hug0, p, 1, rho, 1.72
c-j
composition, compc3, 1.
hug0, p, 1, rho, 1.60
c-j
composition, compc4, 1.
hug0, p, 1, rho, 1.66
c-j
# The following entry is for Cyclotol-78/22
composition, rdx, 78., tnt, 22.
hug0, p, 1, rho, 1.76
c-j
# The following entry is for Cyclotol-77/23
composition, rdx, 77., tnt, 23.
hug0, p, 1, rho, 1.74
c-j
# The following entry is for Cyclotol-75/25
composition, rdx, 75., tnt, 25.
hug0, p, 1, rho, 1.76
c-j
# The following entry is for Cyclotol-75/25
composition, rdx, 75., tnt, 25.
hug0, p, 1, rho, 1.62
c-j
```

Appendix C

```
# The following entry is for Cyclotol-70/30
composition, rdx, 70., tnt, 30.
hug0, p, 1, rho, 1.73
c-j
# The following entry is for Cyclotol-65/35
composition, rdx, 65., tnt, 35.
hug0, p, 1, rho, 1.72
c-j
# The following entry is for Cyclotol-60/40
composition, rdx, 60., tnt, 40.
hug0, p, 1, rho, 1.74
c-j
hug0, p, 1, rho, 1.72
c-j
# The following entry is for Cyclotol-50/50
composition, rdx, 50., tnt, 50.
hug0, p, 1, rho, 1.63
c-j
composition, datb-snl, 1.0
hug0, p, 1, rho, 1.80
c-j
hug0, p, 1, rho, 1.78
c-j
composition, degn, 1.0
hug0, p, 1, rho, 1.38
c-j
composition, dipm, 1.0, tnt, 0.0000000001
hug0, p, 1, rho, 1.76
c-j
composition, expd, 1.0
hug0, p, 1, rho, 1.55
c-j
hug0, p, 1, rho, 1.48
c-j
composition, hmx, 1.0
hug0, p, 1, rho, 1.89
c-j
hug0, p, 1, rho, 1.60
c-j
hug0, p, 1, rho, 1.40
c-j
hug0, p, 1, rho, 1.20
c-j
hug0, p, 1, rho, 1.00
c-j
hug0, p, 1, rho, 0.75
c-j
composition, hnab, 1.0
hug0, p, 1, rho, 1.60
c-j
composition, hns, 1.0
hug0, p, 1, rho, 1.60
c-j
hug0, p, 1, rho, 1.70
c-j
# The following entry is for LX01
composition, nm, 51.7,tnm,33.2,npro,15.1
hug0, p, 1, rho, 1.24
c-j
##lx14
```

Appendix C

composition, hmx, 95.5, estane, 4.5
composition, hmx, 95.5, estane, 4.5
hug0, p, 1, rho, 1.84
c-j
composition, men, 1.0
hug0, p, 1, rho, 1.02
c-j
composition, ng, 1.0
hug0, p, 1, rho, 1.60
c-j
composition, nm, 1.0
hug0, p, 1, rho, 1.13
c-j
composition, nona, 1.0
hug0, p, 1, rho, 1.70
c-j
composition, nq, 1.0
hug0, p, 1, rho, 1.78
c-j
hug0, p, 1, rho, 1.72
c-j
hug0, p, 1, rho, 1.62
c-j
hug0, p, 1, rho, 1.55
c-j
The following entry is for Octol-78/22
composition, hmx, 77.6, tnt, 22.4
hug0, p, 1, rho, 1.82
c-j
The following entry is for Octol-76/23
composition, hmx, 76.3, tnt, 23.7
hug0, p, 1, rho, 1.81
c-j
The following entry is for Octol-75/25
composition, hmx, 75.0, tnt, 25.0
hug0, p, 1, rho, 1.81
c-j
The following entry is for Octol-60/40
composition, hmx, 60., tnt, 40.
hug0, p, 1, rho, 1.80
c-j
composition, pbx9007, 100.
hug0, p, 1, rho, 1.64
c-j
composition, pbx9011, 100.
hug0, p, 1, rho, 1.77
c-j
composition, pbx9205, 100.
hug0, p, 1, rho, 1.67
c-j
composition, pbx9501, 100.
hug0, p, 1, rho, 1.84
c-j
The following entry is for pentolit 50/50
composition, petn, 50., tnt, 50.
hug0, p, 1, rho, 1.71
c-j
hug0, p, 1, rho, 1.70
c-j
hug0, p, 1, rho, 1.68

Appendix C

```
c-j  
hug0, p, 1, rho, 1.64  
c-j  
# The following entry is for PETN  
composition, petn, 100.  
hug0, p, 1, rho, 1.76  
c-j  
hug0, p, 1, rho, 1.70  
c-j  
hug0, p, 1, rho, 1.60  
c-j  
hug0, p, 1, rho, 1.45  
c-j  
hug0, p, 1, rho, 1.23  
c-j  
hug0, p, 1, rho, 0.99  
c-j  
hug0, p, 1, rho, 0.88  
c-j  
hug0, p, 1, rho, 0.48  
c-j  
hug0, p, 1, rho, 0.30  
c-j  
hug0, p, 1, rho, 0.25  
c-j  
# The following entry is for PICRATOL  
composition, expd, 52., tnt, 48.  
hug0, p, 1, rho, 1.63  
c-j  
# The following entry is for PICRIC ACID  
composition, picric acid, 100.  
hug0, p, 1, rho, 1.76  
c-j  
hug0, p, 1, rho, 1.71  
c-j  
hug0, p, 1, rho, 1.60  
c-j  
# The following entry is for RDX  
composition, rdx, 100.  
hug0, p, 1, rho, 1.80  
c-j  
hug0, p, 1, rho, 1.77  
c-j  
hug0, p, 1, rho, 1.72  
c-j  
hug0, p, 1, rho, 1.66  
c-j  
hug0, p, 1, rho, 1.60  
c-j  
hug0, p, 1, rho, 1.46  
c-j  
hug0, p, 1, rho, 1.40  
c-j  
hug0, p, 1, rho, 1.29  
c-j  
hug0, p, 1, rho, 1.20  
c-j  
hug0, p, 1, rho, 1.10  
c-j  
hug0, p, 1, rho, 1.00
```

Appendix C

```
c-j  
hug0, p, 1, rho, 0.95  
c-j  
hug0, p, 1, rho, 0.70  
c-j  
hug0, p, 1, rho, 0.56  
c-j  
composition, tacot, 100.  
hug0, p, 1, rho, 1.85  
c-j  
# The following entry is for TATB  
composition, tatab, 100.  
hug0, p, 1, rho, 1.88  
c-j  
hug0, p, 1, rho, 1.85  
c-j  
# The following entry is for TETRYL  
composition, tetryl, 100.  
hug0, p, 1, rho, 1.73  
c-j  
hug0, p, 1, rho, 1.71  
c-j  
hug0, p, 1, rho, 1.68  
c-j  
hug0, p, 1, rho, 1.61  
c-j  
hug0, p, 1, rho, 1.40  
c-j  
hug0, p, 1, rho, 1.36  
c-j  
hug0, p, 1, rho, 1.20  
c-j  
hug0, p, 1, rho, 1.00  
c-j  
# The following entry is for TNT  
composition, tnt, 100.  
hug0, p, 1, rho, 1.64  
c-j  
hug0, p, 1, rho, 1.45  
c-j  
hug0, p, 1, rho, 1.36  
c-j  
hug0, p, 1, rho, 1.00  
c-j  
hug0, p, 1, rho, 0.80  
c-j  
# The following entry is for BTF  
composition, btf, 100.  
hug0, p, 1, rho, 1.86  
c-j  
hug0, p, 1, rho, 1.76  
c-j  
composition, hnb, 100.  
hug0, p, 1, rho, 1.97  
c-j  
composition, tnm, 100.  
hug0, p, 1, rho, 1.64  
c-j  
composition, tntab, 100.  
hug0, p, 1, rho, 1.74
```

Appendix C

```
c-j  
composition, fefo, 100.  
hug0, p, 1, rho, 1.59  
c-j  
# The following entry is for LX04  
composition, hmx, 85., viton, 15.  
hug0, p, 1, rho, 1.86  
c-j  
# The following entry is for LX07  
composition, hmx, 90., viton, 10.  
hug0, p, 1, rho, 1.87  
c-j  
composition, LX9, 100.  
hug0, p, 1, rho, 1.84  
c-j  
# The following entry is for LX10  
composition, hmx, 95., viton, 5.  
hug0, p, 1, rho, 1.86  
c-j  
# The following entry is for LX11  
composition, hmx, 80., viton, 20.  
hug0, p, 1, rho, 1.86  
c-j  
composition, ap, 100.  
hug0, p, 1, rho, 1.00  
c-j  
# The following entry is for LX15  
composition, hns, 95., kel-f, 5.  
hug0, p, 1, rho, 1.58  
c-j  
# The following entry is for LX17  
composition, tatab, 92.5, kel-f, 7.5  
hug0, p, 1, rho, 1.91  
c-j  
composition, PBX9010, 100.  
hug0, p, 1, rho, 1.78  
c-j  
composition, BKWC9404, 100.  
hug0, p, 1, rho, 1.84  
c-j  
composition, PBX9407, 100.  
hug0, p, 1, rho, 1.60  
c-j  
# The following entry is for PBX-9502  
composition, tatab, 95.0, kel-f, 5.0  
hug0, p, 1, rho, 1.91  
c-j  
# The following entry is for PBX-9503  
composition, tatab, 80.0, hmx, 15, kel-f, 5.0  
hug0, p, 1, rho, 1.90  
c-j  
STOP
```

Distribution

Alliant Techsystems, Inc.

Attn: Garn Butcher
P. O. Box 98
8400 West 5000 So.
Magna, UT 84044-0098

Brigham Young University (4)

Attn: Merrill Beckstead
Predrag Radulovic
Richard Rowley
L. Douglas Smoot
Department of Chemical Engineering
350 Clyde Building
Provo, UT 84602

California Institute of Technology

Attn: Joe E. Shepherd
306e Guggenheim (GALCIT Building)
1200 East California Boulevard
Pasadena, CA 91125

ChemEnergetics, Inc.

Attn: Remon J. Dihu
799 Roosevelt Road
Building 6, Suite 221
Glen Ellyn, IL 60137

Defense Research Agency

Attn: Philip J. Cheese
Fort Halstead
Sevenoaks, Kent, TN14 7BP, England

DOE Albuquerque Operations Office

Attn: Actg. Director, Weapons Program Div.
Albuquerque, NM 87185

Energetic Materials Laboratory

Attn: Katsumi Tanaka
Ministry of International Trade and Industry
National Institute of Materials and Chemical
Research, Tsukuba Research Center,
Tsukuba, Ibaraki 305 Japan

Enig Associates, Inc. (2)

Attn: Michael Cowperthwaite
J. W. Enig
11120 New Hampshire Avenue, Suite 500
Silver Spring, MD 20904-2633

Fraunhofer Institut (FCT)

Attn: Fred Volk
Josef von Fraunhofer Strasse, Germany

ICI Explosives

Attn: Graeme A. Leiper
K80, ICI plc
Stevenston, Ayrshire, KA20 3LN, Scotland

IIT Research Institute (3)

Attn: Allen J. Tulis
James L. Austing
Ron Pape
10 West 35th Street
Chicago, IL 60616-3799

Lawrence Livermore National Lab. (17)

Attn: Dennis Baum
Tom Deboni
Mark Hoffman
Al Holt
Michael Howard
John Kury
Ronald S. Lee
Jon L. Maienschein
Mike Murphy
Albert Nichols III
David Price
Francis H. Ree
Randy Simpson
Clark Souers
Bill Tao
Craig Tarver
Paul A. Urtiew
P. O. Box 808
Livermore, CA 94555

Lockheed-Martin Missiles & Space Co., Inc.

Attn: Erik R. Matheson
1111 Lockheed Way, Sunnyvale, CA 94089

Logicon RDA

Attn: William R. Espander
Laser Technology Department
P. O. Box 9273
Albuquerque, NM 87119-9273

Distribution

Los Alamos National Laboratory (8)

Attn: Blaine Asay (Group DX-2, MS C920)
Langdon Bennett
Mary S. Campbell
Brian Henson
John F. Kramer
Jonathan Mace
Steve Sheffield
Steve Son
P. O. Box 1663
Los Alamos, NM 87545

McGill University (2)

Attn: David Frost
Jean-Philippe Dionne
Mechanical Engineering Department
817 Sherbrooke St. W.
Montreal, Que Canada H3A 2K6

National Defence Research Establishment

Attn: Henric L. Ostmark
Sundybyberg, S-17290, SWEDEN

Naval Air Weapons Center (3)

Attn: Alice I. Atwood
Thom L. Boggs
Don Thompson
China Lake, CA 94555-6001

Naval Reserach Laboratory

Attn: Thomas P. Russell
Chemistry Division, Code 6110
4555 Overlook Ave.
Washington DC 20375

Naval Surface Warfare Center (8)

Attn: Richard R. Bernecker
Charles S. Coffey
Ruth M. Doherty
R. Guirguis
Philip J. Miller
Susan Peters
Harold W. Sandusky
Gerrit T. Sutherland
Indian Head, MD 20640

New Mexico Tech. (3)

Center for Explosives Technology Research
Attn: Per-Anders Persson
Doug Olsen
L. D. Libersky
RCEM, Campus Station
Socorro, NM 87801

North Carolina State University

Attn: Yasuyuki Horie
Department of Mech. and Aero. Eng.
Box 7908
Raleigh, NC 27695-7908

Polytechnic University

Attn: Leonard I. Stiel
333 Jay Street
Brooklyn, NY 11201

Princeton University

Attn: Richard A. Yetter
Department of Mech. and Aero. Eng.
D312 Engineering Quadrangle
Princeton, NJ 08544-5263

Prins Maurits Laboratory TNO (2)

Attn: Ries Verbeek
Albert C. van der Steen
Lange Kleiweg 137
Rijswijk, 2280 AA The Netherlands

Redstone Arsenal

Attn: Barbara P. Marsh
Propulsion Directorate, Bldg 7156
Redstone Arsenal, AL 35898

Southwest Research Institute

Attn: Robert D. Young
Materials and Structures Division
6220 Culebra Road
P. O. Drawer 28510
San Antonio, Texas 78228-0510

Stanford Reserach Institute

Attn: Tom Cooper
333 Ravenswood Avenue
Menlo Park, CA 94025

Distribution

Thiokol Corporation

Attn: Paul C. Braithwaite
Robert G. Jones
P. O. Box 707
Brigham City, UT 84302-0707

University of Delaware

Attn: Thomas B. Brill
Department of Chemistry and Biochemistry
003 Lammot DuPont Laboratory
Newark, DE 19711

University of Illinois

Attn: Herman Krier
Department of Mechanical Engineering
1206 W. Green Street
Urbana, IL 61801

University of Iowa

Attn: P. Barry Butler
Department of Mechanical Engineering
2208 Engineering Bldg.
Iowa City, IA 52245

University of Maryland

Attn: Herman L. Ammon
Rm. B214, Chemistry Building
Lanham, MD 20706

University of Notre Dame

Attn: Joe Powers
Department of Mechanical Eng. and Aerospace
Notre Dame, IN 46556

University of Toronto

Attn: Susan McCahan
Dept. of Mechanical and Industrial Engineering
5 King's College Road
Toronto, Ontario, Canada M5S 3G8

U. S. Army Armament Research (5)

Attn: Ernest Baker
B. Fishburn
Gail Tutt
R. Gentner
Daniel Stec
Development and Engineering Center
Picatinny Arsenal, NJ 07806-5000

U.S. Army Ballistic Research Lab. (3)

Attn: Douglas E. Kooker
Robert B. Frey
John Starkenberg
Aberdeen Proving Grounds, MD 21005-5066

Washington State University

Attn: Yogendra M. Gupta
Physical Science 948A
Pullman, WA 99164-2814

Wilfred Baker Engineering, Inc.

Attn: Craig Doolittle
8700 Crownhill, Suite 310
San Antonio, TX 78209-1128

Wright Lab./Armament Directorate (6)

Attn: Gary H. Parsons
Joseph C. Foster Jr.
Robert L. McKenney Jr.
Paul Bolduc
Phillip Mendicki
David R. Wagnon
2306 Perimeter Road
Eglin Air Force Base, FL 32542-6009

Internal Distribution

MS	Org.	Name
9052	8361	L. L. Baxter
9052	8361	Behrens, R.
9052	8361	Margolis, S. B.
9056	8120	Thorne, L. R.
9104	8120	Christensen, G. J.
1421	1152	Samara, G. A.
1421	1152	Graham, R. A.
0614	1522	Mitchell, D. E.
1452	1552	Harlan, J. G.
1452	1552	Loyola, V. M.
1452	1552	Massis, T. M.
1452	1552	Merson, J. A.
1453	1553	Bickes, R. W.
1453	1553	Benham, R. A.
1453	1553	Fischer, S. H.
1453	1553	Grubelich, M. C.
1453	1553	Harris, S. M.
1453	1553	Vigil, M. G.
1454	1554	Bonzon, L. L.
1454	1554	Fleming, K. J.
1454	1554	Renlund, A. M.
0841	9100	Hommert, P. J.
0841	9101	Bickel, T. C. (Route to 9113)

Distribution

0826	9111	Hermina, W. L.
0834	9112	Ratzel, A. C.
0834	9112	Baer, M. R.
0834	9112	Erickson, K. L.
0834	9112	Gross, R. J.
0834	9112	Hobbs, M. L. (25)
0834	9112	Schmitt, R. G.
0834	9112	Trott, W. M.
0827	9114	Griffith, R.O. (Route to 9114)
0825	9115	Rutledge, W. H. (Route 9115)
0836	9116	Peterson, C. W. (Route 9116)
0836	9116	Tieszen, S. R.
0820	9232	Kipp, M. E.
0820	9232	Yarrington, P.
0820	9232	Boslough, M. B.
0820	9232	Silling, S. A.
0439	9234	Eldred, M. S.
1423	2000	Schmitt, H. W.
9018	8940-2	Central Tech Files (2)
0899	4414	Technical Library (5)
0115	10300	McGee, R. H., Jr.
0619	12690	Review & Approval Desk (5) for DOE/OSTI
0871	14405	McGee, B. C. (2)